Chapter 11

Pleistocene Antarctic Climate Variability: Ice Sheet – Ocean – Climate Interactions

David J. Wilson[1], Tina van de Flierdt[2], Robert M. McKay[3], Tim R. Naish[3]

[1]Department of Earth Sciences, University College London, London, UK
[2]Department of Earth Science and Engineering, Imperial College London, London, UK
[3]Antarctic Research Centre, Victoria University of Wellington, Wellington, New Zealand

Abstract:

During the Pleistocene, Earth experienced high-amplitude fluctuations in global temperature, atmospheric composition, ice sheet extent, and sea level that were forced by orbital variations in the seasonal distribution of solar energy across the planet. Subtle cyclical variations in forcing were greatly amplified by internal feedbacks in the Earth system, with processes in the polar regions influential for pole-to-equator temperature gradients and atmospheric carbon dioxide levels. Exploring the behaviour of the polar ice sheets and the Southern Ocean during this interval is crucial for understanding how the climate system operates and for constraining its sensitivity to future changes. Southern Ocean processes, including wind-driven upwelling, sea ice formation, deep water production, and biological productivity, were instrumental in regulating Earth's atmospheric carbon dioxide levels through Pleistocene glacial-interglacial cycles. On millennial timescales, rapid changes in ocean and atmospheric circulation were influenced by meltwater input from unstable ice sheet margins in both hemispheres, leading to highly variable regional and interhemispheric climate responses. This chapter provides an overview of the tools used in marine sediment and ice core archives to reconstruct Pleistocene changes in the Earth system. We discuss the mechanisms that controlled Earth's climate over different timescales, and review the latest evidence that is revealing how the Antarctic Ice Sheet has both influenced and responded to Pleistocene climate change, including during intervals when Earth's climate was similar to near-future projections. Despite experiencing ice volume changes that were modest in comparison to the advance and retreat of large Northern Hemisphere ice sheets, Antarctica has been a very active player in the ice sheet-ocean-climate system of the past 2.6 million years, and evidence increasingly suggests that it could respond dramatically to anthropogenic warming.

Key words:

Pleistocene, Antarctica, paleoclimate, orbital forcing, ocean circulation, sea ice, productivity, sea level, geochemistry, ice sheet modelling

11.1 Background and motivation

11.1.1 Introduction

Following the warm Mid Pliocene interval, Earth's climate cooled through the late Pliocene and passed a threshold causing intensification of glaciation in the Northern Hemisphere, with periodic expansion and retreat of ice sheets in Eurasia and North America since ~2.6-2.7 Ma (Raymo, 1994; Lisiecki and Raymo, 2005; Lawrence et al., 2006; DeConto et al., 2008; Bailey et al., 2013). This event marked the onset of the Pleistocene epoch (0-2.6 Ma) and, for the first time in the Cenozoic, Earth's climate system was characterised by bipolar glaciation (Zachos et al., 2001). Pleistocene glacial-interglacial cycles were paced by orbital forcing on ~21, ~41, and ~100 kyr timescales (Hays et al., 1976; Imbrie et al., 1992; Imbrie et al., 1993), leading to high-amplitude fluctuations in global temperature, atmospheric composition, ice sheet extent, and sea level (Chappell and Shackleton, 1986; Petit et al., 1999; Lisiecki and Raymo, 2005; Elderfield et al., 2012). The prevailing view is that ice volume variance over the Pleistocene has been dominated by ice sheets expanding to cover large parts of North America and Eurasia during glacial periods, and mostly disappearing during interglacials, with only Greenland remaining partially glaciated during all but the warmest interglacials. For the past 800,000 years, these changes in climate were consistently accompanied by atmospheric carbon dioxide (CO_2) variability, which ranged between ~180 ppm during glacials and ~280 ppm during the warmest interglacials (Figure 11.1).

The Earth is currently in the Holocene (0-11.7 ka BP), an interglacial period with a remarkably stable climate state. However, human interference in the Earth system, in particular through greenhouse gas emissions, has significantly perturbed this stability and has already resulted in atmospheric CO_2 levels that exceed 400 ppm. Such atmospheric conditions are not thought to have existed since the Pliocene, leading to the proposal that we have entered a new epoch known as the Anthropocene (Crutzen and Stoermer, 2000). Assessments by the Intergovernmental Panel on Climate Change indicate that it is virtually certain that these elevated CO_2 levels will prevent an orbitally-induced inception of glaciation before the end of the next millennium, even under reduced emission scenarios (Masson-Delmotte et al., 2013). It is clear that, due to anthropogenic activity, we are entering into a non-analogue state of the Earth system, and one in which changes in Antarctica may play a relatively more important role than they did during the glacial-interglacial cycles of the Pleistocene.

Exploring paleoclimate and paleoenvironmental change during the Pleistocene has proven fundamental to our understanding of the Earth's climate system. Important advances have included testing the orbital theory of ice ages (Milankovitch, 1941; Hays et al., 1976), assessing oceanic mechanisms for centennial scale climate perturbations (Marcott et al., 2014; Chen et al., 2015), and quantifying sea level rise from melting polar ice sheets (Dutton et al., 2015; DeConto and Pollard, 2016). These three examples highlight, respectively, the critical role of Earth system feedbacks for climate, the potential for rapid non-linear changes to occur in the Earth system, and the value of geological evidence for predicting future changes in response to our evolving anthropogenic experiment. Much is known, but many important questions remain unanswered, particularly in the Southern Ocean and Antarctica, and it is against this backdrop that the present chapter is set.

Perhaps the most pressing of these questions is how, and how fast, the polar ice sheets will respond to a future warming climate, which has significant implications for global sea level rise (IPCC, 2019). The Antarctic Ice Sheet contains a potential contribution to global sea levels of ~58 m (Fretwell et al., 2013; Morlighem et al., 2020), comprising ~4 m of marine-based ice in West Antarctica and ~19 m of marine-based ice and ~34 m of terrestrial-based ice in East Antarctica (Fretwell et al., 2013). Whereas the terrestrial portions of the Antarctic Ice Sheet are expected to be relatively stable, the

idea that the marine-based sectors could be susceptible to retreat or collapse under only moderate climate warming was recognised some time ago (Mercer, 1978). Theoretical calculations and modern observations suggest that two key factors affecting ice sheet mass balance could be critical for such retreat. First, where marine-based ice sheets rest on a reverse sloping bed that deepens inland, they are susceptible to marine ice sheet instability, a positive feedback process governing ice flow that enables rapid retreat following an initial perturbation (Weertman, 1974; Schoof, 2007). Second, most ice streams are significantly supported by offshore buttressing ice shelves, whose thinning or removal would reduce the back-stress on the ice and accelerate upstream ice sheet flow (Rignot et al., 2004; Dupont and Alley, 2005; Fürst et al., 2016). Recent observations indicate that marine ice sheet instability is potentially already underway in parts of West Antarctica (Joughin et al., 2014; Rignot et al., 2014; Wouters et al., 2015), while the West Antarctic ice shelves are currently losing mass (Paolo et al., 2015). Despite recognising the importance of these processes, the levels of atmospheric or ocean warming required to generate retreat of the marine-based portions of the Antarctic Ice Sheet are not well constrained, making it essential to assess their past behaviour under different climatic regimes. Since reverse sloping beds developed in the late Pliocene (Bart et al., 1999; De Santis et al., 1999; Bart and Iwai, 2012; McKay et al., 2019), and the ice shelves became more persistent and extensive with Pleistocene cooling (McKay et al., 2009), the Pleistocene interval provides the closest analogue for the modern and future Antarctic Ice Sheet (Colleoni et al., 2018).

11.1.2 Orbital cyclicity and climate

Building on earlier work by James Croll, who had proposed that an orbital influence on seasonality and winter snowfall led to the development of past ice ages (Croll, 1864), Milutin Milankovitch took the critical step of linking high-latitude summer insolation in the Northern Hemisphere to the growth of continental scale ice sheets during the Pleistocene (Milankovitch, 1941). In the Milankovitch model, intervals with low summer insolation are predicted to produce fewer positive degree days and a positive ice mass balance over multiple seasons, thereby enabling ice sheet expansion. Seasonal and spatial variations in insolation are themselves determined by the Earth's orbital configuration, with significant periodic variations on timescales of ~21 kyr (precession), ~41 kyr (obliquity, or axial tilt) and ~100 kyr (orbital eccentricity). In support of the Milankovitch theory, Earth's climate during the early Pleistocene (~2.6 Ma to ~900 ka) was largely characterised by ~41 kyr cycles forced by obliquity (Imbrie et al., 1992; Lisiecki and Raymo, 2005), with intervals of low obliquity leading to reduced seasonality, cooler summers, and ice sheet growth. Whereas the early Pleistocene glacial and interglacial periods had similar durations and climate responded fairly linearly to insolation changes, the climate cyclicity changed significantly during the Mid Pleistocene Transition (MPT), which occurred gradually over a few hundred thousand years at ~900 ka (Ruddiman et al., 1989). Glacial-interglacial cycles since the MPT have been strongly asymmetric, with long glacial periods and shorter interglacials recurring on a quasi-100 kyr timescale (Figure 11.1a) (Lisiecki and Raymo, 2005), indicating a more complex non-linear response of the Earth system to orbital forcing (Imbrie et al., 1993).

In detail, the exact manner by which orbital insolation has controlled the Pleistocene glacial-interglacial cycles remains a matter of debate, with several questions remaining to be fully answered. These include:

(i) the detailed timing of glacial-interglacial transitions in relation to orbital forcing (Kawamura et al., 2007; Drysdale et al., 2009; Thomas et al., 2009);

(ii) the importance of peak summer insolation values (Milankovitch model) versus summer duration, seasonally-integrated insolation, or latitudinal insolation gradients (Huybers, 2006; Huybers and Denton, 2008) in forcing Earth's climate;

(iii) the cause of temporal shifts in the expression of different orbital frequencies in Earth's ice volume and climate records, as seen at the MPT (Ruddiman et al., 1989; Maslin and Brierley, 2015);

(iv) the extent to which the late Pleistocene 100 kyr cycles reflect a non-linear earth system response to eccentricity forcing (Imbrie et al., 1993); forcing by multiple obliquity cycles (Huybers and Wunsch, 2005), by combined obliquity and precession cycles (Ruddiman, 2006; Huybers, 2011), or by multiple precession cycles (Cheng et al., 2016); or internal oscillations of the climate system (Berger, 1999; Rial et al., 2013);

(v) the necessity for orbital and millennial scale processes to combine to cause glaciation and deglaciation (Anderson et al., 2009; Cheng et al., 2009; Barker et al., 2011); and

(vi) the relative importance of Northern Hemisphere versus Southern Hemisphere forcing, and in particular the role of local insolation in governing the ice sheet mass balance of terrestrial and marine-based ice sheets (Knorr and Lohmann, 2003; Huybers, 2006; Raymo et al., 2006; Huybers and Denton, 2008; Laepple et al., 2011; He et al., 2013).

11.1.3 Antarctic feedbacks in the global climate system

Although orbital forcing is recognised as the pacemaker of Pleistocene glacial cycles, it is important to emphasise that the globally-integrated annual insolation budget is insensitive to obliquity and precession, and only weakly sensitive to eccentricity. Therefore, the direct effect of orbital forcing on Earth's energy balance is inadequate to explain glacial-interglacial cycles. Instead, a series of internal Earth system processes and feedbacks are required to translate and amplify subtle regional and seasonal changes driven by orbital forcing into the large-scale Pleistocene climate cycles (Imbrie et al., 1993; Shackleton, 2000; Ruddiman, 2006). These feedbacks arise from interactions between different components of the climate system, including pole-to-equator temperature gradients (which alter the atmospheric and ocean circulation), the biosphere, the cryosphere, and the carbon cycle. The close link between a global stack of benthic foraminiferal oxygen isotope records ($\delta^{18}O$), indicating Earth's climate state (i.e. a combination of ice volume and deep ocean temperature), and the ice core records of atmospheric CO_2 concentrations exemplifies these critical feedbacks (Figure 11.1a,c). Exploring and quantifying how these feedbacks operated in the past represents a key step in understanding the Earth's climate system and informing us about possible future changes that will arise from anthropogenic forcing.

Historically, explanations for Pleistocene climate change focused on the Northern Hemisphere ice sheets, which made the major contribution to sea level variability, and on Atlantic Ocean processes, which can convey climate signals into the Southern Hemisphere and globally. However, ice core records indicate a striking correlation between local Antarctic temperatures and atmospheric CO_2 concentrations (Figure 11.1b,c). As such, research is increasingly recognising the critical importance of Southern Ocean processes, such as sea ice formation, ocean stratification, upwelling, deep water formation, and biological productivity, in the Pleistocene climate system (Sigman and Boyle, 2000; Martinez-Garcia et al., 2011; Ferrari et al., 2014; Kohfeld and Chase, 2017). Furthermore, evidence is emerging for a more dynamic behaviour of the Antarctic Ice Sheet in response to Pleistocene climate cycles than had previously been recognised (McKay et al., 2012b; Dutton et al., 2015; Wilson et al., 2018; Rohling et al., 2019; Turney et al., 2020). Therefore, the Antarctic Ice Sheet may be both an active player in the interconnected climate system (Weaver et al., 2003; Fogwill et al., 2015; Schloesser et al., 2019) and a highly sensitive component that could respond dramatically to future anthropogenic warming (DeConto and Pollard, 2016; Golledge et al., 2017; Rintoul et al., 2018).

While this chapter will touch on some of the above debates concerning the operation of the Pleistocene climate system, including mechanisms for the MPT, we do not seek to provide an authoritative review of Pleistocene glacial-interglacial cycles or their link with orbital forcing at a

global scale. Such a topic would be deserving of an entire book in itself. Instead, we focus on changes in Antarctic climate and the Antarctic Ice Sheet during this interval, and the role of Southern Ocean and Antarctic processes in the interconnected global Earth system. We make a particular effort to discuss some of the key interactions between the Antarctic Ice Sheet, ocean circulation, and global carbon cycle changes, across orbital and millennial timescales.

11.1.4 Strengths of Pleistocene research on Antarctica

Although we now appear to be entering into a world in which large Northern Hemisphere ice sheets will no longer exert such a dominant influence on global climate variability, an understanding of the Earth system behaviour during the Pleistocene epoch is highly relevant for constraining ice sheet-ocean-climate interactions on the modern and future Earth. Below we highlight some of the key strengths of research on this interval:

(i) Boundary conditions: Geological boundary conditions during the Pleistocene were close to those of the modern day, in terms of the latitudinal distribution and topography of the continents, the bathymetry and geometry of ocean gateways, and the subglacial topography beneath ice sheets. These are important factors that determine atmospheric and ocean circulation, global heat transport, and ice sheet stability and dynamics. The Pleistocene behaviour is therefore expected to provide a useful guide to how a wide range of climate feedbacks could operate and interact in future, with the similarities in boundary conditions beneficial for climate modelling.

(ii) Temporal resolution: When compared to earlier intervals of the Cenozoic, Pleistocene paleoclimate records from archives such as ocean sediments, lake sediments, and speleothems generally benefit from better temporal resolution and a wider range of precise dating methods. This geological evidence provides the opportunity to constrain processes operating in the climate system from orbital to sub-centennial timescales, with the potential in some cases to determine rates of change, although this latter goal remains challenging beyond the Last Glacial Maximum (LGM).

(iii) Ice core records: Extremely well resolved records of late Pleistocene polar temperatures and atmospheric compositions are contained in ice cores, which span the last ~100 kyr in Greenland and ~800 kyr in Antarctica (Figure 11.1). These archives provide critical evidence on the local climate forcing acting on the ice sheets at an annual to centennial resolution, as well as recording global carbon cycle changes and interhemispheric patterns of climate variability.

(iv) Spatial integration: Pleistocene sediment records are readily obtained from the seafloor and lake beds using shallow coring techniques, as well as extended piston coring, leading to a wide spatial coverage of climate archives. Combining well-dated highly-resolved records from widely-distributed geological archives and polar ice cores reveals interhemispheric patterns of climate variability and connections between different components of the climate system. As such, and in combination with climate modelling, it is possible to constrain how the critical processes and feedbacks that amplify climate responses are operating.

(v) Cold climates: The glacial periods of the late Pleistocene represent a good example of Earth system behaviour in a significantly colder climate state than the modern day, which provides a robust test for our understanding of the climate system, and in particular for the processes and parameterisations employed in ocean, ice sheet, and climate models. Critically, we are also able to explore Earth system responses to natural warming events that had a similar magnitude to projected scenarios for the future, such as the 5-6 °C of global warming during the last glacial termination.

(vi) Future analogues: The warmest interglacials of the Pleistocene were globally ~1-2 °C warmer than the pre-industrial Holocene, and potentially warmer than this for short intervals in Antarctica due to polar amplification (Figure 11.1b). Therefore, records from these periods provide insight into

Earth system behaviour under levels of modest warming that are relevant to climate projections for the coming decades.

11.2 Archives of Pleistocene Antarctic climate and climate-relevant processes

11.2.1 Polar ice cores

11.2.1.1 Background and characteristics of ice core records

Continuous deep ice cores have been recovered in Antarctica extending back to ~800 ka, providing highly-resolved records of Antarctic temperatures and atmospheric carbon dioxide (CO_2) concentrations over the last eight glacial-interglacial cycles (Figure 11.1b,c). Past temperatures can be derived from the isotopic composition of oxygen ($\delta^{18}O_{ice}$) or deuterium (δD_{ice}) in the ice, while past concentrations of atmospheric CO_2 and other greenhouse gases are recorded in the trapped gas bubbles. Recent discussions of Antarctic ice core science, including the historical background, theoretical and practical considerations, and interpretations of the records, can be found in reviews by Alley (2010), Jouzel (2013), and Brook and Buizert (2018), and only a short summary is given below.

The earliest deep drilling was carried out at Byrd Station in West Antarctica (Gow et al., 1968), but it was several decades before the first continuous record covering multiple glacial-interglacial cycles was recovered, at Vostok Station in East Antarctica (Petit et al., 1999) (Figure 11.2). The Vostok record extends through four glacial cycles to ~420 ka, while the European Programme for Ice Coring in Antarctica (EPICA) project subsequently recovered an even longer core from Dome C (EDC) (Figure 11.2), which extends from the present day to ~800 ka (EPICA Community Members, 2004; Jouzel et al., 2007). To achieve such long records spanning multiple glacial-interglacial cycles, drilling was carried out on the East Antarctic Plateau, where low snow accumulation rates and slow ice flow mean that old ice can be reliably obtained from deep parts of the ice sheet. However, low accumulation rates also limit the temporal resolution of the records and restrict the ability to date the ice by layer-counting, so dating in these settings requires a combination of glaciological ice flow/snow accumulation modelling and orbital tuning.

At lower-lying settings, including coastal regions and West Antarctica, snow accumulation rates are higher and annual layers are thicker. This scenario enables dating by layer-counting (at least in the upper portions of cores where there has been less compaction) and the acquisition of highly-resolved climate records for the last glacial cycle. Recent examples include the deglacial record from the West Antarctic Ice Sheet (WAIS) Divide ice core (WDC) (WAIS Divide Project Members, 2013; Marcott et al., 2014) and a Holocene record from the Roosevelt Island Climate Evolution (RICE) core (Bertler et al., 2018) (Figure 11.2). Since these settings experience a stronger marine influence than the East Antarctic Plateau, they may also provide more sensitive records of changes in ocean circulation and sea ice in the Southern Ocean (WAIS Divide Project Members, 2013; Bertler et al., 2018), making them highly complementary to the interior records. In addition, comparisons between records from the Atlantic, Indian, and Pacific sectors of the ice sheet can provide evidence on the spatial patterns of climate variability and sea ice extent (Stenni et al., 2011; Holloway et al., 2017; Buizert et al., 2018). By comparing records between multiple ice cores, there is also potential to recover past changes in local ice sheet elevation, which may in turn provide evidence on ice sheet mass balance, ice flow, and glacio-isostatic adjustment (Bradley et al., 2012; Sutter et al., 2020).

For the last glacial cycle, records of Northern Hemisphere climate have also been recovered using ice cores in Greenland, thereby enabling interhemispheric comparisons. In particular, the ice cores recovered by the European Greenland Ice-core Project (GRIP) and the Greenland Ice Sheet Project 2 (GISP2) were instrumental in providing high-resolution records of millennial and centennial climate change in the North Atlantic region during the last glacial period and the last deglaciation (Johnsen et al., 1992; Dansgaard et al., 1993; Grootes et al., 1993). More recently, the North Greenland Ice-core Project (NGRIP) recovered a core from a more northerly site, providing a record that extends further back into the last interglacial period (NGRIP Members, 2004). Chronologies in Greenland are generally based on layer counting in the upper portions of cores, with age uncertainties of less than ~1 kyr back to 60 ka in the GICC05 chronology (Svensson et al., 2008), but approaches such as glaciological flow modelling, orbital tuning, and correlations based on volcanic ash layers or methane content are required at deeper depths where the layers are more compressed.

11.2.1.2 Ice core climate proxies

Past Antarctic temperatures can be derived from measurements of $\delta^{18}O_{ice}$ or δD_{ice} in the ice, using an approach based on the relatively well understood process of Rayleigh distillation. As water vapour is transported through the atmosphere, colder temperatures lead to more removal as rain or snow, which preferentially removes the heavy isotopes (^{18}O, D) and leads to a lighter isotopic composition (i.e. more ^{16}O, H) in the remaining vapour, which is ultimately recorded in the ice core record (Jouzel et al., 2007). This relationship appears relatively simple in the modern day, but additional considerations are required when applying it to the past, such as changes in the nature and location of the moisture source, changes in seasonality, and changes in ice sheet elevation (Jouzel et al., 2003; Bradley et al., 2012). Evidence of past climate change can also be preserved more directly in the temperature of the ice itself, enabling independent estimates of temperature changes during the last deglaciation to be obtained by modelling of borehole thermometry data (Cuffey et al., 2016). For times of rapid climate change, modelling of the isotopic composition of nitrogen ($\delta^{15}N$) trapped in gas bubbles can also be used to reconstruct temperature changes (Severinghaus and Brook, 1999), although this approach has been more widely used in Greenland than in Antarctica (Cuffey et al., 2016). Overall, the application of these alternative methods has provided temperature estimates that add confidence to the high-resolution reconstructions based on $\delta^{18}O_{ice}$ or δD_{ice}.

Atmospheric compositions are recorded in trapped bubbles of gas, enabling reconstructions of past changes in greenhouse gas concentrations, such as CO_2, methane, and nitrous oxides (Petit et al., 1999; Spahni et al., 2005). However, gas bubbles continuously exchange with the atmosphere and only become trapped (or 'locked-in') when snow is converted to ice, which typically occurs at ~50-120 metres depth depending on local site conditions (Parrenin et al., 2013). Therefore, in any given sample, the gas compositions are always younger than the surrounding ice, with the gas-ice age offset (Δ_{age}) determined by the lock-in depth and the accumulation rate. For Antarctic coastal sites with rapid accumulation rates, Δ_{age} is typically only ~200-1500 y during the last glacial period, whereas it can be as high as ~6-8 kyr where accumulation rates are low on the East Antarctic Plateau (Marcott et al., 2014).

When comparing records of gas composition (e.g. atmospheric CO_2) to records obtained on the ice itself (e.g. $\delta^{18}O_{ice}$), a correction is routinely applied for Δ_{age}. However, this correction introduces an uncertainty which limits the ability to resolve the detailed phasing between atmospheric composition and climate. Suggestions that deglacial warming in Antarctica preceded the atmospheric CO_2 increase by a few hundred years at the start of the last deglaciation (Fischer et al., 1999; Monnin et al., 2001) may have underestimated the uncertainty in Δ_{age}, whereas a more recent analysis with improved age constraints indicates that the onset of deglacial CO_2 and temperature change was synchronous within error (Parrenin et al., 2013). Most recently, using data from the

WAIS Divide Core (WDC), which benefits from high snow accumulation rates and a small Δ_{age} (~200-300 years), it has been suggested that atmospheric CO_2 changes may actually have slightly led the temperature changes for much of the deglaciation (Marcott et al., 2014).

Measurements of methane gas concentrations serve two additional purposes, beyond quantifying its role as a greenhouse gas. First, because changes in atmospheric methane concentrations are virtually synchronous across the globe, comparison of the methane signal allows for synchronisation of ice core age models between Greenland and Antarctica, which is crucial for evaluating the interhemispheric phasing of climate (Blunier and Brook, 2001; EPICA Community Members, 2006; WAIS Divide Project Members, 2015). In principle, a similar approach would be possible using CO_2 records, but the Greenland ice cores do not provide reliable CO_2 reconstructions due to in-situ production from chemical impurities. Second, since the atmospheric methane budget is believed to be dominated by Northern Hemisphere processes, methane records may provide markers within ice cores for rapid Northern Hemisphere climate changes (e.g. Dansgaard-Oeschger warming events). An interesting consequence is that measurements of methane and CO_2 on the same gas phase in an Antarctic ice core can be used to make a direct comparison (independent of uncertainty in Δ_{age}) between the timing of Northern Hemisphere processes (recorded by methane concentrations) and changes in the global carbon cycle (recorded by CO_2 concentrations) (Marcott et al., 2014).

Many other chemical constituents can also be measured in ice cores to provide proxy evidence on regional or global climate forcings and responses. Examples include past sea ice extent (recorded by sea-salt sodium fluxes, ssNa), dust deposition rates (recorded by non-sea-salt calcium fluxes, nssCa), and inputs of biological aerosols (e.g. methanesulphonate or sulphate) (Wolff et al., 2006). While providing highly valuable records, source and transport effects typically need to be considered for a full understanding of those proxies (Levine et al., 2014), and the relative role of these processes may differ between ice core locations and through time. To complement the dust records, measurements of radiogenic isotopes (e.g. neodymium, strontium, and lead) can be used to trace the dust source regions (Grousset and Biscaye, 2005; Aciego et al., 2009; Vallelonga et al., 2010) and therefore to evaluate changes in dust emission and/or atmospheric circulation patterns in the past. Similarly, records of volcanic eruptions can be obtained from tephra layers in ice, providing evidence on the volcanic forcing of climate (Sigl et al., 2015), as well as being a useful chronological tool for dating and correlating records (Narcisi et al., 2005; Hillenbrand et al., 2008; Parrenin et al., 2013; Turney et al., 2020).

11.2.1.3 Recent advances in ice core proxies and attempts to obtain ice older than one million years

Recent pioneering advances in generating climate records from Antarctic ice cores include the development of analytically challenging measurements on the gas bubbles and the recovery of ice older than ~800 ka. Isotopic measurements have previously been made on the oxygen gas ($\delta^{18}O_{air}$) to monitor changes in the atmospheric oxygen cycle, which is linked to variability in the global monsoon (Petit et al., 1999; Severinghaus et al., 2009). More recently, methods have been developed to measure carbon isotopes of the trace constituent CO_2 ($\delta^{13}C_{CO2}$), providing novel constraints on the sources and sinks of atmospheric CO_2 and new insights into the global carbon cycle (Bauska et al., 2016). Another pioneering development is the measurement of the krypton/nitrogen (Kr/N_2) ratio, which serves as a proxy for global mean ocean temperature because the solubility of each gas has a different temperature-dependence (Bereiter et al., 2018).

Whereas the existing East Antarctic ice cores provide a continuous climate record back to ~800 ka, a major long term goal is to obtain older records, in particular to resolve the nature and causes of the MPT at ~900 ka (Jouzel and Masson-Delmotte, 2010). One recent approach has involved drilling

horizontal blue-ice sections from marginal settings of the ice sheet where old ice upwells towards the surface. This method has obtained discontinuous snapshots of older ice from short intervals at ~1 Ma, ~1.5 Ma, and ~2 Ma (Higgins et al., 2015; Yan et al., 2019), providing new constraints on the carbon cycle-climate relationship before the MPT. However, those data remain challenging to interpret because they represent short time intervals and are subject to large dating uncertainties. To circumvent those issues, and to provide a continuous record through the MPT, a number of efforts are underway to obtain a deep Antarctic ice core that extends to ~1.5 Ma, which modelling studies suggest is a feasible goal (Fischer et al., 2013; Sutter et al., 2019). The 'Beyond EPICA' project proposed that a suitable site exists at Little Dome C near Concordia Station on the East Antarctic Plateau and drilling operations were set to begin in the 2020-2021 field season.

11.2.2 Deep-sea paleoceanographic records

Deep-sea sediment cores have been collected from throughout the global oceans and provide relatively continuous archives of past changes in ocean properties. Analyses on such cores have enabled reconstructions of many aspects of ocean chemistry, biology, and physics, from which changes in regional and global climate states and oceanic and atmospheric processes can be inferred. The general approach is well demonstrated by the series of international programmes that have used riserless drilling to recover long sediment cores from the seafloor, namely the Deep Sea Drilling Project (DSDP, 1968-1983), Ocean Drilling Program (ODP, 1983-2003), Integrated Ocean Drilling Program (IODP, 2003-2013), and International Ocean Discovery Program (IODP, 2013-2023). These programmes have been running for more than half a century and have facilitated many of the major advances made in the earth sciences over this interval, in particular in paleoceanography and paleoclimate. Since Pleistocene sediments are generally accessible to a wider range of drilling and coring approaches than sequences from older epochs, a large number of cores have also been collected during expeditions led by particular countries or institutes. These endeavours have typically provided records from the last deglaciation, but in some cases longer records have been recovered extending through multiple glacial-interglacial cycles.

11.2.2.1 Proxies for climate and ocean-atmosphere-ice sheet processes

By analysing the fossil and mineral contents, grain sizes, magnetic properties, and chemical and isotopic compositions of various fractions of the sediment, it is possible to recover both qualitative and quantitative evidence on a multitude of climate-relevant parameters. These parameters include global ice volume, deep-ocean temperatures, sea surface temperatures (SST), salinity, water mass sourcing, ocean current strength, biological productivity, nutrient utilisation, pH, carbonate ion concentration, nutrient content, iceberg rafting, sediment provenance, dust input, and sea ice extent. In general, observations and measurements on sediment cores provide 'proxies' for the parameter of interest, rather than enabling a direct reconstruction. Therefore, such proxies must be tested and calibrated using a combination of theoretical calculations, laboratory experiments, core-top calibrations, and numerical ocean modelling. General reviews of paleoceanographic approaches and proxies can be found in the literature (Henderson, 2002; Katz et al., 2010; Robinson and Siddall, 2012) and details of methodology and proxy developments are beyond the scope of this contribution. Here we restrict ourselves to listing a range of the most widely applied proxies, together with notes highlighting some important aspects of their application, and selected references to guide the reader towards pioneering studies and recent instructive updates (Table 11.1).

11.2.2.2 Pleistocene age models

In order to apply such proxy methods in the past, and to make comparisons between marine sediment cores and ice cores, it is necessary to generate age models that convert sediment core depths to calendar ages. For sediments of Pleistocene age, a wide range of approaches are possible and these techniques are often used in combination to achieve the most robust and/or highest resolution age model:

(i) Radiocarbon ($\Delta^{14}C$) dating of carbonate fossils or organic matter: This method provides absolute ages for individual sediment layers, subject to consideration of surface reservoir ages (Skinner et al., 2019) and conversion from radiocarbon years to calendar years (Reimer et al., 2013). Due to the short half-life of radiocarbon, this method is only applicable back to ~40 ka. In addition, bioturbation or reworking of microfossils and inputs of aged terrestrial organic carbon can present challenges, particularly on the Antarctic continental shelf (Anderson et al., 2014).

(ii) Correlation of carbonate $\delta^{18}O$ records to a benthic $\delta^{18}O$ stack: This method is routinely used where foraminiferal carbonate is available in a sediment core, but carbonate is sparse and typically absent from Southern Ocean and Antarctic margin sediments. In this region, other types of proxy records can be used for correlation with a benthic $\delta^{18}O$ stack, but this approach leads to greater uncertainties when assessing leads and lags with far-field records. Some caution is also needed because deep ocean $\delta^{18}O$ changes are not synchronous on millennial timescales (Skinner and Shackleton, 2005), while $\delta^{18}O$ stacks are typically constructed using orbital tuning with an assumed phase lag between insolation changes and the climate response (e.g. SPECMAP, Martinson et al., 1987; LR04, Lisiecki and Raymo, 2005).

(iii) Biostratigraphy using carbonate or siliceous microfossils and nannofossils: Although it usually provides lower resolution age constraints than the above two methods, diatom biostratigraphy is widely and effectively used in the Southern Ocean where carbonate is often absent (Gersonde and Barcena, 1998; Cody et al., 2012). However, it is limited by the need to assume linear sedimentation rates between datums that are often widely separated in time, and by the reworking processes that affect many depositional settings on the Antarctic shelf (McKay et al., 2019). A specific challenge for the late Pleistocene is the lack of species turnover events, with only 9 diatom events spanning the last 800 kyr (Cody et al., 2012), only one of which is a first appearance datum (FAD), whereas the majority are last appearance datums (LADs) that are susceptible to reworking.

(iv) Tephrostratigraphy: Discrete tephra layers in sediment cores can be identified from their mineralogy and geochemistry, providing a valuable tool for regional correlation and dating that is often used in combination with other approaches. In Antarctica, this approach is most promising in regions of active volcanism associated with the West Antarctic Rift system. For example, ^{40}Ar-^{39}Ar dating of tephra deposits provides absolute constraints for the development of Neogene chronologies in the Ross Sea (Naish et al., 2009). In addition, the recognition of distinct tephra or crypto-tephra layers can also enable correlation between Antarctic marine sediments and ice core records (Narcisi et al., 2005; Hillenbrand et al., 2008; Parrenin et al., 2013; Di Roberto et al., 2019; Turney et al., 2020).

(v) Magnetostratigraphy: Magnetic measurements are routinely conducted on cores during IODP expeditions, enabling precise stratigraphic alignment at major reversals (e.g. Brunhes-Matayama boundary; Bassinot et al., 1994) and coarse-scale interpolation in between, often assuming constant sedimentation rates. Additional approaches such as relative paleo-intensity are also being developed to provide finer resolution age models away from magnetic reversals (Laj et al., 2004).

(vi) Correlation to ice core records: In the North Atlantic region, high-resolution age models for glacial periods have been generated based on correlation of North Atlantic SST proxies to Greenland ice core climate records (Shackleton et al., 2000) or synthetic tuning targets (Barker et al., 2015), based on the assumption that rapid millennial climate events are effectively synchronous across the region. Although Pleistocene climate changes in the Southern Ocean were generally less abrupt than

in Greenland, SST records in South Atlantic and Southern Ocean cores typically show a strong similarity to Antarctic ice core temperatures on glacial-interglacial and millennial timescales, enabling the inter-comparison of marine and ice core records (Mortyn et al., 2003). The validity of transferring Antarctic ice core age scales to sediment cores in this way has recently been demonstrated (Hoffman et al., 2017). However, because of the assumption of synchronicity between these signals, caution is required when considering the relative phasing of climate events between marine and ice core records. In certain Southern Ocean settings, distinct glacial-interglacial and millennial timescale changes in dust inputs have also been inferred from proxies in marine sediment cores (e.g. iron content, leaf waxes, or magnetic susceptibility), enabling correlation to dust records in Antarctic ice cores (Pugh et al., 2009; Martinez-Garcia et al., 2011; Weber et al., 2012).

(vii) Correlations using sediment core properties: It is often possible to correlate between records from the same region where there is systematic climate-related variability in sediment properties such as carbonate percent, colour index, or magnetic susceptibility. This correlation can allow an age model to be transferred from a core with a well-established chronology and depositional model to another core that may have fewer age constraints.

11.2.2.3 Bioturbation and resolution

Unlike ice cores, sediment cores are generally subject to bioturbation, in which burrowing organisms living in oxic or sub-oxic conditions mix sediment components vertically over depths of up to tens of centimetres. Ocean sediments can also experience periods of erosion or non-deposition related to ocean current strength, sea level change, submarine channel activity, or iceberg scouring. In combination, bioturbation, hiatuses, and low or variable sedimentation rates limit the age resolution that is achievable in proxy records to typically a few hundred to a few thousand years. However, higher resolution paleoceanographic records can be obtained in settings with high accumulation rates, such as sediment drifts where sediment is locally focused, or highly productive regions with high biogenic particle fluxes. Nearshore sites with significant terrestrial inputs can also generate high resolution records, but much of the Antarctic continental shelf has been characterised by polar glacial regimes during the late Pleistocene that are sediment-starved due to limited discharge of turbid meltwater (McKay et al., 2009). An additional challenge in the cold, corrosive waters of the Southern Ocean arises from the poor preservation of carbonate microfossils, which can further limit sediment accumulation rates, age model resolution, and the range of proxy approaches available.

11.2.2.4 Deep-sea coral archives

Since they are not subject to bioturbation or highly variable sedimentation rates, deep-sea scleractinian corals have emerged as a promising archive that is suitable for absolute dating and the application of multiple geochemical tracers (Robinson et al., 2014). Measurements on fossil corals are particularly valuable in the Southern Ocean because it circumvents the challenges of carbonate dissolution and age model resolution that affect foraminifera-based proxies. As such, deep-sea corals have enabled glacial and deglacial reconstructions of Southern Ocean ventilation (radiocarbon; Burke and Robinson, 2012; Hines et al., 2015), water mass sourcing (neodymium isotopes; Robinson and van de Flierdt, 2009; Wilson et al., 2020), pH (boron isotopes; Rae et al., 2018), and surface nutrient utilisation (nitrogen isotopes; Wang et al., 2017). Future research in the Southern Ocean will be significantly enhanced by an increasing spatial and temporal coverage of deep-sea coral measurements and an expansion in the range of proxy measurements, as well as by integrating evidence from deep-sea corals with sediment and ice core records.

11.2.3 Ice-proximal sedimentary records

Globally-distributed sediment cores provide evidence on large scale changes in Earth's climate system, with reconstructions of global deep water chemistry being particularly informative on processes occurring in the polar regions where deep waters form (Lisiecki and Raymo, 2005; Gebbie and Huybers, 2011). However, a full understanding of Antarctic changes requires evidence from sites that are more proximal to the Antarctic Ice Sheet, for a number of reasons. First, because of the polar amplification of climate, a knowledge of globally-averaged temperatures is not sufficient for understanding the local climate forcing acting on the Antarctic Ice Sheet. Given the strong oceanic influences on ice sheet mass balance for Antarctica's marine-based ice sheets, records from both the surface and subsurface of the high latitude Southern Ocean are required. Second, changes in sea ice extent, biological productivity, and sub-surface water mass properties can vary spatially over short distances, such as across Southern Ocean fronts, which necessitates an array of well-distributed local records. Third, and crucially for reconstructing past changes in ice sheet behaviour, local records of iceberg rafted debris (IRD), sediment provenance, and sedimentary signatures of glacial grounding can be obtained. Since each catchment of the Antarctic Ice Sheet likely has a different sensitivity to climate and ocean forcing (Golledge et al., 2017), reconstructions of past ice sheet behaviour and proximal ocean dynamics need to be made on a sector-by-sector basis.

Proximal sites include the Antarctic continental shelves, the nearby continental rise, and the deep ocean. Records from shelf sites provide the only way to obtain direct evidence on past changes in ice sheet extent, based on the evidence of subglacial versus open marine sedimentation (McKay et al., 2012b; Smith et al., 2019) or the erosion and deformation signatures produced by ice grounding (Domack et al., 1999; McKay et al., 2012b; Reinardy et al., 2015). However, these settings are often characterised by discontinuous records with low sedimentation rates, poor core recovery, and significant erosional hiatuses due to glacial over-riding, making them difficult to date. Conventional dating tools using foraminiferal $\delta^{18}O$ or SST reconstructions are rarely available, and dating is generally achieved at a coarse resolution using magnetostratigraphy, biostratigraphy, and tephrostratigraphy, as well as radiocarbon where possible.

Where foraminifera are present at shelf sites, radiocarbon-based approaches are viable to generate age models covering the last ~40 kyr, but such records are rare (e.g. Mackintosh et al., 2011; McKay et al., 2016; Hillenbrand et al., 2017; Bart et al., 2018). Many studies rely on radiocarbon dating of bulk organic matter or its acid-insoluble fraction, but in shelf settings characterised by low sedimentation rates and extensive glacial reworking of pre-LGM deposits, such measurements are usually compromised by the presence of reworked fossil carbon leading to anomalously old ages (Anderson et al., 2014). However, novel approaches are being developed to overcome the influence of such contamination, including ramped pyrolysis (Rosenheim et al., 2013) and compound-specific analyses (Ohkouchi et al., 2003), which attempt to extract the youngest populations of organic carbon present in the sediment. In the Ross Sea, recent studies have observed in-situ calcareous foraminifera in certain sub-ice-shelf and grounding-line-proximal settings (Bart et al., 2016), which has provided better radiocarbon constraints for records of the last deglaciation (Bart et al., 2018), as well as enabling more robust radiocarbon age models to be developed based on a combination of bulk, compound-specific, and foraminiferal analyses (Prothro et al., 2020).

On the continental rise and in the deep ocean, depositional settings with more continuous sedimentation are more common, allowing the recovery of longer records with fewer (if any) erosional hiatuses that are more suitable for dating. While the general lack of carbonate sediments restricts conventional $\delta^{18}O$-based approaches in much of the Southern Ocean, methods including magnetostratigraphy, biostratigraphy, and cyclostratigraphy are generally applicable. In specific settings, these methods may be supplemented by correlating proxy records for dust with Antarctic ice core records (Pugh et al., 2009), or by assuming a link between biological productivity and glacial-interglacial climate state (Bonn et al., 1998; Hillenbrand et al., 2009; Wu et al., 2017). Although the

continental rise is typically located hundreds or thousands of kilometres from ice sheet margins (Figure 11.2), sediment sequences recovered from levees on the banks of canyons influenced by turbidity currents have proven to be a valuable archive of orbital-scale continental margin processes (Escutia et al., 2011; Wilson et al., 2018). Aspects of past ice sheet behaviour are recorded by proxies including IRD fluxes (Patterson et al., 2014; Weber et al., 2014; Wilson et al., 2018; Wu et al., 2021) and mineralogical or geochemical provenance signatures of the sediments (Farmer et al., 2006; Roy et al., 2007; Hillenbrand et al., 2009; Licht and Hemming, 2017; Wilson et al., 2018; Wu et al., 2021). Records of IRD indicate the presence of ice grounded at sea level, and can be used to infer dynamic ice margin behaviour. However, it is important to emphasise that IRD accumulation rates are not simply related to ice volume (or to changes in ice volume), since they are also influenced by the original sediment content of the ice, variability in the loss of basal sediment during ice shelf and iceberg transport (Clark and Pisias, 2000; Smith et al., 2019), and ocean temperatures and ocean currents which determine the locus of deposition (Cook et al., 2014; Licht and Hemming, 2017). Provenance of the fine-grained or bulk sediment provides information about the source rocks undergoing subglacial erosion on the proximal continent (Roy et al., 2007), and can therefore be used to infer changes in erosional sources linked to past ice sheet extent (Wilson et al., 2018) or to indicate sediment transport pathways (Simões Pereira et al., 2018). The other advantage of records from such offshore settings is that they are usually well-located to provide complementary evidence (often in the same samples) on paleoceanographic and climate changes, enabling records of ice sheet behaviour to be integrated with regional and global climate forcings and effects.

11.3 Records of global and Southern Ocean climate during the Pleistocene

In this section we present a compilation of key records of global and Southern Ocean climate, derived from sediment cores and ice cores over the last 800 kyr (Figure 11.3) and from sediment cores over the last 3 Myr (Figure 11.4). Lisiecki and Raymo (2005) combined benthic foraminiferal $\delta^{18}O$ records from 57 globally-distributed sites to generate a Plio-Pleistocene reference curve (the "LR04 stack") that reflects a combination of deep ocean temperature and ice volume. The LR04 stack indicates glacial-interglacial cycles in global climate superimposed on a progressive cooling during the Pleistocene, which was mostly expressed in more extreme glacial conditions (Figure 11.4g). The stack also demonstrates two major climate shifts (Lisiecki and Raymo, 2005): a switch in cyclicity from dominantly ~41 kyr to ~100 kyr cycles at the MPT (~900 ka, yellow bar in Figure 11.4), and an increase in interglacial intensity since the Mid Brunhes Event (MBE, ~430 ka, yellow bar in Figure 11.3) (Jansen et al., 1986).

11.3.1 Global sea level

While the LR04 stack provides an excellent stratigraphic tool for the Pleistocene (Lisiecki and Raymo, 2005), it is influenced by changes in both global ice volume and deep ocean temperatures (Shackleton, 2000), and their relative contributions to that record have varied through time (Elderfield et al., 2012). By combining records of benthic foraminiferal $\delta^{18}O$ and Mg/Ca ratios in the same sediment core, the $\delta^{18}O$ signal can be deconvolved into separate deep ocean temperature and "ice volume" components (Sosdian and Rosenthal, 2009; Elderfield et al., 2012) (Figure 11.3b, light blue line). However, converting the ice volume component in an individual record into a global ice volume or sea level record is complicated by local hydrographic (salinity) changes and also requires assumptions about the $\delta^{18}O$ compositions of past ice sheets (Jakob et al., 2020). A similar deconvolution approach has been proposed using a global compilation of planktonic $\delta^{18}O$ records and SST estimates (Shakun et al., 2015), while other methods have included scaling benthic $\delta^{18}O$

records to coral-derived sea levels for the last deglaciation (Waelbroeck et al., 2002) or combining benthic $\delta^{18}O$ data with ice sheet modelling (Bintanja et al., 2005). An alternative approach for generating continuous sea level reconstructions has exploited planktonic foraminiferal $\delta^{18}O$ records from the Red Sea (Rohling et al., 2004; Grant et al., 2014) and the Mediterranean Sea (Rohling et al., 2014), by modelling the hydrographic response of these restricted basins to eustatic sea level change and local isostatic adjustments. The Red Sea record provides a sea level reconstruction back to ~500 ka (Grant et al., 2014) (Figure 11.3b, solid blue line), while the Mediterranean Sea record extends back into the Pliocene (Figure 11.3b and Figure 11.4a, dashed blue line), although with larger uncertainties for the earlier section (Rohling et al., 2014). A recent statistical approach has combined a number of the above records with other similar ones to provide a late Pleistocene sea level stack for the last ~800 kyr (Spratt and Lisiecki, 2016) (Figure 11.3a).

The above methods largely agree on the scale of the late Pleistocene sea level changes (Figure 11.3a,b), indicating glacial-interglacial fluctuations of up to ~130 m since the MBE, with smaller changes both before the MBE and during the Marine Isotope Stage (MIS) 10-9 and MIS 8-7 transitions. However, the individual records are subject to quite large uncertainties (e.g. compare the two records in Figure 11.3b), and a statistical treatment indicates uncertainties of 9-12 m (1σ) for the sea level stack (Spratt and Lisiecki, 2016) (Figure 11.3a). Therefore, while these approaches provide valuable evidence on global sea level change through the late Pleistocene on orbital timescales, they are not well suited for resolving changes in Antarctic ice volume, which are expected to represent only ~10 % of the global sea level signal during this interval (Tigchelaar et al., 2018). A particular issue here is that coral-based reconstructions indicate peak sea levels higher than the Holocene for certain recent interglacials (e.g. 6-9 m during MIS 5e (~116-129 ka), 6-13 m during MIS 11; Dutton et al., 2015), which would implicate ice loss from the Antarctic Ice Sheet, but this magnitude of past sea level variability is not resolvable in the marine proxy records given their uncertainties. It is also important to note that the sea level estimates from sediment cores provide a globally-integrated measure of ice volume, and cannot identify the locations where ice volume changes occurred, or the phasing of ice sheet advance and retreat between hemispheres. Therefore, while Elderfield et al. (2012) suggested that an expansion of global ice volume at ~900 ka during the MPT (Figure 11.4b) may have included a significant Antarctic contribution, direct evidence is needed to test the location of this ice growth.

11.3.2 Sea surface temperatures

In terms of Earth's surface climate, the best global coverage of past changes is derived from proxy-based SST reconstructions in widely-distributed marine cores. The construction of a stack from these records minimises the effects of local changes in ocean currents or frontal positions, as well as proxy uncertainties, and enhances the signal/noise ratio to produce a meaningful global reconstruction. A global alkenone-based SST stack based on 10 high-resolution Pleistocene records (Martínez-Botí et al., 2015a) indicates glacial-interglacial changes of ~3-4 °C in the late Pleistocene since the MBE (Figure 11.3c, black line), ~2-3 °C before the MBE, and ~1-2 °C in the early Pleistocene (Figure 11.4c, black line). In addition, a multi-proxy compilation of over 20,000 SST data points (including alkenones, Mg/Ca, and foraminiferal and radiolarian transfer functions) from 59 marine cores was used to generate a 2 Myr long record of global average surface temperature (GAST) by spatially weighting the SST data in latitudinal bands and converting to GAST using a climate model (Snyder, 2016). This reconstruction indicates glacial-interglacial GAST changes of ~5-6 °C in the late Pleistocene since the MBE (Figure 11.3c, dashed black line), compared to ~4-5 °C in the interval preceding the MBE, and ~2-3 °C in the earlier Pleistocene (1.2-2.0 Ma) (Figure 11.4d, dashed black line). Note that the larger changes in GAST than in SST reconstructions arise because larger temperature changes occur over land than over the ocean.

We plot three individual alkenone-based SST records to demonstrate changes in different regions of the Southern Ocean. Two records are from the Subantarctic Zone, in the South Atlantic (PS2489-2/ODP Site 1090; Martinez-Garcia et al., 2010) and the Southeast Pacific (PS75/34-2; Ho et al., 2012). The third record is from the Subtropical Zone, just north of the modern Subtropical Front, in the Tasman Sea (DSDP Site 593; McClymont et al., 2016). These records all demonstrate glacial cooling, resulting from a combination of global cooling, polar amplification, and shifts in Southern Ocean fronts. The magnitude of glacial-interglacial temperature changes in the subantarctic South Atlantic and Southeast Pacific Ocean were very similar, with both recording glacial cooling of ~6-8 °C since the MBE in comparison to glacial cooling of ~4-6 °C in the interval immediately before it (Martinez-Garcia et al., 2009; Ho et al., 2012) (Figure 11.3d). These results are also in good agreement with subantarctic South Atlantic estimates from foraminiferal transfer functions over the last 550 kyr (Becquey and Gersonde, 2003). For the Tasman Sea, which today is influenced by subtropical waters, the late Pleistocene glacial-interglacial changes were slightly larger at ~8-10 °C, suggesting northward glacial shifts of the Subtropical Front (McClymont et al., 2016), with no distinct change at the MBE (Figure 11.3d). In both subantarctic and subtropical settings, the glacial-interglacial variability during the early Pleistocene was muted compared to the late Pleistocene (Figure 11.4d), being ~2-4 °C in the subantarctic South Atlantic (Martinez-Garcia et al., 2010) and ~4-5 °C in the Tasman Sea (McClymont et al., 2016).

11.3.3 Intermediate and deep ocean temperatures

Antarctic Intermediate Water (AAIW) forms today in the vicinity of the Subantarctic Front and propagates northwards at intermediate depths into each ocean basin. Therefore, a record of its changing properties reflects changes in surface conditions in the Subantarctic Zone of the Southern Ocean and/or changes in the location or mode of AAIW formation. Benthic foraminiferal Mg/Ca measurements at DSDP Site 593 in the Tasman Sea have been used to establish AAIW temperatures through the Pleistocene (McClymont et al., 2016). Glacial-interglacial variability in AAIW temperature was ~3-4 °C since the MPT and ~3 °C during the early Pleistocene, superimposed on a long term cooling trend since ~1.3 Ma (Figure 11.4e). Note that the trends in the Pliocene and early Pleistocene intervals of that record are sensitive to poorly constrained seawater Mg/Ca ratios for that time, but the mid to late Pleistocene cooling is a robust feature (McClymont et al., 2016).

A large proportion of the global deep ocean is filled by deep waters that form in the Antarctic Zone of the high latitude Southern Ocean i.e. Antarctic Bottom Water (AABW) and Lower Circumpolar Deep Water (LCDW) (Gebbie and Huybers, 2011). Therefore, past deep water temperatures reflect conditions in the regions of deep water formation near Antarctica. At ODP Site 1123, benthic foraminiferal Mg/Ca ratios provide a record of past LCDW temperatures in the pathway of the largest inflow of Antarctic-sourced deep waters into the Pacific Ocean. At this site, glacial temperatures have persistently been -1 to -2 °C (i.e. close to the freezing point of seawater) for the past ~1.5 Myr (Figure 11.4f) (Elderfield et al., 2012). Before the MBE, interglacial temperatures were ~1-2 °C and glacial-interglacial variability was ~2-3 °C, whereas since the MBE there have been slightly higher interglacial peak temperatures (~2-3 °C) and enhanced glacial-interglacial variability (~3-4 °C) (Figure 11.3e).

11.3.4 Antarctic temperatures and atmospheric CO_2

Antarctic air temperature reconstructions for the last 800 kyr based on ice core δD_{ice} indicate a distinct ~100 kyr cyclicity and a sawtooth pattern of slow stepped cooling and rapid warming that mirrors the LR04 benthic $\delta^{18}O$ stack (Figure 11.1). Late Pleistocene glacial-interglacial variations were ~10-12 °C since the MBE, compared to ~7-8 °C before the MBE (Figure 11.3g). This difference arose mostly as a result of the significantly cooler 'lukewarm' interglacials that preceded the MBE, whereas

glacial temperatures changed by only ~1 °C across the MBE (Jouzel et al., 2007). In comparison to estimates of GAST, Antarctica experienced polar amplification of around 1.6 times (2σ range of 1.2 to 2.3 times) in the late Pleistocene (Snyder, 2016). It is also important to note that peak Antarctic temperatures during the last four interglacials (MIS 5e, MIS 7, MIS 9, and MIS 11) were warmer than the Holocene by 2-4 °C for a few thousand years (Jouzel et al., 2007) (Figure 11.3g).

Atmospheric CO_2 concentrations from a compilation of Antarctic ice core records (Bereiter et al., 2015) demonstrate a very close link to Antarctic temperature variations. Since the MBE, glacial-interglacial variability in atmospheric CO_2 concentrations has averaged ~90 ppm, fluctuating between ~180-190 ppm during glacial periods and ~270-290 ppm during interglacials (Figure 11.3h). Before the MBE, the glacial-interglacial variability was smaller (~60-70 ppm), with glacial CO_2 levels similar to the more recent glacials (~170-190 ppm) while interglacial CO_2 levels were lower (peaks of ~240-260 ppm) (Figure 11.3h). Beyond the ice core record, atmospheric CO_2 reconstructions for the early Pleistocene are based on foraminiferal boron isotope records (Figure 11.4h), which have larger uncertainties but appear to indicate slightly higher glacial CO_2 concentrations before the MPT (Chalk et al., 2017), as well as a decline in CO_2 concentrations since the late Pliocene and earliest Pleistocene (Martínez-Botí et al., 2015a).

11.3.5 Sea ice extent and dust supply

Other processes in the Southern Ocean region also varied on a ~100 kyr timescale, although sometimes with different magnitudes or timing within a glacial cycle. Reconstructions of Southern Ocean sea ice extent based on ice-core ssNa content (Wolff et al., 2006) indicate initial expansions in sea ice at the onset of glaciation (e.g. MIS 5e to MIS 5d transition), with further enhancements towards maximum sea ice extent during full glacials (e.g. MIS 4) and glacial maxima (e.g. MIS 2) (Figure 11.3f). Although quantitative interpretation of the ssNa proxy faces some challenges, ssNa fluxes vary by up to a factor of four and show a striking similarity to Antarctic temperature records (Figure 11.3f cf. Figure 11.3g). Interglacials prior to the MBE experienced higher ssNa than more recent interglacials (Figure 11.3f), suggesting that interglacial sea ice retreat was more muted during the lukewarm interglacials before the MBE.

Atmospheric dust supply to the Antarctic region is recorded in ice cores by non sea-salt calcium fluxes (nssCa) (Wolff et al., 2006), which vary by a factor of ~20 through glacial cycles (Figure 11.3i), in a similar pattern to iron fluxes. Glacial periods were characterised by an increased dust supply that was particularly pronounced during glacial maxima (Figure 11.3i). While changes in atmospheric transport to Antarctica may influence dust fluxes, the temporal patterns are well reproduced in dust flux records from Southern Ocean marine cores, such as ODP Site 1090 in the Subantarctic Zone of the South Atlantic (Martinez-Garcia et al., 2011) (Figure 11.3j, brown) and PS75/076-2 in the South Pacific (Figure 11.3j, orange), albeit with smaller relative glacial-interglacial changes. In combination with grain-size evidence for minimal variations in the wind-driven Antarctic Circumpolar Current during the LGM and Holocene (McCave et al., 2013), the agreement among these dust records suggests that a major part of the signal was due to changes in continental aridity, local wind strength, or shelf exposure in the Southern Hemisphere dust source regions (e.g. Patagonia). Whereas highly-resolved sea ice reconstructions are lacking beyond the oldest ice core record at ~800 ka, high resolution marine records provide dust reconstructions for the entire Pleistocene and indicate an approximate doubling of glacial dust fluxes to the Southern Ocean at the MPT (Martinez-Garcia et al., 2011) (Figure 11.4i).

11.4 Late Pleistocene carbon cycle and climate dynamics

11.4.1 Controls on glacial-interglacial atmospheric CO_2

Changes in the carbon cycle were a fundamental feature of late Pleistocene glacial-interglacial cycles (Figure 11.3) and were crucial for translating orbital forcing into changes in Earth's energy balance and mean global temperature. While colder ocean temperatures during glacial periods (Figure 11.3c-e) would have directly enhanced oceanic uptake of CO_2 due to its greater solubility in cold water, thereby creating a positive feedback loop, the effect of these changes was modest in comparison to the full magnitude of glacial-interglacial atmospheric CO_2 changes (Sigman and Boyle, 2000). Furthermore, this temperature effect was almost cancelled out by opposing effects from reduced carbon storage in a saltier glacial ocean and the reduced size of the terrestrial biosphere (Sigman and Boyle, 2000). Therefore, more active mechanisms of carbon storage must have been operating to explain the consistent ~90 ppm decrease in atmospheric CO_2 during each glacial period since the MBE (Figure 11.3h).

Because the deep ocean contains approximately 60 times more carbon than the atmosphere, it has been recognised for some time that carbon storage in the deep ocean was probably key to explaining these atmospheric CO_2 variations. Various mechanisms were proposed involving changes in deep ocean circulation, ocean nutrient inventories, marine productivity, and alkalinity (Boyle, 1988b; Broecker and Denton, 1989; Martin, 1990; Rickaby et al., 2010). Much of the early focus was on global ocean nutrient chemistry and North Atlantic Deep Water (NADW) formation, whereas more recently there has been a shift towards Southern Ocean carbon cycle mechanisms (Sigman and Boyle, 2000; Sigman et al., 2010). A significant role for processes in this region is supported by the close correlation between Antarctic temperatures and atmospheric CO_2 during the last deglaciation (Monnin et al., 2001; Parrenin et al., 2013) and throughout the last 800 kyr (Jouzel et al., 2007; Luthi et al., 2008; Bereiter et al., 2015) (Figure 11.1). Since the temporal evolution of Antarctic temperature differed from Northern Hemisphere temperatures, this powerful observation has driven a search for theories and data to constrain the role of Antarctic and Southern Ocean processes in the global carbon cycle.

11.4.2 Southern Ocean mechanisms based on sea ice, ocean circulation, and deep stratification

An important role for Southern Ocean circulation in the glacial-interglacial carbon cycle was proposed by Toggweiler (1999), who suggested that changes in the strength and/or position of the Southern Hemisphere westerly winds could determine the structure of the overturning circulation and hence its capacity to store carbon (Toggweiler et al., 2006; Menviel et al., 2018). In simple terms, equatorward shifts in the westerly winds during glacial periods could weaken the wind forcing over the Antarctic Circumpolar Current, leading to reduced Southern Ocean upwelling and weaker overturning. This scenario would decrease CO_2 release to the atmosphere through the Southern Ocean surface (i.e. reduced upwelling), and simultaneously increase carbon storage in the deep ocean through the combination of the low-latitude biological pump and a longer water residence time in the deep ocean (i.e. reduced overturning). The glacial expansion of sea ice in response to high-latitude cooling was proposed as an additional driver of deep ocean carbon storage, since it would restrict gas exchange between upwelling Southern Ocean deep waters and the atmosphere (Elderfield and Rickaby, 2000; Keeling and Stephens, 2001).

More recently, the magnitude of the wind-driven mechanism proposed by Toggweiler (1999) has been challenged because eddy compensation in the Antarctic Circumpolar Current weakens the link between wind strength and Southern Ocean upwelling (Farneti et al., 2010). However, while our detailed understanding has evolved since the original hypothesis, the general concept remains influential, and a related idea has emerged that combines aspects of both the ventilation and sea ice

mechanisms. Specifically, it has been proposed that changes in sea ice extent in the Southern Ocean control the surface ocean buoyancy forcing and hence the global deep ocean circulation structure (Adkins, 2013; Ferrari et al., 2014; Watson et al., 2015). The glacial expansion of sea ice would shoal the boundary between northern-sourced (NADW) and underlying southern-sourced (AABW) water masses, effectively increasing the volume of the deep overturning cell (Figure 11.5). In addition, a shoaled boundary would occupy a water depth where there is less rough seafloor bathymetry and significantly weaker vertical mixing, leading to reduced mixing between the two cells and increased deep stratification (Figure 11.5). This scenario would significantly enhance the capacity for glacial carbon storage in the deep overturning cell (Brovkin et al., 2007; Lund et al., 2011; Ferrari et al., 2014; Watson et al., 2015; Marzocchi and Jansen, 2019; Stein et al., 2020).

Observations consistent with those ideas include the enhanced salinity of glacial southern-sourced deep waters based on pore water chlorinity profiles (Adkins et al., 2002), increased glacial deep ocean stratification inferred from benthic foraminiferal carbon isotopes ($\delta^{13}C$) (Hodell et al., 2003; Curry and Oppo, 2005), increased glacial density stratification derived from $\delta^{18}O$ gradients (Lund et al., 2011), and restriction of NADW from the lower overturning cell inferred from neodymium isotopes (Wilson et al., 2020). There is also strong evidence from sediment cores and deep-sea corals to support enhanced carbon storage in a more isolated glacial deep ocean and rapid carbon release during the deglaciation, which is derived from radiocarbon (Skinner et al., 2010; Burke and Robinson, 2012; Skinner et al., 2017), boron isotopes (Martínez-Botí et al., 2015b; Rae et al., 2018), and oxygenation proxies (Jaccard et al., 2016; Anderson et al., 2019). These changes in ocean carbon storage and the associated changes in tracer distributions are also supported by recent ocean modelling studies (Mariotti et al., 2016; Menviel et al., 2018).

Perhaps the biggest challenge in testing the finer details of these sea ice-based mechanisms arises from the difficulty in obtaining direct evidence on past sea ice processes and areal extent. Estimates of circum-Antarctic sea ice extent for the LGM are predominantly based on diatom and radiolarian transfer functions (Gersonde et al., 2005), which indicate a doubling of the modern area of winter sea ice and a northward shift of ~5-10 degrees in the winter sea ice edge in the Indian and Atlantic sectors. Recent studies have improved constraints on the Pacific sector at the LGM, supporting a northward shift of ~5 degrees latitude in the winter sea ice extent (Benz et al., 2016), and provide a clearer view on deglacial changes in the Atlantic sector (Xiao et al., 2016). However, past sea ice extent in some regions, such as the Pacific entrance to the Drake Passage, remains poorly constrained. Beyond reconstructing winter sea ice extent, it is challenging to obtain a more holistic view of past sea ice behaviour, although the distributions of organic biomarkers such as highly branched isoprenoids (HBIs) may provide complementary evidence on summer sea ice extent and seasonality (Collins et al., 2013), which appears to have been enhanced during the LGM (Green et al., 2020). Such evidence will be essential for distinguishing between different sea ice-based processes that control the deep ocean structure, because some mechanisms are based on changes in the summer sea ice position (Ferrari et al., 2014) whereas others are sensitive to sea ice formation rates (Nadeau et al., 2019).

For a full understanding of ocean-atmosphere-climate interactions in the Southern Ocean, it is also important to establish the exact timing of past sea ice changes, particularly during transitions such as the last deglaciation. Challenges arise from age model uncertainties and the limited latitudinal distribution of sediment cores, although sea ice records have been recovered from all the major ocean basins, including the Atlantic (Shemesh et al., 2002; Allen et al., 2005; Collins et al., 2012; Xiao et al., 2016), Indian (Crosta et al., 2004; Xiao et al., 2016), and Pacific Oceans (Ferry et al., 2015). A complimentary approach, with potential to provide highly-resolved records of past changes, is based on sea ice proxies such as ssNa in ice cores (Wolff et al., 2006). While atmospheric transport is a major control on ssNa input to Antarctic ice core sites on interannual timescales, ssNa levels over

geological timescales appear to be linked to sea ice extent because the sea ice surface is the major source of ssNa (Levine et al., 2014). Despite uncertainties arising from transport processes, records of ssNa and methane sulphonic acid (MSA) (Abram et al., 2013) appear to be useful semi-quantitative proxies for past sea ice extent, and are particularly useful for recording the timing of rapid sea ice changes. Future observational and modelling studies will be important for translating ice core ssNa and MSA records into a more quantitative understanding of past sea ice behaviour. Better sea ice implementation in ocean and climate models is also required, since the existing models give widely different results and struggle to reproduce a sea ice field for the LGM that is consistent with data constraints (Roche et al., 2012), although that situation is improving (Green et al., 2020). A related challenge arises from modelling bottom water formation around Antarctica, specifically the contribution of dense shelf water production to AABW (Snow et al., 2016), because this process is not included in most current climate models.

11.4.3 Southern Ocean mechanisms based on dust supply, productivity, and nutrient utilisation

The other major way in which Southern Ocean processes could influence the global carbon cycle is through changes in surface ocean productivity. The high-latitude Southern Ocean is presently a high-nutrient low-chlorophyll area, where iron and possibly other micronutrients limit biological productivity (Martin, 1990). In the modern (interglacial) ocean, nutrients in this region are not fully utilised, which leads to a leak in the biological pump. Upwelling deep waters release regenerated CO_2 to the atmosphere, while the subduction of water masses with high preformed nutrient levels reduces the efficiency of carbon sequestration for a given global ocean nutrient inventory (and for a given ocean circulation structure and strength) (Sigman et al., 2010). Recognising this scenario for the modern day led to the “iron hypothesis”, in which it was proposed that increased glacial dust supply to this region could have provided the missing dissolved iron, thereby enhancing Southern Ocean productivity and nutrient utilisation, and increasing glacial carbon storage in the deep ocean (Martin, 1990).

Antarctic ice core records provide a test for the iron hypothesis because dust fluxes can be inferred from nssCa fluxes (Wolff et al., 2006; Lambert et al., 2008). Those records support a major increase in dust supply from Patagonia during glacial periods (Figure 11.3i), although with the caveat that dust transport to Antarctic ice cores may have differed from dust transport to the Southern Ocean. Evidence that this signal is broadly representative of dust input to the Southern Ocean is found in dust records from marine cores (Figure 11.3j), which indicate glacial increases in dust fluxes by a factor of 5-10 at ODP Site 1090 in the Subantarctic Zone of the South Atlantic Ocean (Martinez-Garcia et al., 2011), and by a factor of ~3 at a number of sites in the South Pacific sector of the Southern Ocean (Lamy et al., 2014). Complementary studies have confirmed the carbon cycle impact of this mechanism, by demonstrating that increased dust fluxes led to both increased productivity (from alkenone fluxes) and increased nutrient utilisation (from foraminiferal nitrogen isotopes) in the Subantarctic Zone (Martinez-Garcia et al., 2014). A recent compilation of dust records indicates that the dust signal was circumpolar in extent, but also highlights the potential for spatial differences in carbon sequestration linked to geographical variations in dust fluxes and the effect of frontal shifts on nutrient supply (Thöle et al., 2019).

The Subantarctic Zone was probably the key region where increased dust fluxes could have enhanced glacial carbon sequestration, because increased sea ice coverage, reduced upwelling, and increased near-surface stratification in the Antarctic Zone probably reduced the importance of this latter region for carbon exchange during glacial periods. Indeed, glacial increases in Antarctic Zone nutrient utilisation (diatom nitrogen isotopes) coincided with reduced productivity (opal and barium proxies) for at least the last two glacial cycles (Francois et al., 1997; Studer et al., 2015), which can

only be reconciled by a reduction in nutrient supply from below. However, a full mechanistic understanding of the changes in upwelling, near-surface stratification, nutrient supply, iron fertilisation, and export productivity across all sectors of the Antarctic and Subantarctic Zones is yet to be established. The challenge in establishing a full Southern Ocean carbon budget is complex because of the interactions between each of these regions, but modelling studies generally agree that subantarctic iron fertilisation could cause a decline in glacial atmospheric CO_2 of ~30-40 ppm (Brovkin et al., 2007; Hain et al., 2010).

In marine records, it is possible to take a further step in assessing the influence of iron fertilisation on the carbon cycle because multiple proxies can be used to simultaneously trace not only dust input and marine export productivity, but also the effect on bottom water (or pore water) carbon chemistry and oxygen content (Gottschalk et al., 2016; Jaccard et al., 2016). As a result, it may be possible to separate changes in deep ocean carbon storage that occurred due to productivity variations (predominantly in the Subantarctic Zone) from changes that were linked to stratification and deep ocean ventilation (predominantly in the Antarctic Zone). Evidently, both mechanisms are required to explain CO_2 changes through glacial-interglacial cycles (Jaccard et al., 2013; Jaccard et al., 2016), and they likely also played a role in carbon cycle dynamics on millennial timescales (Gottschalk et al., 2016; Jaccard et al., 2016).

11.4.4 Sequence of changes through the last glacial cycle

Explaining glacial-interglacial cycles in terms of changes in the atmospheric CO_2 budget between glacial and interglacial states is not sufficient for a full understanding of how the Earth's climate system operated. In addition, transient events must be studied to address questions such as what triggered glaciation or deglaciation, what feedbacks were operating, and how fast these feedbacks acted. Ongoing efforts are seeking to refine proxies and age models, to generate high resolution paleo-records, and to integrate them with modelling approaches to delve into the mechanisms.

Here we summarise such efforts to constrain the sequence and timing of changes that operated in the progression towards full glaciation, drawing heavily on a recent compilation of regional SST records and other proxy reconstructions for the last glacial cycle (Kohfeld and Chase, 2017) (Figure 11.6). Early in the glacial cycle, at the MIS 5e to MIS 5d transition, both hemispheres experienced SST changes that were largest at high latitudes and probably linked to a major decline in summer insolation forcing (Kohfeld and Chase, 2017). The direct effect of cooling would only have been a modest CO_2 drawdown due to the solubility effect, but the indirect effects were larger. Antarctic ice core ssNa records indicate an expansion of winter sea ice at this time (Wolff et al., 2006), although marine diatom records indicate that the sea ice expansion was moderate and spatially variable (Figure 11.6). These changes were accompanied by increased nutrient utilisation in the Antarctic Zone (Studer et al., 2015) (Figure 11.6), probably because near-surface stratification caused by seasonal melting of sea ice led to a restricted supply of nutrients from below. Together, the cooling, sea ice expansion, and increased surface stratification would have restricted carbon release to the atmosphere and increased deep ocean carbon storage (Keeling and Stephens, 2001; Sigman et al., 2010), helping to explain the ~35 ppm drop in atmospheric CO_2.

At the MIS 5 to MIS 4 transition, there was further global cooling, leading to average SST ~3 °C cooler than during interglacials, with the most pronounced changes at high latitudes (Kohfeld and Chase, 2017). It was accompanied by Antarctic sea ice expansion (Figure 11.6) and major changes in ocean circulation, as recorded by benthic $\delta^{13}C$ (Oliver et al., 2010) and neodymium isotope records (Piotrowski et al., 2005; Wilson et al., 2015) (Figure 11.6). These circulation changes could have arisen directly from polar cooling and sea ice expansion (Ferrari et al., 2014) (Figure 11.5), with an additional potential influence from AABW formation by brine rejection (Bouttes et al., 2010; Adkins,

2013). Dust fluxes increased significantly at the MIS 5 to MIS 4 transition, as recorded in ice cores (Wolff et al., 2006; Lambert et al., 2008) (Figure 11.6) and Southern Ocean sediment cores (Martinez-Garcia et al., 2009; Martinez-Garcia et al., 2014) (Figure 11.3j), indicating that increased nutrient utilisation by iron fertilisation of the Subantarctic Zone was restricted to this later step. Hence, a combination of sea ice expansion, ocean circulation changes, and iron fertilisation could explain the ~40 ppm drop in atmospheric CO_2. Modelling studies also suggest that the switch in deep ocean structure could have magnified the CO_2 drawdown effect of the polar surface ocean stratification and sea ice changes that emerged in MIS 5d (Hain et al., 2010), leading to additional carbon storage at this time.

After increases in atmospheric CO_2 of ~20-30 ppm during MIS 3, the lowest glacial CO_2 values were reached during MIS 2. Many of the proxies that changed during the MIS 5 to MIS 4 transition reached their most extreme values at the LGM (Figure 11.6), indicating maximum contributions to carbon drawdown from high latitude temperatures, ocean circulation, and iron fertilisation of the Subantarctic Zone.

11.4.5 Millennial climate variability and the bipolar seesaw

Glacial climates were also highly variable on sub-orbital timescales, and here we discuss some of the records of those changes and the mechanisms responsible. Early evidence for millennial and sub-millennial climate change in the North Atlantic region during the last glacial period and deglaciation was provided by Greenland ice core $\delta^{18}O_{ice}$ records (Dansgaard et al., 1993). Rapid fluctuations of more than 10 °C between cold stadial and warm interstadial intervals were termed Dansgaard-Oeschger events (Figure 11.7; Figure 11.8a), which were also observed in reconstructions of regional North Atlantic climate (Figure 11.8b) and IRD input to the oceans (Bond et al., 1997; McManus et al., 1999). Specific incidences of partial ice sheet collapse from the North American ice sheet, known as Heinrich events, were recorded by distinct IRD layers in marine sediment cores during some of the longest stadials (Bond et al., 1992; Alley and MacAyeal, 1994; Hemming, 2004).

In comparison to the relative stability of Holocene climate, the greater variability of regional and global climate during late Pleistocene glacial and deglacial periods has been attributed to climatic and oceanographic boundary conditions that led to a bi-stable ocean circulation mode in the Atlantic Ocean (Broecker et al., 1985; Broecker et al., 1990; Ganopolski and Rahmstorf, 2001). Comparing ice core climate records from Greenland and Antarctica reveals that this signal was region-specific, with the Southern Ocean warming during cold Greenland stadials (yellow bars in Figure 11.7), and then starting to cool following the rapid onset of Greenland interstadials (Blunier and Brook, 2001; EPICA Community Members, 2006) (Figure 11.7). This anti-phased bipolar pattern is pervasive and has also been recognised in SST reconstructions from North and South Atlantic sediment cores (Barker et al., 2009). Hence, the concept of a bipolar seesaw emerged (Broecker, 1998), in which a strong Atlantic meridional overturning circulation (AMOC) would lead to warming in the North Atlantic and cooling in the Southern Ocean, whereas a weak AMOC with reduced NADW formation would lead to cooling in the North Atlantic and the accumulation of heat in the South Atlantic and Southern Ocean (Broecker, 1998; Ganopolski and Rahmstorf, 2001; Stocker and Johnsen, 2003). The more gradual changes in Antarctica than Greenland (Figure 11.7) were initially linked to the large volume of the Southern Ocean which could act as a heat capacitor (Stocker and Johnsen, 2003), supported by the observation that longer stadial events in Greenland coincided with greater warming in Antarctica (EPICA Community Members, 2006).

The concept of a bipolar seesaw has often been used to refer to both the observed anti-phasing in polar temperatures and the ocean circulation mechanism that may be behind it, even though the forcing mechanisms responsible have yet to be fully established. For example, it is not clear whether

the forcing originates from processes controlling deep water formation in the North Atlantic (Ganopolski and Rahmstorf, 2001) or the Southern Ocean (Buizert and Schmittner, 2015), or some combination. It has also not been established whether oceanic processes (WAIS Divide Project Members, 2015) or atmospheric teleconnections (Hogg et al., 2016) play the dominant role in transferring the climate signal. Regardless of the mechanism, there are many examples of the signal of Dansgaard-Oeschger or Heinrich events being transmitted globally and almost instantaneously, leading to changes in multiple components of the Earth system. For stadials and/or Heinrich events, the effects include weakening of the Asian monsoon system (Wang et al., 2001), a southward shift of the intertropical convergence zone (Peterson et al., 2000; Wang et al., 2004; Mulitza et al., 2017), South Atlantic warming (Barker et al., 2009), and a strengthening and/or southward shift of the southern westerly winds (Lamy et al., 2007; Anderson et al., 2009; Whittaker et al., 2011). With highly-resolved and absolute-dated reconstructions, it may be possible to distinguish specific roles for oceanic and atmospheric processes in transmitting such signals (WAIS Divide Project Members, 2015). Records from the WDC ice core indicate roles for both the atmosphere and the ocean, with an instantaneous but spatially-variable atmospheric response in the southern westerly winds being followed a few hundred years later by a spatially-uniform oceanic response (Buizert et al., 2018).

There is also an increasing wealth of evidence indicating deep ocean circulation changes on millennial timescales during the last glacial cycle, including records from the Bermuda Rise in the deep Northwest Atlantic (Henry et al., 2016) (Figure 11.8c,d), the Portuguese margin of the Northeast Atlantic (Martrat et al., 2007), and the Cape Basin of the deep Southeast Atlantic (Piotrowski et al., 2005; Gottschalk et al., 2018). What remains less clear is the exact nature of the link between deep ocean circulation changes and these millennial events. While Heinrich events could force ocean circulation changes by freshening the North Atlantic surface ocean in regions of deep water formation (Ganopolski and Rahmstorf, 2001), iceberg discharge may also simply provide a positive feedback that lengthens or deepens a stadial following an initial perturbation (McManus et al., 1999). Recent evidence supports this latter view, because SST changes occurred before IRD input during Heinrich events in North Atlantic records covering the last ~400 kyr (Barker et al., 2015). The observation that similar circulation changes occurred during most stadials of the last glacial period, both those with and without Heinrich events (Figure 11.8c,d), would also support that view (Henry et al., 2016). However, such observations are not inconsistent with an ocean circulation origin for some abrupt climate events, such as the Younger Dryas (Muschitiello et al., 2019). Regardless of the actual trigger, which could differ between events, it is possible to effectively model spatial and temporal patterns of millennial climate variability during Heinrich stadials, and also many of the related changes in atmospheric and Southern Ocean processes, using North Atlantic freshwater hosing experiments (Ganopolski and Rahmstorf, 2001; Menviel et al., 2018).

Other components of the Southern Ocean atmosphere-ocean system also record sub-orbital scale variability. For example, millennial variability is seen in records of the Agulhas leakage (Marino et al., 2013), which is the ‘warm water return route’ which advects salt from the Indian Ocean via the southern tip of Africa to the Atlantic Ocean. Increases in the Agulhas leakage during North Atlantic stadials may have influenced the AMOC by resupplying salt to the Atlantic Ocean, leading to the potential for a dynamic feedback through the influence of the southern westerly winds and Southern Ocean fronts on the Agulhas leakage (Marino et al., 2013). Changes in the Agulhas leakage could also have influenced late Pleistocene glacial terminations by preconditioning the interglacial resumptions of AMOC (Peeters et al., 2004). The strength of the subantarctic portion of the Antarctic Circumpolar Current in the northern Drake Passage also appears to have fluctuated on millennial timescales during the last glacial period and deglaciation, with enhanced flow during Antarctic warm periods (North Atlantic stadials), possibly linked to southward shifts of the southern westerly winds to better align with the Drake Passage (Lamy et al., 2015). Similar to the effects of the Agulhas leakage on the warm water return route, these changes could have influenced the ‘cold water return route’ to the

North Atlantic Ocean on both millennial (Lamy et al., 2015) and orbital or longer timescales (Toyos et al., 2020), although their origin and dynamics are yet to be fully understood.

Understanding millennial climate variability is important because it may have played a crucial role in determining the timing and sequence of events during late Pleistocene glacial terminations (Anderson et al., 2009; Cheng et al., 2009; Denton et al., 2010; Roberts et al., 2010; Barker et al., 2011; Shakun et al., 2012; Menviel et al., 2018). As summarised by Denton et al. (2010), North Atlantic freshwater forcing during Heinrich Stadial 1 and the associated AMOC weakening could have led to Southern Ocean warming, sea ice retreat, and a southward shift of the southern westerly winds. In combination, these changes would have acted to enhance near-surface upwelling and reduce deep ocean stratification, thereby allowing carbon stored in the deep ocean to escape to the atmosphere (Anderson et al., 2009; Martínez-Botí et al., 2015b; Rae et al., 2018). The ubiquitous association between such bipolar seesaw oscillations and late Pleistocene terminations (Barker et al., 2011) suggests that a particularly large or sustained millennial event, in combination with appropriate orbital forcing, could enable the climate system to cross a critical threshold that allows further positive feedbacks to move the system into a full interglacial period. We also note that the reinvigoration of AMOC at the start of the Bolling-Allerod warm period has been identified as the likely origin of a centennial-scale CO_2 release from the ocean to the atmosphere (Marcott et al., 2014; Chen et al., 2015), highlighting just how fast the ocean-atmosphere system can act.

It is also important to understand the role of AMOC variability in heat transport, because the bipolar seesaw can cause significant local warming of the ocean and atmosphere in the vicinity of either Greenland or Antarctica that is above the expected 'background' levels for a given climate state. Such warming could be crucial for both atmospheric and ocean-driven mechanisms that influence ice sheet stability (Golledge et al., 2014; Weber et al., 2014; Clark et al., 2020). In this regard, we note that the operation of a bipolar seesaw is not restricted to glacial periods of the late Pleistocene, since it has also been observed during the early Pleistocene (Birner et al., 2016), with evidence also emerging for AMOC instability during recent interglacial periods (Galaasen et al., 2020). Therefore, when considering Antarctic climate records and the response of the Antarctic Ice Sheet, the operation of a bipolar seesaw should be considered as a pervasive (although likely variable) factor over at least the duration of the Pleistocene. Changes in the bipolar seesaw and southern westerly winds were probably also important earlier in the Neogene, with the influence of Antarctic cooling on the Agulhas leakage potentially contributing to the onset of Northern Hemisphere Glaciation (McKay et al., 2012a).

11.5 Antarctic Ice Sheet dynamics in the late Pleistocene

11.5.1 Climate context

The predominantly marine-based WAIS (~4 m sea level equivalent) and marine-based sectors of the EAIS (~19 m sea level equivalent) are susceptible to retreat through a combination of reduced buttressing through ice shelf thinning and marine ice sheet instability, as outlined earlier. To constrain the levels of atmospheric or ocean warming required to generate ice sheet retreat, it is essential to assess past ice sheet behaviour in response to different climatic and oceanographic regimes, in particular during times that were warmer than today. Recent Pleistocene interglacials provide a good target, because both Antarctic ice cores and other globally-distributed marine and terrestrial paleoclimate reconstructions indicate that certain interglacials have been warmer than the pre-industrial Holocene, in particular MIS 5e, MIS 9, and MIS 11 (Jouzel et al., 2007; Lang and Wolff, 2011; Capron et al., 2014; Yin and Berger, 2015; Snyder, 2016; Holloway et al., 2017) (Figure 11.3).

In terms of average global SSTs, MIS 5e was probably warmer than pre-industrial conditions by only around 0.5-1 °C (McKay et al., 2011; Hoffman et al., 2017) (Figure 11.3c), although larger changes occurred at high latitudes (Capron et al., 2014; Hoffman et al., 2017). In Antarctica, peak temperatures during MIS 5e, MIS 9, and MIS 11 reached 2-4 °C warmer than the Holocene (Jouzel et al., 2007) (Figure 11.3g). Given similar greenhouse gas forcing to the Holocene (Figure 11.3h), the Antarctic warmth of these previous interglacials likely reflects differences in insolation forcing (Yin and Berger, 2015) and differences in interhemispheric heat transport by the AMOC (Holden et al., 2010). It has also been suggested that some component of the peak interglacial warming of Antarctica and the Southern Ocean could have arisen as a local consequence of feedbacks from WAIS collapse (Holden et al., 2010), although evidence for WAIS collapse during the late Pleistocene remains inconclusive. Changes in sea ice extent and atmospheric transport could also have contributed to changes in ice core records during these intervals of peak warmth (Holloway et al., 2016).

11.5.2 Global evidence on the Antarctic Ice Sheet

Global sea level reconstructions based on benthic foraminiferal $\delta^{18}O$ records provide constraints on the magnitude and timing of past changes in globally-integrated ice volumes (Figure 11.3a,b, Figure 11.4a,b). However, as discussed earlier, a number of caveats and uncertainties limit the precision of these methods, severely restricting their ability to quantitatively reconstruct past peak interglacial sea levels or the timing of Antarctic changes. Furthermore, such approaches cannot resolve where a given sea level change originated from, which is a critical factor when thinking about specific contributions from Antarctica through time as well as the local fingerprints of future sea level change on a warming planet (Hay et al., 2014).

Instead, the most robust evidence on global sea levels during late Pleistocene interglacials is based on reconstructions from absolute-dated coral terraces, once corrections are made for tectonic uplift and glacio-isostatic adjustments (GIA) that affect local sea levels (Raymo and Mitrovica, 2012; Dutton et al., 2015). Such studies indicate elevated global mean sea levels during warm late Pleistocene interglacials, with estimates of ~6-9 m during MIS 5e (Kopp et al., 2009; Dutton and Lambeck, 2012) and ~6-13 m during MIS 11 (Raymo and Mitrovica, 2012). An additional source of error in those estimates comes from uncertainty in the GIA corrections that arises from differences in the size and distribution of the Northern Hemisphere ice sheets at the preceding glacial maxima. In light of the possibility that a greater proportion of Northern Hemisphere ice was in Eurasia rather than North America at the penultimate glacial maximum compared to the LGM, it has been suggested that global mean sea level during MIS 5e may have been another ~2 m higher than those estimates (Rohling et al., 2017).

Since a significant amount of ice remained on Greenland during MIS 5e, a reduction in the Greenland ice sheet likely contributed no more than ~2 m to global sea level rise above Holocene levels (Colville et al., 2011; Dahl-Jensen et al., 2013; Yau et al., 2016a; Clark et al., 2020). Noble gas measurements in ice cores indicate a short-lived global mean ocean warming of ~1.1 ± 0.3 °C above Holocene levels at ~129 ka and lasting for around 2 kyr, leading to a sea level contribution from thermal expansion of 0.7 ± 0.3 m, followed by a return to stable temperatures similar to the Holocene for the remainder of MIS 5e (Shackleton et al., 2020). Given the above constraints, the global sea level estimate of ~6-9 m for MIS 5e implies significant ice loss from Antarctica (Dutton et al., 2015; Clark et al., 2020). In addition, ice loss in Greenland and Antarctica may not have occurred synchronously (Capron et al., 2014; Yau et al., 2016b; Rohling et al., 2019; Clark et al., 2020), and therefore simply subtracting the Greenland contribution from the total sea level change during MIS 5e (i.e. the 'mass balance' approach) could underestimate Antarctic contributions to sea level change. Ice loss from Antarctica

during MIS 11 is subject to more uncertainty, because of the wider range in global mean sea level estimates (~6-13 m), as well as evidence for a greater sea level contribution from Greenland ice sheet collapse (Reyes et al., 2014; Irvalı et al., 2020). Overall, the sea level evidence points to a reduced ice volume in Antarctica during both MIS 5e and MIS 11, presumably from retreat of some combination of the WAIS and the marine-based sectors of the EAIS, but the location of ice loss is not resolved by the sea level records.

Compared to absolute sea level estimates, the magnitude and rates of sea level variability within interglacials remain less well constrained and are strongly debated. Significant sea level fluctuations of several metres were proposed to have occurred within MIS 5e (Kopp et al., 2009), whereas recent studies indicate relatively stable sea levels (Barlow et al., 2018; Polyak et al., 2018). For example, Polyak et al. (2018) reported phreatic overgrowths on coastal speleothems from Mallorca that indicate a stable local sea level during MIS 5e, which (after GIA adjustments) is consistent with an early MIS 5e peak in global mean sea level followed by a gradual decline. In terms of rates of change, estimates based on coral terraces suggest maximum rates of sea level rise within MIS 5e of ~3-7 mm/yr (Kopp et al., 2013; Barlow et al., 2018). In contrast, while subject to large uncertainties, the sea level reconstruction from the Red Sea (Figure 11.3b) suggests potentially much higher rates of sea level rise of up to ~9-35 mm/yr for the most rapid millennial event within MIS 5e, which has been attributed mostly to changes in the Antarctic Ice Sheet volume (Rohling et al., 2019).

11.5.3 Regional studies of Antarctic Ice Sheet behaviour before the LGM

During the LGM, the Antarctic Ice Sheet extended across the continental shelves, reaching the shelf break along many but not all margins (RAISED Consortium, 2014). Hence, the glacial Antarctic Ice Sheet was characterised by a different geometry than today, with thickening near the present day ice margins and an overall increase in ice volume (see Chapter 12 for details). Such LGM and deglacial reconstructions draw heavily on radiocarbon-based dating of shelf sediments and terrestrial deposits (e.g. lake sediments, raised beaches, and moraines), as well as using cosmogenic nuclides (e.g. ^{10}Be, ^{14}C, ^{26}Al) to constrain past rock exposure and ice sheet elevation. Our understanding of the LGM provides a useful context for assessing the likely geometry and volume of the ice sheet through previous glacial-interglacial cycles, but such reconstructions are more challenging due to the effects of LGM erosion and the difficulty in dating events in shelf and terrestrial records beyond the radiocarbon dating window. Recent advances in understanding the LGM and Holocene ice sheet have particularly benefited from the use of in-situ ^{14}C exposure dating (e.g. Nichols et al., 2019), which is more sensitive to recent changes in the ice sheet and less susceptible to inheritance than cosmogenic ^{10}Be or ^{26}Al methods. For previous glacial cycles, ^{14}C exposure dating is unavailable, while ^{10}Be and ^{26}Al data are more suitable for understanding the long term evolution of the ice sheet than for detailed reconstructions of variability within individual glacial or interglacial periods. The likelihood of multi-stage exposure and burial histories means that interpretations are typically non-unique (e.g. Jones et al., 2017 and references therein), while the relatively long half-lives of ^{10}Be and ^{26}Al preclude their use to constrain short climate events. For the above reasons, most of our knowledge of the earlier Pleistocene behaviour of the Antarctic Ice Sheet comes from offshore marine sediment cores and ice sheet modelling, which therefore form our main focus below.

11.5.4 Regional evidence on the West Antarctic Ice Sheet

In light of the sea level contributions that appear to be required from Antarctica during recent warm interglacials, and the sensitivity of West Antarctic catchments such as the Pine Island/Thwaites Glacier system (Amundsen Sea Embayment) and the Siple Coast (Ross Sea) (Figure 11.2) to ocean warming in models (Golledge et al., 2017), a partial or full collapse of the WAIS might be suspected

for MIS 5e and/or MIS 11. However, geological evidence either supporting or refuting this suggestion has been hard to obtain. There is direct evidence for WAIS collapse during at least one late Pleistocene interglacial within the past 1.1 Myr, which comes from the discovery of Pleistocene open-ocean diatoms in tills beneath the modern Whillans Ice Stream at the Siple Coast (Scherer et al., 1998). Such a late Pleistocene collapse is also supported by faunal evidence from bryozoans for a trans-Antarctic seaway (Barnes and Hillenbrand, 2010). However, while Scherer et al. (1998) provide unequivocal evidence for at least one collapse event, neither study was able to determine which interglacial such collapse occurred in, how long it lasted, or whether collapse occurred multiple times. Future studies based on the molecular genetics of benthic marine species may provide better constraints on past gateway openings (Strugnell et al., 2018), but the detailed timing of any such Pleistocene events are yet to be resolved by this method (e.g. Collins et al., 2020).

Offshore sedimentary evidence from the late Pleistocene has been obtained from sediment cores on the Ross Sea shelf during the Antarctic Drilling Project (ANDRILL; see also Chapter 10) (Figure 11.2). An extensive sequence of Pliocene sediments was recovered in core AND-1B and indicates significant Pliocene variability in the WAIS, including events of ice sheet advance across the Ross Sea shelf (recorded by subglacial diamictites) as well as extended intervals of retreat (recorded by diatomite) (Naish et al., 2009). The AND-1B record extends into the Pleistocene, where sediments indicative of ice retreat become less prominent, but open ocean deposition is indicated for some Pleistocene intervals (Naish et al., 2009). The Pleistocene record was analysed in detail by McKay et al. (2012b), who suggested that the late Pleistocene sedimentary environment generally fluctuated between two states: subglacial or grounding zone sedimentation during glacial periods, and deposition beneath a floating ice shelf during interglacials. Critically, loss of the Ross Ice Shelf at some point in the last ~250 kyr is indicated by a thick layer of reworked volcanic glass sourced from Mt Erebus, which suggests that WAIS deglaciation occurred during either MIS 5e or MIS 7 (McKay et al., 2012b). The ANDRILL records can be challenging to interpret because of the combined influences of EAIS and WAIS dynamics on ice flow in the Ross Sea (McKay et al., 2012b), but the above interpretation is consistent with models that indicate a strong link between removal of the Ross Ice Shelf and WAIS deglaciation (Martin et al., 2019). Other limitations in acquiring a detailed late Pleistocene reconstruction from AND-1B arise from the presence of major erosional hiatuses and a lack of dating constraints (McKay et al., 2012b), indicating the need for further research in this region. The broader context of the Plio-Pleistocene AND-1B record, including a comparison to more proximal records from the Southern Victoria Land margin and geological sequences in the Transantarctic Mountains, can be found in Levy et al. (2012).

Pleistocene evidence from the vicinity of the Amundsen Sea Embayment (Figure 11.2) is rather limited, but sequences from the continental rise have been used to address the possibility of a late Pleistocene WAIS collapse. In an early study, no collapse was inferred to have occurred over the past ~1.8 Ma, based on the absence of distinct sedimentological changes that would be expected to have characterised such an event (Hillenbrand et al., 2002). However, subsequent research revealed an extended interval of MIS 13-15 that was characterised by elevated productivity and distinctive sediment inputs from the hinterland that hinted at WAIS collapse during this time (Hillenbrand et al., 2009). Collapse or retreat during this lukewarm late Pleistocene interglacial may have been aided by the extended duration of warmth (Figure 11.3g) or by shifts in the Amundsen Sea low pressure system that led to increased incursions of warm Circumpolar Deep Water (CDW) onto the shelf since the MPT (Konfirst et al., 2012). However, if the WAIS collapsed during MIS 13-15, it might seem surprising to find no evidence here for more recent collapse events, given the warmer interglacial temperatures since the MBE, both globally and in Antarctica (Figure 11.3). In light of modelling outputs indicating that WAIS deglaciation in the Amundsen Sea Embayment could potentially occur without removal of the Ross Ice Shelf (Clark et al., 2020), it will be important to obtain better constraints on the late Pleistocene ice sheet history in this region.

Sedimentary records providing evidence on the Antarctic Peninsula Ice Sheet were recovered from the continental rise of the Bellingshausen Sea during ODP Leg 178 (Sites 1095, 1096, 1101; Figure 11.2). Clay mineral constraints (Hillenbrand and Ehrmann, 2005) and sedimentological changes (Cowan et al., 2008) both indicate Pleistocene advance and retreat of the Antarctic Peninsula Ice Sheet across the shelf, but a more detailed understanding is limited by the low resolution of those records. Since the Antarctic Peninsula Ice Sheet may survive even while the WAIS retreats significantly (Sutter et al., 2016), records from this region may not provide strong constraints on past or future behaviour of the WAIS or on global sea level contributions from West Antarctica.

Overall, the offshore sedimentary records provide support for late Pleistocene variability of the WAIS, including retreat or collapse in certain interglacials, but the record is fragmentary and does not provide a clear picture of a consistent response between sectors during each of the recent warm interglacials. While ongoing marine geological studies are seeking to significantly improve this picture, alternative approaches are exploring how an ice sheet change such as WAIS collapse would be imprinted on Antarctic ice core records. For example, ice core $\delta^{18}O_{ice}$ or δD_{ice} records could be affected directly by changes in ice sheet elevation and glacio-isostatic adjustment, or indirectly through the impacts of ice sheet melting on ocean and atmospheric temperatures, sea ice extent, and atmospheric circulation (Bradley et al., 2012; Steig et al., 2015). Unfortunately, the direct effect of ice sheet elevation changes linked to WAIS collapse may not have had a significant impact at the location of existing East Antarctic ice cores (Bradley et al., 2012) (Figure 11.2), thereby limiting the ability to resolve such a change, which points to a need for ice cores in targeted locations. Modelling studies have also suggested that peaks in ice core $\delta^{18}O_{ice}$ or δD_{ice} that occurred early in MIS 5e could record the effect of significant reductions in sea ice linked to warm SSTs, without requiring WAIS collapse (Holloway et al., 2016).

The latest evidence indicating changes to the WAIS during MIS 5e is emerging from blue-ice sites. Both δD_{ice} and other geochemical tracers measured on MIS 5e ice at the Mount Moulton blue-ice site in Marie Byrd Land of West Antarctica are consistent with the regional climate changes that would be expected to result from WAIS collapse (Korotkikh et al., 2011; Steig et al., 2015). In addition, a blue-ice record from the Patriot Hills Blue Ice Area, located ~50 km inland from the modern grounding line of the Filchner-Ronne Ice Shelf, provides indirect constraints on ice sheet changes in the Weddell Sea Embayment (Turney et al., 2020). Measurements of δD_{ice} in a short section of ice corresponding to Heinrich Stadial 11 suggest that temperatures were elevated above Holocene levels during the penultimate deglaciation. Critically, a subsequent hiatus between 130 ka and 80 ka appears to indicate a retreated grounding line in the Weddell Sea Embayment which, in combination with ice sheet modelling, would support significant mass loss from both the WAIS and the Recovery Basin of the EAIS during the last interglacial (Turney et al., 2020). Future studies of horizontal blue-ice cores can be expected to provide additional new insights, but research is also required to test the relationship between ice sheet grounding line positions and upstream flow patterns, as well as the origin of unconformities in blue-ice records (e.g. Winter et al., 2016).

11.5.5 Regional evidence on the East Antarctic Ice Sheet

Until recently, evidence constraining the behaviour of the EAIS through late Pleistocene glacial-interglacial cycles (and during many other time periods) had been limited by the lack of suitable sedimentary archives recovered from this challenging and remote region (Figure 11.2). Early views on the EAIS generally favoured a history of stable behaviour through the Neogene because of its predominantly terrestrial-based geometry (Sugden et al., 1993), although counter-arguments for more dynamic behaviour were put forward (Webb and Harwood, 1991). It is now clear that nearly one-third of the ice in East Antarctica (~19 m sea level equivalent; Fretwell et al., 2013) is contained

within marine-based catchments underlain by deep subglacial basins, notably the Wilkes, Aurora, and Recovery Subglacial Basins (Figure 11.2). For these regions, ice sheet modelling suggests that the dynamics were probably quite different from the continental-based EAIS interior (Fogwill et al., 2014; Mengel and Levermann, 2014; DeConto and Pollard, 2016; Golledge et al., 2017).

Recent studies from the continental shelf offshore of the Aurora Basin (Figure 11.2) provide support for a dynamic EAIS. Specifically, marine geophysical data indicative of a surface-meltwater rich subpolar glacial system supports retreat of this marine margin in the Oligocene and Miocene (Gulick et al., 2017), with a transition to a polar environment occurring in the late Miocene. Marine sequences from the Prydz Bay area, recovered from the uplifted terrestrial margin and from offshore sites during ODP Leg 188 (Sites 1165-1167; Figure 11.2), also clearly indicate dynamic behaviour of the EAIS during the Pliocene (Hambrey and McKelvey, 2000; Quilty et al., 2000; Cook et al., 2014). For example, characteristic $^{40}Ar/^{39}Ar$ ages indicate that far-travelled IRD from the vicinity of the Aurora Subglacial Basin reached ODP Site 1165 during the Pliocene (Cook et al., 2014). At the same time, cosmogenic isotope data from the Ross Sea (core AND-1B) (Figure 11.2) supports the idea that the terrestrial portion of the EAIS has remained largely intact and has not retreated significantly over at least the last 8 Myr (Shakun et al., 2018). Based on the above studies, it is clear that attention should be focused on the marine basins when assessing possible EAIS variability during the Pleistocene, with the caveat that the specific subglacial bedrock topography of each basin may result in significant spatial variability in ice sheet behaviour between sectors (Golledge et al., 2017; Morlighem et al., 2020). Furthermore, both the onshore and offshore bedrock topography of Antarctica has evolved over geological timescales, in response to multiple tectonic, erosional, and sedimentary processes, with implications for past ice sheet size and stability (e.g. Jamieson et al., 2010; Austermann et al., 2015; Colleoni et al., 2018; Paxman et al., 2019; Paxman et al., 2020). Only recently have continent-scale topographic reconstructions for multiple time slices been attempted (e.g. Paxman et al., 2019), and these will require ongoing validation and refinement using geological records.

Evidence constraining the late Pleistocene behaviour of the EAIS has come from cosmogenic isotopes, distal Southern Ocean IRD records, and more proximal studies of sedimentology and geochemical provenance. Cosmogenic isotope analyses adjacent to the Skelton Glacier, an outlet glacier that drains a portion of the EAIS into the Ross Sea, indicate that it had surface elevations at least ~200 m higher than today for a significant portion of the Pleistocene, presumably representing past glacial periods with an expanded ice sheet (Jones et al., 2017). Since cosmogenic isotope studies do not indicate thickening of the EAIS interior during Pleistocene glacial periods (e.g. Lilly et al., 2010; Suganuma et al., 2014), elevation changes in the transition regions between the interior and the marine margins may have been driven by ice shelf and marine processes (Jones et al., 2017). While the Dronning Maud Land region of East Antarctica experienced very limited elevation changes during the last deglaciation, more than 500 m of long-term thinning is indicated for the EAIS in this region during the Pleistocene (Suganuma et al., 2014). Thinning of the EAIS interior since the Pliocene is also reported in other regions (Yamane et al., 2015), and may have been linked to global cooling, sea ice expansion, and reduced atmospheric moisture transport, leading to reduced accumulation rates (Suganuma et al., 2014; Yamane et al., 2015). Overall, while the cosmogenic isotope evidence points to spatially-variable Pleistocene elevation changes of the EAIS, these data do not constrain the lateral extent of the ice sheet, and are not well-suited for constraining the possibility of past short-lived retreat events leading to ice surface elevations similar to or lower than today.

Teitler et al. (2010) presented distal IRD records from ODP Leg 177 Site 1090 in the Agulhas Basin of the Southeast Atlantic covering multiple glacial cycles over the past ~500 kyr. These authors observed almost continuous IRD deposition over that interval, but significantly more IRD during

glacial periods, which they attributed to an influence of cold SSTs on iceberg survivability into lower latitudes. The mineralogical provenance of the IRD indicates a dominantly EAIS source, such that the continuous presence of IRD was used to infer persistent marine margins of the EAIS across this interval (Teitler et al., 2010). That inference is consistent with sea level reconstructions during late Pleistocene interglacials (Dutton et al., 2015) and the stability of the interior EAIS (Shakun et al., 2018), because even sea level contributions from Antarctica of up to ~6-13 m (Dutton et al., 2015) would not imply retreat of the ice sheet margins onto land. However, the strong control of iceberg survivability makes their record highly sensitive to climate variability, limiting the ability to infer changes in iceberg production and to draw conclusions on the dynamic behaviour of EAIS margins (Teitler et al., 2010).

For the Lambert Glacier-Amery Ice Shelf system, which drains a large catchment of the EAIS into Prydz Bay (Figure 11.2), data from ODP Legs 119 and 188 provide information on its Plio-Pleistocene behaviour. Focusing on ODP Site 1166 on the continental shelf and ODP Site 1167 on the continental slope (Figure 11.2), Passchier et al. (2003) presented sedimentological evidence indicating a switch in behaviour between the early and late Pleistocene. Alternations between glacially-derived debrites and fine-grained pelagic interbeds at ODP Site 1167 during the early Pleistocene were attributed to advance and retreat of the grounding line, implying that the Lambert Glacier was a highly dynamic ice stream (Passchier et al., 2003). In contrast, since the MPT, grounding-line debrites were replaced by glacio-marine deposition, from which it was inferred that the glacial advances of the Lambert Glacier became less extreme and no longer reached the shelf edge, suggesting a less dynamic ice sheet (Passchier et al., 2003). Nevertheless, clay mineralogy and IRD records from the Prydz Bay continental rise covering the last ~500 kyr do indicate late Pleistocene variability in the Lambert Glacier-Amery Ice Shelf system (Wu et al., 2021). As well as providing evidence for glacial advances across the shelf and interglacial retreat, differences in clay mineralogy between individual glacial and interglacial periods suggest a sensitive response of the ice sheet in this region to subtle differences in oceanic and atmospheric forcing (Wu et al., 2021).

The most prominent developments in understanding the past behaviour of the EAIS have come from IODP Expedition 318, which retrieved sediment cores from the continental shelf and rise in the vicinity of the Wilkes Subglacial Basin (Escutia et al., 2011) (Sites U1355-1361; Figure 11.2). While many new insights from that expedition concerned earlier periods of glacial history, Pleistocene sections were recovered from the continental rise sites, including Site U1361, which provides important constraints on the late Pleistocene variability of the EAIS in this region. A recent study used neodymium and strontium isotope measurements on the bulk and fine-grained sediment fractions to trace changes in sediment provenance during the late Pleistocene (Figure 11.9e), from which variability of the ice sheet margin was inferred (Wilson et al., 2018). These authors proposed that the ice margin retreated in the vicinity of the Wilkes Subglacial Basin during MIS 5e, MIS 9, and MIS 11, based on provenance signatures that differed from the Holocene sediments but which could be explained by a greater contribution from Ferrar Large Igneous Province and associated Beacon lithologies that are found inland in the Wilkes Subglacial Basin (Ferraccioli et al., 2009). Differing responses for those warm interglacials compared to the Holocene and MIS 7 indicate that retreat occurred when Antarctic air temperatures were at least 2 °C warmer than pre-industrial temperatures for 2,500 years or more (Jouzel et al., 2007) (Figure 11.9a), suggesting a role for extended warmth (rather than the absolute magnitude of peak interglacial temperatures) in forcing the ice sheet behaviour (Wilson et al., 2018).

Overall, the Site U1361 record fingerprints a contribution to late Pleistocene interglacial sea levels from ice loss at the EAIS margin (Wilson et al., 2018), but those data are not able to quantify the extent of retreat or the total sea level contribution. However, the striking similarity between this

record (Figure 11.9) and changes during the Pliocene (Cook et al., 2013; Bertram et al., 2018) is an important observation. In light of global climate cooling since the Pliocene (Figure 11.4c), the occurrence of similar ice sheet behaviour suggests that the late Pleistocene EAIS in the vicinity of the Wilkes Subglacial Basin has been more sensitive to glacial-interglacial changes than might have been anticipated. Because of the lower atmospheric CO_2 levels of Pleistocene interglacials compared to the Pliocene, and the slightly cooler global average surface temperatures, it appears that other factors may have compensated to maintain a sensitive ice sheet. One key factor may have been the operation of a stronger bipolar seesaw in ocean heat transport during the late Pleistocene (Stocker and Johnsen, 2003; Barker et al., 2011), which could have played a major role in generating peak interglacial Antarctic temperatures that were ~2-4 °C warmer than the Holocene (Jouzel et al., 2007; Holden et al., 2010) (Figure 11.9a). Sea ice feedbacks may also have contributed to localised Southern Ocean warming (Holloway et al., 2016). Regardless of the combination of mechanisms responsible for the local warmth, it appears critical to consider local rather than global temperatures in forcing the ice sheet behaviour (Rohling et al., 2019; Clark et al., 2020). An additional contributing factor may have been the deepening of bedrock topography in the Wilkes Subglacial Basin through time (Colleoni et al., 2018), which could have enhanced the sensitivity of this catchment to ocean forcing, although only modest changes have been reconstructed between the Pliocene and late Pleistocene (Colleoni et al., 2018; Paxman et al., 2020).

Two complementary studies have recently emerged, providing apparently contrasting views on the interglacial stability of ice in the Wilkes Subglacial Basin. Blackburn et al. (2020) showed that subglacial opal and calcite precipitates in the Wilkes Subglacial Basin record a level of ^{234}U enrichment that is consistent with a major ice margin retreat during MIS 11 followed by the isolation of a marine-derived fluid reservoir beneath the ice sheet since this time (Blackburn et al., 2020). To first order, those data agree with the offshore marine record, which also recorded the most extreme provenance changes during MIS 11 (Figure 11.9e; Wilson et al., 2018), together providing support for a globally significant sea level contribution from the Wilkes Subglacial Basin of up to 3-4 metres at that time. In contrast, no such major retreat is inferred for MIS 5e (Blackburn et al., 2020), which may indicate that the MIS 5e retreat indicated by the marine record (Figure 11.9e) was more limited in extent. Evidence on the local ice sheet elevation during MIS 5e from $\delta^{18}O_{ice}$ values in the Talos Dome (TALDICE) ice core (Figure 11.2) also appears to rule out a collapse on the scale inferred for MIS 11, which restricts MIS 5e sea level contributions from the Wilkes Subglacial Basin to a maximum of ~0.4-0.8 m (Sutter et al., 2020). Therefore, while Wilson et al. (2018) highlighted the value in comparing recent super-interglacials to the slightly cooler Holocene or MIS 7 intervals, the response of the ice sheet to subtle differences between super-interglacials should also be explored.

A major question to be addressed with future research is whether the EAIS in the vicinity of the Wilkes Subglacial Basin could even have been more sensitive to environmental change than the WAIS. If so, it would challenge a long-standing assumption that WAIS collapse would precede EAIS collapse, opening up the possibility that feedbacks from retreat of EAIS margins could contribute to WAIS collapse (Fogwill et al., 2015; Phipps et al., 2016). It will also be important to obtain similar constraints on the late Pleistocene behaviour of the EAIS margin in other regions, which are likely to have differing sensitivities to oceanic and atmospheric warming (Golledge et al., 2017). Late Pleistocene paleoenvironmental work is underway at the Sabrina Coast offshore of the Aurora Subglacial Basin (Holder et al., 2020; Tooze et al., 2020), and in Prydz Bay offshore of the Lambert Glacier-Amery Ice Shelf system (Wu et al., 2021), but much more extensive sediment provenance data will be required from these regions. In addition, the integration of ice sheet models with both erosion models and bedrock geology maps holds significant potential to improve interpretations of detrital provenance records in terms of past ice sheet dynamics (Aitken and Urosevic, 2021).

11.5.6 Mechanisms of Antarctic Ice Sheet retreat and insights from ice sheet modelling

The above evidence from geological reconstructions is important for constraining ice sheet models. In particular, the requirement for ice margin retreat in the Wilkes Subglacial Basin during Pleistocene super-interglacials (Wilson et al., 2018; Blackburn et al., 2020) (Figure 11.9e), similar to the Pliocene (Cook et al., 2013; Bertram et al., 2018), may implicate dynamic mechanisms such as ice shelf hydrofracture and ice cliff failure (in addition to marine ice sheet instability) in increasing the sensitivity of the Antarctic Ice Sheet to warm ocean temperatures (Pollard et al., 2015; DeConto and Pollard, 2016). With those processes incorporated, the output from the Penn State University ice sheet model (PSU-ISM) for MIS 5e (Figure 11.10c) appears to be in agreement with the geological data (Figure 11.9) and suggests that Antarctica could contribute ~6-7 m to global mean sea level during this time (DeConto and Pollard, 2016). That scenario involves local ice margin retreat into the subglacial basins of East Antarctica, and also the loss of large parts of the WAIS (Figure 11.10c), consistent with the observations from Turney et al. (2020). In contrast, running the same model without implementing hydrofracture or ice cliff failure led to no collapse of the WAIS and virtually no changes in East Antarctica (Figure 11.10d). The initial boundary conditions can also affect estimates of sea level change from ice sheet models, although they have a modest effect compared to differences in model physics. For example, the choice of glacial versus modern initial conditions leads to a difference of ~1.5 m in the predicted peak MIS 5e sea level rise (Figure 11.10b cf. Figure 11.10c), because the deeper bed elevations resulting from a glacial starting point act to enhance ice margin retreat (DeConto and Pollard, 2016).

From the above data-model comparison, it could be inferred that models lacking the ice cliff failure mechanism, such as the Parallel Ice Sheet Model (PISM) used by Golledge et al. (2017), or other statistical approaches (Ritz et al., 2015), may underestimate the sensitivity of the Antarctic Ice Sheet to ocean warming. However, significant caution is warranted here, because ice sheet collapse in the Wilkes Subglacial Basin (as required to explain the geological data from past super-interglacials) has been simulated using the PISM model (Mengel and Levermann, 2014) under a similar warming scenario to that used by DeConto and Pollard (2016). Indeed, a recent statistical analysis suggests that MIS 5e retreat could be achieved in the DeConto and Pollard (2016) model even without applying cliff failure mechanisms (Edwards et al., 2019). Most recently, using a revised version of the PSU-ISM model, it was proposed that marine ice cliff failure cannot be excluded as a major ice loss mechanism unless the Antarctic Ice Sheet contribution to peak MIS 5e sea levels was less than 3.5 m, while Antarctic contributions of over 6 m would require the operation of an ice cliff failure mechanism (Gilford et al., 2020). With the present observational constraints from MIS 5e, it is unclear whether such dynamic mechanisms are required, but constraining the role of ice cliff instability during past retreat events would represent a major step for accurately modelling the rates of change associated with Antarctic contributions to past interglacial sea levels. Furthermore, evidence on whether these processes were at play in the past would provide essential information to constrain the high-end predictions of future sea level change and to project near-future rates of sea level change (Edwards et al., 2019; Gilford et al., 2020).

While atmospheric forcing for an ice sheet model can reasonably be approximated based on Antarctic ice core temperature reconstructions (Jouzel et al., 2007; DeConto and Pollard, 2016; Blasco et al., 2019) or using local insolation and atmospheric CO_2 forcing (Tigchelaar et al., 2018), past ocean forcing of the Antarctic Ice Sheet is harder to implement. Challenges arise from the lack of suitable paleoceanographic archives from the Southern Ocean, in particular from sites proximal to the ice sheet where the forcing acts, and a lack of understanding of local ocean dynamics under ice shelves and near ice sheet grounding lines. Therefore, our present understanding of the mechanisms that may have influenced ocean forcing and contributed to melting of the Antarctic Ice Sheet is

largely based on modern observations and modelling. As described above, changes in ocean heat transport linked to the bipolar seesaw (Stocker and Johnsen, 2003; Holden et al., 2010) may have been a major factor behind the elevated Southern Ocean warmth affecting surface, intermediate, and deep waters during deglacial or interglacial periods (Figure 11.9b-c). Alternatively, enhanced melting of the Antarctic Ice Sheet during MIS 5e could have been linked to warming of CDW arising from changes in the temperature of NADW or its fractional contribution to CDW (Duplessy et al., 2007; Rohling et al., 2019). Regardless of the exact controlling mechanisms, CDW temperatures are important because where this water mass is able to cross the Antarctic continental shelves (such as in deep channels or where the shelves are narrow), its warmth can melt the undersides of ice shelves or the deep portions of an ice sheet near its grounding line (Pritchard et al., 2012; Alley et al., 2016; Silvano et al., 2016; Turner et al., 2017; Nakayama et al., 2019). If CDW was no more than ~1 °C warmer during MIS 5e than during the pre-industrial Holocene (Duplessy et al., 2007; Shackleton et al., 2020), these changes may have been insufficient on their own to cause the magnitude of retreat proposed to have occurred (Figure 11.10c). However, increases in the upwelling of CDW and/or more efficient transport of CDW across the Antarctic shelves could also have been important for increasing the heat supply to the ice sheet margins (Fogwill et al., 2014; Hillenbrand et al., 2017; Turner et al., 2017). Hence, the possibility arises for forcing by atmospheric processes because of their control on CDW upwelling and transport (Anderson et al., 2009; Fogwill et al., 2014; Turner et al., 2017).

In the absence of a full understanding of the above processes, ocean forcing has often been applied in a fairly simplistic way in ice sheet models, for example using a spatially uniform warming (Mengel and Levermann, 2014; DeConto and Pollard, 2016; Golledge et al., 2017; Turney et al., 2020). Where an ocean climatology derived from an atmosphere-ocean general circulation model was applied to an ice sheet model, both the climate forcing and the modelled ice sheet response were found to be inconsistent with paleoclimate records (Sutter et al., 2016), such that the application of a uniform warming was recommended. Regardless of the detailed approach, the majority of models applying an ocean forcing have suggested that collapse of the WAIS during MIS 5e was feasible in light of paleoclimate constraints (Capron et al., 2014; Hoffman et al., 2017). Specifically, modelled collapses occurred under regional ocean warming of ~0.5 °C (Golledge et al., 2017), ~1 °C (Turney et al., 2020), ~2 °C (DeConto and Pollard, 2016), and ~2-3 °C (Sutter et al., 2016), and also in a model with transient variations in ocean forcing derived from a general circulation model that was forced to replicate reconstructed AMOC variability (Clark et al., 2020). In addition, a high-resolution modelling study using the BISICLES model also indicates the sensitivity of WAIS to collapse on centennial to millennial timescales in response to CDW incursions and ice shelf removal from any of its major ice shelves (Amundsen Sea, Ronne, or Ross) (Martin et al., 2019). While not specifically targeted at MIS 5e, and probably somewhat extreme in the forcing assumed, that study indicates one mechanism through which the WAIS could respond to ocean warming and reduced ice shelf buttressing during MIS 5e. In contrast, one recent modelling study found that WAIS collapse during late Pleistocene interglacials only occurred when forced by sub-surface warming of ~4 °C (Tigchelaar et al., 2018), which the authors considered to be unrealistically high, but their suggestion that both the WAIS and EAIS were relatively stable creates a problem in explaining the global sea level data from MIS 5e and MIS 11. Marine Isotope Stage 11 has received less targeted attention from modelling, but a recent study simulated WAIS collapse during this interval with an intermediate ocean warming of only ~0.4 °C when sustained for ~4 kyr (Mas e Braga et al., 2021), which represents warming that is around an order of magnitude lower than in Tigchelaar et al. (2018). It will be important to resolve the causes of such model differences, which will require higher resolution ice sheet models, the inclusion of both sea ice processes and cross-shelf CDW transport in coupled ocean-ice sheet models (Nakayama et al., 2019), and the incorporation of dynamical ice sheet-ocean-climate feedbacks, as well as better high latitude paleotemperature constraints and verification with geological records.

Finally, it is important to emphasise that the relative contributions of different processes to ice loss are likely to differ between sectors of Antarctica and to vary with the climate state (Golledge et al., 2017; Morlighem et al., 2020). Although late Pleistocene and near-future changes are likely to occur in marine basins, variable contributions can be expected from atmospheric and ocean warming, with WAIS catchments most sensitive to ocean warming and EAIS catchments sensitive to a combination of atmospheric and ocean warming (Golledge et al., 2017). Given the likelihood of differing sensitivities between regions, the existing late Pleistocene constraints on the Wilkes Subglacial Basin (Wilson et al., 2018; Blackburn et al., 2020; Sutter et al., 2020) are not sufficient on their own to validate or tune an ice sheet model. It will therefore be important to obtain further geological evidence from other sectors of the EAIS and WAIS in order to test the sensitivity of specific Antarctic catchments to atmospheric and/or ocean warming. Another major target for the future will be data constraining the possibility of WAIS collapse in each of the recent late Pleistocene interglacials, because at present the evidence is sparse and equivocal. Nevertheless, whereas earlier model studies tended to implicate MIS 7 as the late Pleistocene interglacial with the greatest potential for Antarctic Ice Sheet retreat due to the high insolation peak at this time (e.g. Pollard and DeConto, 2009; de Boer et al., 2014), recent models have indicated greatest retreat during MIS 5e and MIS 11 (e.g. Sutter et al., 2019), in better agreement with constraints from the Wilkes Subglacial Basin (Wilson et al., 2018; Blackburn et al., 2020) and with global sea level reconstructions (Dutton et al., 2015; Spratt and Lisiecki, 2016).

11.5.7 Millennial variability and ice sheet-ocean-climate feedbacks

A recent assessment of global sea level variability during MIS 5e, based on the Red Sea $\delta^{18}O$ record in combination with a salinity reconstruction from the surface ocean near Greenland, has implicated asynchronous ice volume changes between Greenland and Antarctica during this interval (Rohling et al., 2019). These authors suggested that an early MIS 5e sea level high stand at ~129-125 ka was caused by Antarctic melting during and following Heinrich Stadial 11, and that these changes preceded significant melting in Greenland. Given the coincidence of Antarctic melting with a cool interval in the Northern Hemisphere, and the asynchronicity with Greenland retreat, this millennial scale response of the Antarctic Ice Sheet has been attributed to changes in the supply of warm water to the Antarctic shelves linked to the bipolar seesaw (Holden et al., 2010; Marino et al., 2015; Clark et al., 2020; Turney et al., 2020). In addition to warming of the interior ocean and Southern Ocean during Heinrich Stadial 11 (Duplessy et al., 2007; Shackleton et al., 2020), southward shifts in the southern westerly winds likely occurred as a bipolar seesaw response to weakening of the AMOC (Menviel et al., 2018) and could have enhanced incursions of warm CDW onto the shelves (Fogwill et al., 2014).

Millennial changes in the Antarctic Ice Sheet have also been proposed for the last glacial period. Sea level reconstructions from the Red Sea indicate sea level rise of up to ~30 m at ~20 mm/yr during the Antarctic warm events of MIS 3, which was originally attributed to approximately equal contributions from Antarctic and Northern Hemisphere ice sheets (Rohling et al., 2004). However, an Antarctic contribution of ~15 m would appear to be an over-estimate, since it would match or exceed the deglacial changes in Antarctica between the LGM and the Holocene (RAISED Consortium, 2014; Tigchelaar et al., 2018). A recent ice sheet model supports ice loss from the Antarctic Ice Sheet in response to millennial scale climate variability during the last glacial period, but of a smaller magnitude, with ocean warming contributing to sea level rise of up to ~6 m from a combination of both WAIS and EAIS margins (Blasco et al., 2019). Evidence for rapid drops in global sea level during the last glacial period has also been reported, including a sea level fall of ~17 m towards the end of the LGM (Yokoyama et al., 2018), although a large proportion of that ice growth was presumably in the Northern Hemisphere. Regardless, these data suggest that ice sheets may also gain volume

rapidly, so the origin of such ice growth events must be explored for a better understanding of ice sheet dynamics.

Whereas salinity reconstructions and IRD records have provided extensive evidence on millennial variability of the North American and Greenland ice sheets during the late Pleistocene (Hemming, 2004; Rohling et al., 2019), comparable marine geological evidence on the Antarctic Ice Sheet has been more limited. In an early pioneering study, IRD records from the high latitude Southeast Atlantic Subtropical Zone (Cape Basin core TNO57-21) and Antarctic Zone (ODP Site 1094) were used to infer millennial variability in iceberg discharge from the Weddell Sea sector of the WAIS during MIS 3 (Kanfoush et al., 2000). These authors suggested that such changes may have been linked to rapid sea level variability or to the enhanced warmth of CDW due to increased NADW contributions during Northern Hemisphere interstadials (Figure 11.7d,e). However, such a mechanism would seem inconsistent with the Red Sea and modelling studies described above, in which Antarctic retreat was linked to Northern Hemisphere stadials, and it might be suspected that complications from iceberg survivability in this setting make it challenging to infer the exact timing of discharge events from the Antarctic Ice Sheet.

A more recent study used IRD records from cores in Iceberg Alley in the Scotia Sea to explore millennial variability in the Antarctic Ice Sheet during the last deglaciation (Weber et al., 2014). That study revealed centennial to millennial scale fluctuations in IRD content during the deglaciation, potentially indicating variability in ice sheet processes on very short timescales. Pronounced deglacial IRD peaks occurred during early Heinrich Stadial 1 (~17-16 ka) and at the onset of the Antarctic Cold Reversal (~15-14 ka), with the latter consistent with an Antarctic contribution to meltwater pulse (MWP) 1A (Weber et al., 2014). Although it is difficult to quantify the contribution of local icebergs from the Antarctic Peninsula (or the Weddell Sea region more generally) versus far-travelled icebergs from East Antarctica in those records, future geochemical and mineralogical provenance studies may provide this information. Unfortunately, the effects of changes in basal sediment content and its survival, both in ice shelves as they flow to the calving line (Smith et al., 2019) and in icebergs in the open ocean (Clark and Pisias, 2000), may challenge a simple interpretation of ice dynamics, but it is interesting to note that ice sheet models have reproduced a very similar temporal pattern in Antarctic ice discharge through the deglaciation (Golledge et al., 2014). The debate concerning the origin of MWP-1A is active and ongoing, with the case also being made for a dominantly Northern Hemisphere meltwater source (Mackintosh et al., 2011), while a recent data-model comparison using planktonic $\delta^{18}O$ records is consistent with significant contributions from both hemispheres (Yeung et al., 2019).

The Antarctic Ice Sheet may not only respond to changes in AMOC and interhemispheric heat transport on millennial timescales, but it could also melt through local positive feedbacks following an initial perturbation. In particular, meltwater input and surface stratification could generate further local subsurface warming in the Southern Ocean, thereby enhancing ice shelf and ice sheet melting and accelerating ice sheet retreat (Golledge et al., 2014; Fogwill et al., 2015; Bronselaer et al., 2018; Schloesser et al., 2019). Such a positive feedback mechanism has been proposed to explain Antarctic melting during MWP-1A during the last deglaciation (Golledge et al., 2014; Weber et al., 2014), as well as during early MIS 5e (Rohling et al., 2019). However, it is also worth noting that local processes near an ice margin could lead to negative feedbacks as well as positive ones. For example, the expansion of large ice shelf cavities in response to ice sheet retreat from the continental shelves could trigger extensive supercooling of near-surface waters and sea ice growth, thereby reducing ice shelf melting and slowing retreat (e.g. Ashley et al., 2021). As well as causing local changes, Antarctic meltwater inputs could also affect the global ocean circulation, because stratification of the near-surface ocean would restrict AABW formation, as suggested for MWP-1A (Golledge et al., 2014) and early MIS 5e (Hayes et al., 2014). Furthermore, since meltwater inputs would be likely to enhance

sea ice formation and generate surface cooling, they could cause northward shifts in ocean fronts and atmospheric circulation patterns, with the effects extending even to the intertropical convergence zone (Bronselaer et al., 2018). Therefore, in a case where Antarctic ice sheet melting arose from Southern Ocean warming and southward-shifted westerly winds linked to an AMOC reduction, these meltwater-induced changes could potentially provide a negative feedback on the original global-scale ocean and atmospheric circulation changes. With millennial variability of the Antarctic Ice Sheet only now starting to be addressed in ice sheet models (Golledge et al., 2014; Blasco et al., 2019; Martin et al., 2019; Clark et al., 2020), these kinds of dynamic ice sheet-ocean-climate feedbacks (both local and global) will need to be incorporated for these models to be effective.

11.6 Antarctica during earlier Pleistocene climate states

11.6.1 Lukewarm interglacials

Before the MBE at ~430 ka, interglacial periods in Antarctica were cooler than the more recent ones and are often described as "lukewarm" interglacials (Jouzel et al., 2007) (Figure 11.3g). Interglacial atmospheric CO_2 concentrations were also lower during this interval (Figure 11.3h), consistent with a greenhouse gas influence on global temperatures, but a complete explanation for the changes at the MBE is lacking. While oceanic processes play a major role in setting atmospheric CO_2 levels, there is currently little evidence to suggest significant differences in deep water source regions or ocean circulation across the MBE. Benthic $\delta^{13}C$ and neodymium isotope data from the deep North Atlantic Ocean (Site U1313) during the early Pleistocene indicate that similar glacial and interglacial modes of deep ocean circulation have operated since the onset of significant glacial Southern Ocean stratification and sea ice expansion at the start of the Pleistocene (Lang et al., 2016). Similarly, high resolution neodymium isotope data spanning the last ~800 kyr from the mid-depth equatorial Atlantic (ODP Site 929) record no evidence of interglacial changes in Atlantic Ocean circulation across the MBE (Howe and Piotrowski, 2017), indicating a clear decoupling from atmospheric CO_2 and Antarctic temperatures. Since sea ice proxies in ice cores record a shift across the MBE that resembles Antarctic temperature changes (Wolff et al., 2006) (Figure 11.3f), Southern Ocean processes are a strong candidate to explain interglacial changes across the MBE. This suggestion is also supported by increases in interglacial Antarctic Zone productivity and deep water ventilation at ODP Site 1094 after the MBE (Jaccard et al., 2013).

Here we highlight this interval because constraints on the Antarctic Ice Sheet response to the lukewarm interglacials could complement the evidence on more recent super-interglacials such as MIS 5e and MIS 11. However, there is currently a dearth of evidence from Antarctica during this interval. The ANDRILL cores from the Ross Sea are challenging to interpret during the lukewarm interglacials because clearly defined ice shelf sediments are less frequent than during the more recent interglacials, although there may have been an episode of ice shelf retreat and/or open ocean conditions during one of these interglacials (McKay et al., 2012b). As described earlier, the possibility of retreat or collapse of the WAIS during MIS 13-15 was put forward based on elevated productivity and distinctive sediment inputs in an Amundsen Sea core (Hillenbrand et al., 2009). If correct, this result would imply either the importance of extended warmth rather than peak warmth in triggering WAIS retreat, or a role for local ocean forcing at this time (Hillenbrand et al., 2009), but more evidence from other settings is required to confirm this event.

For the EAIS, a clay minerology record from Prydz Bay also hints at enhanced retreat of the Lambert Glacier-Amery Ice Shelf system during MIS 13 (Wu et al., 2021), but that possibility needs to be tested with additional proxies and a longer record. At Site U1361 offshore of the Wilkes Subglacial

Basin, it was not possible to conduct provenance work on the lukewarm interglacials due to core disturbance (Wilson et al., 2018). However, recent studies using other piston cores from this East Antarctic margin have provided paleoenvironmental records that extend back into interglacials prior to the MBE (Tolotti et al., 2018; Jimenez-Espejo et al., 2020). On the basis of elemental chemistry and XRF core-scanning records, Jimenez-Espejo et al. (2020) suggested that the lukewarm interglacials were characterised by a reduced variability in ocean conditions and ice sheet size, while Tolotti et al. (2018) indicated changes in diatom assemblages at the MBE. Future work using isotopic provenance and IRD records in this region could therefore provide further constraints on the behaviour of the ice sheet in the Wilkes Subglacial Basin during lukewarm interglacials.

11.6.2 Super-interglacial MIS 31

Similar to MIS 5e and MIS 11, certain early Pleistocene interglacials also experienced warmer than usual interglacial conditions, both in Antarctica and globally. A distinctive example is MIS 31 (1.08-1.06 Ma), when the high latitude Southern Ocean warmed by several degrees above modern day values (Scherer et al., 2008; Villa et al., 2008; Beltran et al., 2020), accompanied by deep ocean warming and/or global ice volume decrease (Lisiecki and Raymo, 2005; Raymo et al., 2006) (Figure 11.4g). This interval provides an additional test for the Antarctic Ice Sheet response to high latitude warming above present day temperatures, similar to the Pliocene but under more comparable ice sheet boundary conditions to the modern day. Notably, recent data from MIS 31 include SST reconstructions that indicate warming of ~5 °C at the Antarctic margin, based on organic biomarkers ($U^{k'}_{37}$; Long Chain Diol Index, LDI) at Site U1361 offshore of the Wilkes Subglacial Basin and at ODP Site 1101 offshore of the Antarctic Peninsula (Beltran et al., 2020) (Figure 11.2). This excess warmth has been linked to a specific alignment of orbital parameters (i.e. high obliquity and eccentricity) that led to an unusually high summer insolation anomaly at high latitudes (Berger and Loutre, 1991). However, such a magnitude of warming cannot be explained by insolation forcing alone, leading to the suggestion that a minor initial warming triggered ice sheet collapse, with subsequent dynamic ice sheet-ocean-climate feedbacks leading to the major warming event (Beltran et al., 2020).

The best constraints on the Antarctic Ice Sheet behaviour during MIS 31 come from the Ross Sea, in the form of an unusual carbonate unit at Cape Roberts Project site CRP-1 (Scherer et al., 2008) and an interval of extended sedimentation of diatomite and volcanic sands at AND-1B (Naish et al., 2009; McKay et al., 2012b) (Figure 11.2). Both observations indicate sea ice retreat and open ocean deposition, and have been interpreted to indicate retreat of the Ross Ice Shelf and the WAIS as a whole. This scenario can also be reproduced in ice sheet models forced by warm ocean waters, with model outputs suggesting ~6-8 m sea level rise, with ~4 m from WAIS collapse and the remainder from small-scale retreat or ice thinning in the subglacial basins of East Antarctica (DeConto et al., 2012; Beltran et al., 2020).

These changes in the WAIS may also have had more widespread global consequences. As discussed earlier, freshwater input linked to ice sheet retreat could generate a series of feedbacks in the climate system, through reduced AABW formation, increased sea ice formation, and shifts in atmospheric circulation (Bronselaer et al., 2018). Retreat of the WAIS during MIS 31 (McKay et al., 2012b) may provide such an example, because it is proposed to have played a role in reducing AABW formation and inflow to the deep Southwest Pacific (Hall et al., 2001), and to have influenced the remarkably warm interglacial temperatures at Lake El'gygytgyn in Siberia through feedbacks involving ocean circulation and/or sea level change (Melles et al., 2012).

Unfortunately, geological constraints on the EAIS during this interval are rather poor, making it difficult to test ice sheet model outputs that typically suggest only minor changes (DeConto et al., 2012; Beltran et al., 2020). Teitler et al. (2015) compared IRD records through MIS 31 from a

proximal site on the Prydz Bay continental rise (ODP Site 1165) (Figure 11.2) and a distal South Atlantic site (ODP Site 1090). At the distal ODP Site 1090, there was a significantly reduced IRD content during this warm interval, similar to MIS 5e and MIS 11, which was likely controlled by SST warming. The proximal ODP Site 1165 in Prydz Bay recorded increased sedimentation rates and increased IRD supply during MIS 31, coupled to evidence for ocean warming from the elevated foraminiferal carbonate content. Therefore, these data do not support loss of the marine ice margin, consistent with model studies (Beltran et al., 2020), but do suggest some local instability and/or ice margin retreat. However, detailed stratigraphy is challenging through this period, in both ODP Site 1165 (Teitler et al., 2015) and the Ross Sea records (McKay et al., 2012b), and future research will be required to provide better constraints on Antarctic Ice Sheet dynamics during MIS 31.

11.6.3 Mid Pleistocene Transition

At the MPT (~900 ka), there was an intensification of glacial conditions and a major switch in the predominant cyclicity of global climate records (Figure 11.4). The ~41 kyr cycles of the early Pleistocene were replaced by ~100 kyr cycles in the late Pleistocene (Ruddiman et al., 1989; Lisiecki and Raymo, 2005), but the cause of this event remains unexplained. Early ideas included the crossing of a CO_2 threshold that made the Northern Hemisphere ice sheets more resistant to melting (Berger et al., 1999) or which influenced their sensitivity to integrated summer insolation forcing (Huybers, 2006); a change in the dynamics of those ice sheets linked to regolith removal from their base (Clark and Pollard, 1998); a transition from predominantly terrestrial-based ice sheets to expanded marine-based ice sheets in Antarctica (Raymo et al., 2006); or a change in bottom water formation around Antarctica that enhanced glacial ocean carbon storage (Paillard and Parrenin, 2004). While the Northern Hemisphere mechanisms continue to be explored (Willeit et al., 2019), here we focus on the two mechanisms linked to Antarctica and discuss the new constraints that have emerged in recent years to test them.

11.6.3.1 Role of Antarctic Ice Sheet dynamics

Raymo et al. (2006) suggested that the MPT may have resulted from a change in Antarctic Ice Sheet dynamics, specifically the development of marine-based ice sheets in Antarctica. In this hypothesis, the dominant 41 kyr signal in global climate records before the MPT is explained as an in-phase response of the Antarctic and Northern Hemisphere ice sheets to obliquity forcing. Because the influence of precession forcing is out of phase between the hemispheres, it was proposed that the precession component of ice sheet variance was out of phase, such that the coincidence of Northern Hemisphere ice sheet advance with Antarctic Ice Sheet retreat led to an approximate cancelling out of the precession signal in globally-integrated $\delta^{18}O$ records. According to this hypothesis, the expansion of marine-based ice sheets in Antarctica at the MPT would have resulted in an increased sensitivity of the Antarctic Ice Sheet to Northern Hemisphere climate and ice volume variability, propagated through changes in ocean circulation and sea level. Hence, more synchronous ice sheet behaviour would emerge at this time, leading to greater overall ice volumes and stronger ~21 kyr and ~100 kyr signals (Raymo et al., 2006). Evidence from a benthic foraminiferal $\delta^{18}O$ record in the deep Southwest Pacific Ocean was taken to support an increase in Antarctic ice volume at the MPT (Elderfield et al., 2012) (Figure 11.4b), but this scenario is equivocal because that record could have been influenced by regional changes in deep ocean circulation (Ford and Raymo, 2020), while the location of ice build-up cannot be determined by this method.

The idea of a switch from a terrestrial to a marine-based EAIS (Raymo et al., 2006) can now be addressed with more direct evidence, in particular from Site U1361 which constrains changes in the vicinity of the Wilkes Subglacial Basin (Figure 11.2). The key observation here, based on a range of sedimentological and geochemical evidence, is that a marine-based ice sheet existed in East

Antarctica from the Early Pliocene to the early Pleistocene (Escutia et al., 2011; Patterson et al., 2014), periodically extending to the continental shelf edge (Reinardy et al., 2015), and also in the late Pleistocene (Wilson et al., 2018) and presumably in between (Bertram, 2018). Therefore, it is hard to support the idea that the MPT originated from a switch from a smaller terrestrial EAIS to an expanded marine-based EAIS. For the WAIS, there is also strong evidence from the Ross Sea (AND-1B) (Figure 11.2) for marine margins in both the Pliocene and Pleistocene (Naish et al., 2009), and for a control on its dynamics by obliquity rather than precession cycles in the Pliocene and early Pleistocene (Naish et al., 2009). In contrast to those observations, and depending on the climate scenario, some ice sheet model runs have suggested that a switch to a marine-based WAIS could have occurred at around the MPT (Sutter et al., 2019). A ~200-kyr long unconformity at around this time in the ANDRILL record would be consistent with the expansion of a marine-based ice sheet in the Ross Sea Embayment at the MPT, and is interpreted as representing a cooling climate in the high southern latitudes that allowed ice shelves to persist into interglacial periods (McKay et al., 2009; McKay et al., 2012b). However, even if the WAIS expanded at this time, it would not be possible to explain the majority of the MPT ice volume signal in this way.

While the above evidence does not support a transition between a terrestrial and a marine Antarctic Ice Sheet at the MPT, it is interesting that temporal shifts in the orbital cyclicity of IRD records from the EAIS have been recorded within the Plio-Pleistocene. For example, Patterson et al. (2014) demonstrate a much earlier switch in the orbital behaviour of the EAIS in the Wilkes Subglacial Basin, with IRD records from Site U1361 indicating ~41 kyr cyclicity during the warm Mid Pliocene followed by a shift to ~21 kyr and ~100 kyr cyclicity around the onset of the Pleistocene. Hence, the idea that local forcing could create ~21 kyr cyclicity in Antarctic Ice Sheet dynamics during the early Pleistocene (Raymo et al., 2006) appears to be supported, and such changes could conceivably have been cancelled out in marine $\delta^{18}O$ records by similar opposing changes in the Northern Hemisphere. However, the significant IRD content indicates the presence of a marine-terminating margin during the early Pleistocene, so this Antarctic precession signal was clearly not the result of a terrestrial EAIS. Instead, Patterson et al. (2014) suggested that an increased sea ice extent linked to Plio-Pleistocene cooling could have shielded the early Pleistocene ice sheet from marine forcing and left it relatively more sensitive to local precession forcing. The growth of Northern Hemisphere ice sheets and an accompanying decrease in global sea level has also been proposed to play a possible role in increasing the stability of the marine sectors of the EAIS within the early Pleistocene (Jakob et al., 2020).

The late Pleistocene IRD record at Site U1361 was generated from material deposited under lower sedimentation rates than during the Pliocene, making it difficult to characterise orbital cyclicity (Wilson et al., 2018). Nevertheless, the observation of IRD pulses during terminations of the last five glacial periods appears consistent with Antarctic Ice Sheet variability that was synchronised to changes in the Northern Hemisphere ice sheets. Modelling studies suggest that synchronisation in the late Pleistocene could arise through a combination of global sea level and CO_2 changes (Tigchelaar et al., 2018; Gomez et al., 2020), and the deglacial sea level forcing acting on the marine margins of the Antarctic Ice Sheet would certainly have increased with the development of larger Northern Hemisphere ice sheets at the MPT. In addition, larger Northern Hemisphere ice sheets since the MPT may have displayed more dynamic behaviour (Hodell et al., 2008), potentially leading to increased millennial variability in the Atlantic deep ocean circulation and a stronger bipolar seesaw (Stocker and Johnsen, 2003). If early interglacial retreat of the Antarctic Ice Sheet occurred in response to heat transport changes during terminal Heinrich Stadial events (Marino et al., 2015; Rohling et al., 2019; Clark et al., 2020), such a scenario could effectively synchronise the ice sheets on orbital timescales, even while the behaviour is asynchronous on millennial timescales. Overall, while changes in the magnitude and length of glacial cycles at the MPT are likely to have affected the

behaviour of the Antarctic Ice Sheet, there is a lack of evidence at present to suggest that a change in Antarctic Ice Sheet dynamics played the significant role in this transition.

11.6.3.2 Role of the Southern Ocean carbon cycle

In light of the dominant control of Southern Ocean processes on the late Pleistocene carbon cycle (Figure 11.6), this region is a strong candidate to have played a role in the declining glacial atmospheric CO_2 levels at the MPT (Figure 11.4h). As proposed by Paillard and Parrenin (2004), changes in SST or sea ice extent could impact on polar ocean stratification, deep ocean circulation, and carbon storage, leading to extended glacial periods that are more resistant to deglaciation. A recent study has tested this idea using paired planktonic and benthic $\delta^{18}O$ records from ODP Site 1094 to reconstruct the surface stratification of the Southern Ocean Antarctic Zone across the MPT (Hasenfratz et al., 2019). These authors demonstrated that a stronger halocline has formed during glacial periods since the MPT, in association with reduced communication between the deep ocean and the Antarctic surface, with these two factors potentially combining to form a positive feedback loop. In this scenario, glacial carbon storage could be enhanced and a stronger orbital forcing would be required to initiate deglacial carbon release, allowing glacial periods to be extended and larger Northern Hemisphere ice sheets to grow (Hasenfratz et al., 2019). This mechanism is supported by atmospheric CO_2 reconstructions from marine boron isotope records (Hönisch et al., 2009; Chalk et al., 2017) (Figure 11.4h) and from Antarctic blue-ice cores (Higgins et al., 2015; Yan et al., 2019), which indicate a decline in glacial CO_2 levels of ~30 ppm at the MPT. A change of this magnitude is readily achievable through changes in the Antarctic Zone (Hain et al., 2010; Watson et al., 2015), but the CO_2 records do not uniquely constrain the mechanism of carbon drawdown. A further complexity is that while a period of global cooling preceding the MPT may have pre-conditioned the Earth for such a mechanism (Snyder, 2016) (Figure 11.4c), the stalling of global average temperatures at ~1.2 Ma suggests that another trigger was ultimately required to generate the ice volume increase at ~800-900 ka (Figure 11.4a,b).

Evidence for changes in deep ocean circulation and chemistry in the Atlantic Ocean is recorded across the MPT, including a weakening or shoaling of the glacial AMOC (neodymium isotopes; Pena and Goldstein, 2014) that coincided with enhanced deep ocean carbon storage (benthic B/Ca and Cd/Ca; Farmer et al., 2019). Those records are consistent with the Southern Ocean circulation changes expected from the Antarctic Zone mechanism (Ferrari et al., 2014; Hasenfratz et al., 2019). Furthermore, the distinct circulation switch during MIS 22-24 (Pena and Goldstein, 2014) appears to have coincided with the glacial ice volume expansion at ~900 ka (Elderfield et al., 2012), which suggests that a sensitive response of the ocean circulation to a combination of forcings may have ultimately determined the timing for the emergence of the 100 kyr cycles. Low orbital eccentricity at ~900 ka has been proposed to play a role, although the extent to which orbital forcing acted as a Northern Hemisphere (Pena and Goldstein, 2014) or Southern Hemisphere (Elderfield et al., 2012) driver remains to be determined. Further work will be required to understand the mechanistic links between near-surface stratification and deep water formation in the Southern Ocean, as well as the feedbacks between Southern Ocean processes, Atlantic Ocean circulation, and the Northern Hemisphere ice sheets during this interval.

Evidence for Subantarctic Zone changes has also been obtained over the MPT, with planktonic foraminiferal Mg/Ca and $\delta^{18}O$ reconstructions at ODP Site 1090 indicating an early cooling and freshening of the surface ocean during glacial periods at ~1250 ka (Rodríguez-Sanz et al., 2012). Those results could indicate either a sea ice expansion or a latitudinal migration of the westerly wind belt driving shifts in the Southern Ocean fronts (Rodríguez-Sanz et al., 2012), which may have helped precondition the Earth system for the changes at the MPT. In addition, glacial dust fluxes in the Subantarctic Zone of the Atlantic sector approximately doubled at the MPT (Martinez-Garcia et al.,

2011) (Figure 11.4i), which suggests that iron fertilisation of surface ocean productivity could have contributed to the glacial carbon drawdown at the MPT and to longer-lasting glacial periods thereafter (Martinez-Garcia et al., 2011; Chalk et al., 2017). Although fertilisation of the Subantarctic Zone in the late Pleistocene is responsible for ~30 ppm glacial CO_2 drawdown (Hain et al., 2010), the dust changes at the MPT might be expected to have arisen as a result of increased global ice volume and reduced sea level, in which case this process may have acted as a positive feedback rather than as the trigger for the MPT, similar to its role during more recent glacial cycles (Figure 11.6).

At present, Antarctic ice core records do not extend across the MPT (Bereiter et al., 2015) and CO_2 reconstructions from marine proxies have lower resolution and larger uncertainties (Hönisch et al., 2009; Chalk et al., 2017) (Figure 11.4h). Therefore, obtaining continuous ice core records across this interval is an important target (Fischer et al., 2013; Sutter et al., 2019). High resolution records of Antarctic climate, sea ice, dust, and atmospheric CO_2, all measured in the same archive, will be invaluable for determining which combination of these mechanisms and feedbacks was responsible for the MPT.

11.7 Future research on Antarctica in the Pleistocene

11.7.1 Motivation and outlook

The boundary conditions and climatic forcing affecting each sector of the Antarctic Ice Sheet, and indeed each ice stream, are different (e.g. subglacial bedrock topography, basal lithology, shelf width and geometry, proximity to CDW inflow, ice shelf extent). Hence, a spatial perspective is critical for understanding the past and future responses of the ice sheet to climate change. While this chapter has highlighted the existing reconstructions that constrain the dynamic behaviour of the WAIS and EAIS in the Pleistocene, their value is limited by the small number of observations and their restricted spatial distribution, as well as in some cases by poor temporal resolution.

With the challenges of drilling in the Southern Ocean and on the Antarctic margin, there have been relatively few expeditions of the IODP (and its precursors) to this region, with only 7 expeditions in its first 50 years from 1968 to 2017 (Figure 11.2; white squares). Following the success of IODP Expedition 318 to the George V Land margin of East Antarctica in 2010, a concerted community effort led to four expeditions to the Antarctic margin and/or high latitude Southern Ocean in 2018 and 2019 (Figure 11.2; yellow squares). It is anticipated that samples from these expeditions will significantly improve upon the existing spatial and temporal resolution of records of Antarctic and Southern Ocean variability in the Pleistocene, particularly along the WAIS margin. However, increased efforts to obtain Pleistocene records of EAIS variability are required, particularly from the margins of the marine-based basins.

As well as records of ice sheet behaviour, improved spatial coverage in records of changing Southern Ocean processes and properties is required, including evidence on sea ice formation, upwelling, deep convection, dust supply, productivity, surface fronts, and oceanic temperatures on the shelves and near the ice margins. In particular, there is a strong need for better records of oceanic temperatures at intermediate water depths near the continental shelf breaks, which models indicate to be a key control on ice shelf thinning that can trigger marine-based ice sheet retreat. Another important target is to constrain changes in Southern Ocean sea ice formation, which influences the locations and strengths of deep convection during the Pleistocene. Both oceanic temperatures and sea ice show complex spatial variability, and neither are well reproduced in the current generation of ocean circulation or climate models. New paleo-data will therefore be important for indicating system behaviour and for ground-truthing new and improved modelling approaches. For sea ice, the

Cycles of Sea-Ice Dynamics in the Earth System (C-SIDE) working group of PAGES has been addressing some of these issues, for example by compiling a database of proxy data for the last glacial cycle, identifying data gaps, and conducting data-model comparisons (Chadwick et al., 2019), with the seasonality of sea ice emerging as an important factor to consider (Green et al., 2020). In combination, better records of sea ice extent, ocean temperatures, and deep water formation will guide a better understanding of the various dynamic feedbacks between the ice sheets and the ocean. More broadly, evidence on ice sheet-ocean-climate interactions in the Southern Ocean is crucial for understanding the role of Southern Hemisphere processes in heat and carbon transport, over timescales ranging from glacial-interglacial cycles through to millennial and sub-centennial climate variability.

By way of introducing some of this exciting future research, we end this chapter with a brief overview of the sediment sequences recovered in four recent IODP expeditions (Figure 11.2). The discussion below is limited to preliminary findings from immediate shipboard observations, whereas the science emanating from those expeditions, both individually and when synthesised together, will fuel at least the next decade of research on the Pleistocene history of Antarctica. It is anticipated that future analysis of these cores will allow us to address many crucial questions that remain about Antarctica's role in the global climate system.

11.7.2 IODP Expedition 374: Ross Sea West Antarctic Ice Sheet History

In 2018, IODP Expedition 374 drilled a latitudinal and depth transect of five sites (U1521-1525) from the shelf to the rise in the Ross Sea (Figure 11.2). The aim was to evaluate the Neogene to Quaternary response of the WAIS to ocean and atmospheric forcing, orbital forcing, and sea level forcing under a range of climatic boundary conditions, and to establish its contribution to far-field sea level change (McKay et al., 2019). In total, 1293 m of high-quality sediment cores from five sites were recovered, spanning the early Miocene to late Pleistocene. Because the shelf sites were located on the outer shelf, they will provide complementary evidence on climate forcing and WAIS behaviour to the existing records from the more ice-proximal ANDRILL sites in the western Ross Sea.

Coring at Sites U1521 and U1522 on the shelf recovered some Pleistocene sections that will help constrain the shelf environment, but recovery was very poor in the Pleistocene intervals of these cores. At the shelf-edge, Site U1523 is well placed to evaluate Plio-Pleistocene changes in the Antarctic Slope Current, which could exert an important control on ice sheet stability because it influences the ability of modified CDW to penetrate onto the Ross Sea shelf. At deeper depths on the continental slope, Site U1525 will provide a complimentary view on the Antarctic Slope Current from early to mid Pleistocene strata. Continental rise Site U1524 is the deepest site, located on the southeastern levee of the Hillary Canyon, one of the largest conduits for newly-formed Ross Sea Bottom Water (a type of AABW). Drilling at this site recovered a mostly continuous ~120 m long Pleistocene record of AABW outflow. This expanded record is particularly exciting because it opens up the prospect of coupling evidence on the ice margin behaviour, based on turbidite activity and IRD/fine-grained sediment provenance, to a highly resolved record of changes in climate, meltwater input, and AABW production (McKay et al., 2019).

11.7.3 IODP Expedition 379: Amundsen Sea West Antarctic Ice Sheet History

The primary goal of IODP Expedition 379 in 2019 was to constrain the past behaviour of the WAIS in the Amundsen Sea Embayment (Gohl et al., 2019) (Figure 11.2), a region that is currently experiencing significant and rapid ice loss (Shepherd et al., 2018) and in which ice sheet retreat by marine ice sheet instability may already be underway (Joughin et al., 2014; Rignot et al., 2014).

Unlike the Ross Sea or Weddell Sea, this setting benefits from the ability to record changes in WAIS dynamics with no direct influence from the EAIS.

Continuous Plio-Pleistocene records were obtained from the continental rise at Sites U1532 and U1533 (Figure 11.2) and are characterised by strong lithological cyclicity. These cycles are inferred to be related to glacial-interglacial changes in glacially-derived sediment inputs to the Southern Ocean, and to oceanographic variability linked to the wind-driven currents of the Antarctic Circumpolar Current. Analyses of IRD accumulation rates and provenance hold the potential to constrain potential retreat or collapse events, and in particular to assess changes during super-interglacials of the late Pleistocene (e.g. MIS 11) and earlier Pleistocene (e.g. MIS 31).

11.7.4 IODP Expedition 382: Iceberg Alley and Subantarctic Ice and Ocean Dynamics

IODP Expedition 382 in 2019 targeted the first deep drilling in the Scotia Sea, with the goal of constraining the Plio-Pleistocene dynamics of the Antarctic Ice Sheet and its role in sea level variations, as well as exploring ice sheet-ocean-atmosphere interactions in the wider region (Weber et al., 2019). The South Scotia Sea lies in the pathway of 'Iceberg Alley', where icebergs escape the coastal ocean into the Antarctic Circumpolar Current, making it an excellent location to trace iceberg calving (IRD fluxes) and sources (geochemical provenance tracing). South Falkland Slope sites were also drilled, in a sensitive location to trace movements of the Subantarctic Front and AAIW properties, as well as westerly wind changes and iron fertilisation of surface ocean productivity.

The Scotia Sea sites (U1536-1538; Figure 11.2) recovered diatom oozes and silty clays that form a continuous Plio-Pleistocene record. The Pleistocene sediments show clear glacial-interglacial variability in physical properties, colour, and biogenic opal content, and will provide crucial evidence on Antarctic Ice Sheet variability, Drake Passage throughflow, and shifts in ocean fronts and sea ice over this interval. These continuous high-resolution records will allow the effects of Northern Hemisphere Glaciation, the MPT, and the MBE to be explored, with preliminary shipboard data indicating the potential for a high fidelity orbital signal to be present in these records. The South Falkland Slope sites (U1534, U1535; outside the map area of Figure 11.2) recovered late Pliocene and Pleistocene foraminifera-bearing silts and clays, including a continuous late Pleistocene section back to ~700 ka that should allow millennial variability in frontal positions and AAIW properties to be reconstructed back to at least MIS 17, as well as providing some earlier Pleistocene and late Pliocene snapshots.

11.7.5 IODP Expedition 383: Dynamics of Pacific Antarctic Circumpolar Current

IODP Expedition 383 to the South and Southeast Pacific in 2019 did not directly target Antarctic Ice Sheet dynamics, but will provide important evidence on Miocene to Holocene atmosphere-ocean-climate dynamics in the Southern Ocean region (Lamy et al., 2019). Specifically, it fills a significant spatial gap in records of the Antarctic Circumpolar Current, which was previously mostly constrained in the Atlantic and Indian sectors. Its main focus was on recovering changes in the past vertical structure of the Antarctic Circumpolar Current on glacial-interglacial and millennial timescales, as well as exploring changes during super-interglacials and the MPT. The results from this expedition will be highly complementary for interpreting the more proximal records of Antarctic Ice Sheet variability from other recent expeditions, both by providing information on the ocean conditions influencing the ice sheet, and by revealing how the ice sheet has influenced ocean circulation and climate.

Sites in the central South Pacific (U1539, U1540, U1541) and eastern South Pacific (U1543) recovered diatom and carbonate oozes from the northern margin of the Antarctic Circumpolar Current at 3.6-4.1 km depth. Site U1539 will provide a particularly valuable Pleistocene record of Lower CDW paleoceanography because of its high late Pleistocene sedimentation rates and its continuation through the MPT. Nearby Site U1540 has a lower sedimentation rate, but extends through much of the Plio-Pleistocene, while sites U1541 and U1543 also contain mostly continuous records that extend back into the Miocene. The Chile margin sites (U1542, U1544) are located at shallower water depths of 1.1 km and 2.1 km and will provide high-resolution late Pleistocene records. Despite the dominance of siliciclastic sediments, these two sites will be suitable for monitoring late Pleistocene changes in AAIW and CDW properties and flow, providing insight into interconnected changes in the Southern Hemisphere ice sheet-ocean-climate system.

Acknowledgments

We thank the reviewers for their positive and helpful comments on this chapter. DJW and TvdF acknowledge the Natural Environment Research Council, the Leverhulme Trust, and the Kristian Gerhard Jebsen Foundation for supporting their Southern Ocean and Antarctic research. RMM was funded by the NZ Marsden Fund (18-VUW-089).

References

Abram, N.J., Wolff, E.W., Curran, M.A.J., 2013. A review of sea ice proxy information from polar ice cores. Quat. Sci. Rev. 79, 168-183.

Aciego, S.M., Bourdon, B., Lupker, M., Rickli, J., 2009. A new procedure for separating and measuring radiogenic isotopes (U, Th, Pa, Ra, Sr, Nd, Hf) in ice cores. Chemical Geology 266, 194-204.

Adkins, J.F., 2013. The role of deep ocean circulation in setting glacial climates. Paleoceanography 28, 539-561.

Adkins, J.F., Cheng, H., Boyle, E.A., Druffel, E.R.M., Edwards, R.L., 1998. Deep-sea coral evidence for rapid change in ventilation of the deep North Atlantic 15,400 years ago. Science 280, 725-728.

Adkins, J.F., McIntyre, K., Schrag, D.P., 2002. The salinity, temperature, and $\delta^{18}O$ of the glacial deep ocean. Science 298, 1769-1773.

Aitken, A.R.A., Urosevic, L., 2021. A probabilistic and model-based approach to the assessment of glacial detritus from ice sheet change. Palaeogeography, Palaeoclimatology, Palaeoecology 561, 110053, doi: 10.1016/j.palaeo.2020.110053

Allen, C.S., Pike, J., Pudsey, C.J., Leventer, A., 2005. Submillennial variations in ocean conditions during deglaciation based on diatom assemblages from the southwest Atlantic. Paleoceanography 20, PA2012, doi: 10.1029/2004PA001055.

Alley, K.E., Scambos, T.A., Siegfried, M.R., Fricker, H.A., 2016. Impacts of warm water on Antarctic ice shelf stability through basal channel formation. Nat. Geosci. 9, 290-293.

Alley, R.B., 2010. Reliability of ice-core science: historical insights. Journal of Glaciology 56, 1095-1103.

Alley, R.B., MacAyeal, D.R., 1994. Ice-rafted debris associated with binge/purge oscillations of the Laurentide Ice Sheet. Paleoceanography 9, 503-511.

Anderson, D.M., Archer, D., 2002. Glacial–interglacial stability of ocean pH inferred from foraminifer dissolution rates. Nature 416, 70-73.

Anderson, J.B., Conway, H., Bart, P.J., Witus, A.E., Greenwood, S.L., McKay, R.M., Hall, B.L., Ackert, R.P., Licht, K., Jakobsson, M., 2014. Ross Sea paleo-ice sheet drainage and deglacial history during and since the LGM. Quat. Sci. Rev. 100, 31-54.

Anderson, R.F., Ali, S., Bradtmiller, L.I., Nielsen, S.H.H., Fleisher, M.Q., Anderson, B.E., Burckle, L.H., 2009. Wind-driven upwelling in the Southern Ocean and the deglacial rise in atmospheric CO_2. Science 323, 1443-1448.

Anderson, R.F., Sachs, J.P., Fleisher, M.Q., Allen, K.A., Yu, J., Koutavas, A., Jaccard, S.L., 2019. Deep-Sea Oxygen Depletion and Ocean Carbon Sequestration During the Last Ice Age. Glob. Biogeochem. Cycle 33, 301-317.

Ashley, K.E., McKay, R., Etourneau, J., Jimenez-Espejo, F.J., Condron, A., Albot, A., Crosta, X., Riesselman, C., Seki, O., Massé, G., Golledge, N.R., Gasson, E., Lowry, D.P., Barrand, N.E., Johnson, K.,

Bertler, N., Escutia, C., Dunbar, R., Bendle, J.A., 2021. Mid-Holocene Antarctic sea-ice increase driven by marine ice sheet retreat. Clim. Past 17, 1-19.

Austermann, J., Pollard, D., Mitrovica, J.X., Moucha, R., Forte, A.M., DeConto, R.M., Rowley, D.B., Raymo, M.E., 2015. The impact of dynamic topography change on Antarctic ice sheet stability during the mid-Pliocene warm period. Geology 43, 927-930.

Bailey, I., Hole, G.M., Foster, G.L., Wilson, P.A., Storey, C.D., Trueman, C.N., Raymo, M.E., 2013. An alternative suggestion for the Pliocene onset of major northern hemisphere glaciation based on the geochemical provenance of North Atlantic Ocean ice-rafted debris. Quat. Sci. Rev. 75, 181-194.

Barker, S., Cacho, I., Benway, H., Tachikawa, K., 2005. Planktonic foraminiferal Mg/Ca as a proxy for past oceanic temperatures: a methodological overview and data compilation for the Last Glacial Maximum. Quat. Sci. Rev. 24, 821-834.

Barker, S., Chen, J., Gong, X., Jonkers, L., Knorr, G., Thornalley, D., 2015. Icebergs not the trigger for North Atlantic cold events. Nature 520, 333-336.

Barker, S., Diz, P., Vautravers, M.J., Pike, J., Knorr, G., Hall, I.R., Broecker, W.S., 2009. Interhemispheric Atlantic seesaw response during the last deglaciation. Nature 457, 1097-1102.

Barker, S., Knorr, G., Edwards, R.L., Parrenin, F., Putnam, A.E., Skinner, L.C., Wolff, E., Ziegler, M., 2011. 800,000 years of abrupt climate variability. Science 334, 347-351.

Barlow, N.L.M., McClymont, E.L., Whitehouse, P.L., Stokes, C.R., Jamieson, S.S.R., Woodroffe, S.A., Bentley, M.J., Callard, S.L., Cofaigh, C.Ó., Evans, D.J.A., 2018. Lack of evidence for a substantial sea-level fluctuation within the Last Interglacial. Nat. Geosci. 11, 627-634.

Barnes, D.K.A., Hillenbrand, C.D., 2010. Faunal evidence for a late Quaternary trans-Antarctic seaway. Global Change Biology 16, 3297-3303.

Bart, P.J., Coquereau, L., Warny, S., Majewski, W., 2016. In situ foraminifera in grounding zone diamict: a working hypothesis. Antarct. Sci. 28, 313-321.

Bart, P.J., De Batist, M., Jokat, W., 1999. Interglacial collapse of Crary Trough-mouth fan, Weddell Sea, Antarctica; implications for Antarctic glacial history. Journal of Sedimentary Research 69, 1276-1289.

Bart, P.J., DeCesare, M., Rosenheim, B.E., Majewski, W., McGlannan, A., 2018. A centuries-long delay between a paleo-ice-shelf collapse and grounding-line retreat in the Whales Deep Basin, eastern Ross Sea, Antarctica. Sci Rep 8, 12392, doi: 10.1038/s41598-018-29911-8.

Bart, P.J., Iwai, M., 2012. The overdeepening hypothesis: how erosional modification of the marine-scape during the early Pliocene altered glacial dynamics on the Antarctic Peninsula's Pacific margin. Palaeogeography, Palaeoclimatology, Palaeoecology 335, 42-51.

Bassinot, F.C., Labeyrie, L.D., Vincent, E., Quidelleur, X., Shackleton, N.J., Lancelot, Y., 1994. The astronomical theory of climate and the age of the Brunhes-Matuyama magnetic reversal. Earth Planet. Sci. Lett. 126, 91-108.

Bauersachs, T., Rochelmeier, J., Schwark, L., 2015. Seasonal lake surface water temperature trends reflected by heterocyst glycolipid-based molecular thermometers. Biogeosciences 12, 3741-3751.

Bauska, T.K., Baggenstos, D., Brook, E.J., Mix, A.C., Marcott, S.A., Petrenko, V.V., Schaefer, H., Severinghaus, J.P., Lee, J.E., 2016. Carbon isotopes characterize rapid changes in atmospheric carbon dioxide during the last deglaciation. Proceedings of the National Academy of Sciences 113, 3465-3470.

Becquey, S., Gersonde, R., 2003. A 0.55-Ma paleotemperature record from the Subantarctic zone: Implications for Antarctic Circumpolar Current development. Paleoceanography 18, 1014, doi: 10.1029/2000PA000576.

Beltran, C., Golledge, N.R., Ohneiser, C., Kowalewski, D.E., Sicre, M.-A., Hageman, K.J., Smith, R., Wilson, G.S., Mainié, F., 2020. Southern Ocean temperature records and ice-sheet models demonstrate rapid Antarctic ice sheet retreat under low atmospheric CO_2 during Marine Isotope Stage 31. Quat. Sci. Rev. 228, 106069, doi: 10.1016/j.quascirev.2019.106069.

Benz, V., Esper, O., Gersonde, R., Lamy, F., Tiedemann, R., 2016. Last Glacial Maximum sea surface temperature and sea-ice extent in the Pacific sector of the Southern Ocean. Quat. Sci. Rev. 146, 216-237.

Bereiter, B., Eggleston, S., Schmitt, J., Nehrbass-Ahles, C., Stocker, T.F., Fischer, H., Kipfstuhl, S., Chappellaz, J., 2015. Revision of the EPICA Dome C CO_2 record from 800 to 600 kyr before present. Geophys. Res. Lett. 42, 542-549.

Bereiter, B., Shackleton, S., Baggenstos, D., Kawamura, K., Severinghaus, J., 2018. Mean global ocean temperatures during the last glacial transition. Nature 553, 39-44.

Berger, A., Li, X.S., Loutre, M.-F., 1999. Modelling northern hemisphere ice volume over the last 3 Ma. Quat. Sci. Rev. 18, 1-11.

Berger, A., Loutre, M.F., 1991. Insolation values for the climate of the last 10 million years. Quat. Sci. Rev. 10, 297-317.

Berger, W.H., 1999. The 100-kyr ice-age cycle: internal oscillation or inclinational forcing? International Journal of Earth Sciences 88, 305-316.

Bertler, N.A.N., Conway, H., Dahl-Jensen, D., Emanuelsson, D.B., Winstrup, M., Vallelonga, P.T., Lee, J.E., Brook, E.J., Severinghaus, J.P., Fudge, T.J., 2018. The Ross Sea Dipole-temperature, snow accumulation and sea ice variability in the Ross Sea region, Antarctica, over the past 2700 years. Clim. Past. 14, 193-214.

Bertram, R.A., 2018. Reconstructing the East Antarctic Ice Sheet during the Plio-Pleistocene using Geochemical Provenance Analysis. PhD thesis, Imperial College London.

Bertram, R.A., Wilson, D.J., van de Flierdt, T., McKay, R.M., Patterson, M.O., Jimenez-Espejo, F.J., Escutia, C., Duke, G.C., Taylor-Silva, B.I., Riesselmann, C.R., 2018. Pliocene deglacial event timelines and the biogeochemical response offshore Wilkes Subglacial Basin, East Antarctica. Earth Planet. Sci. Lett. 494, 109-116.

Bintanja, R., van de Wal, R.S.W., Oerlemans, J., 2005. Modelled atmospheric temperatures and global sea levels over the past million years. Nature 437, 125-128.

Birner, B., Hodell, D.A., Tzedakis, P.C., Skinner, L.C., 2016. Similar millennial climate variability on the Iberian margin during two early Pleistocene glacials and MIS 3. Paleoceanography 31, 203-217.

Blackburn, T., Edwards, G.H., Tulaczyk, S., Scudder, M., Piccione, G., Hallet, B., McLean, N., Zachos, J.C., Cheney, B., Babbe, J.T., 2020. Ice retreat in Wilkes Basin of East Antarctica during a warm interglacial. Nature 583, 554-559.

Blasco, J., Tabone, I., Alvarez-Solas, J., Robinson, A., Montoya, M., 2019. The Antarctic Ice Sheet response to glacial millennial-scale variability. Clim. Past. 15, 121-133.

Blunier, T., Brook, E.J., 2001. Timing of millennial-scale climate change in Antarctica and Greenland during the last glacial period. Science 291, 109-112.

Bond, G., Heinrich, H., Broecker, W., Labeyrie, L., McManus, J., Andrews, J., Huon, S., Jantschik, R., Clasen, S., Simet, C., Tedesco, K., Klas, M., Bonani, G., Ivy, S., 1992. Evidence for massive discharges of icebergs into the North Atlantic Ocean during the last glacial period. Nature 360, 245-249.

Bond, G., Showers, W., Cheseby, M., Lotti, R., Almasi, P., deMenocal, P., Priore, P., Cullen, H., Hajdas, I., Bonani, G., 1997. A pervasive millennial-scale cycle in North Atlantic Holocene and glacial climates. Science 278, 1257-1266.

Bonn, W.J., Gingele, F.X., Grobe, H., Mackensen, A., Futterer, D.K., 1998. Palaeoproductivity at the Antarctic continental margin: opal and barium records for the last 400 ka. Paleogeogr. Paleoclimatol. Paleoecol. 139, 195-211.

Bouttes, N., Paillard, D., Roche, D.M., 2010. Impact of brine-induced stratification on the glacial carbon cycle. Clim. Past. 6, 575-589.

Boyle, E.A., 1988a. Cadmium: Chemical tracer of deepwater paleoceanography. Paleoceanography 3, 471-489.

Boyle, E.A., 1988b. Vertical oceanic nutrient fractionation and glacial/interglacial CO_2 cycles. Nature 331, 55-56.

Boyle, E.A., Keigwin, L.D., 1982. Deep circulation of the North Atlantic over the last 200,000 years: Geochemical evidence. Science 218, 784-787.

Bradley, S.L., Siddall, M., Milne, G.A., Masson-Delmotte, V., Wolff, E., 2012. Where might we find evidence of a Last Interglacial West Antarctic Ice Sheet collapse in Antarctic ice core records? Glob. Planet. Change 88, 64-75.

Bradtmiller, L.I., McManus, J.F., Robinson, L.F., 2014. $^{231}Pa/^{230}Th$ evidence for a weakened but persistent Atlantic meridional overturning circulation during Heinrich Stadial 1. Nature Communications 5, 5817, doi: 10.1038/ncomms6817.

Broecker, W., Clark, E., 2001. An evaluation of Lohmann's foraminifera weight dissolution index. Paleoceanography 16, 531-534.

Broecker, W.S., 1998. Paleocean circulation during the last deglaciation: A bipolar seesaw? Paleoceanography 13, 119-121.

Broecker, W.S., Bond, G., Klas, M., Bonani, G., Wolfli, W., 1990. A salt oscillator in the glacial Atlantic? 1. The concept. Paleoceanography 5, 469-477.

Broecker, W.S., Denton, G.H., 1989. The role of ocean-atmosphere reorganizations in glacial cycles. Geochim. Cosmochim. Acta 53, 2465-2501.

Broecker, W.S., Peteet, D.M., Rind, D., 1985. Does the ocean-atmosphere system have more than one stable mode of operation? Nature 315, 21-26.

Bronselaer, B., Winton, M., Griffies, S.M., Hurlin, W.J., Rodgers, K.B., Sergienko, O.V., Stouffer, R.J., Russell, J.L., 2018. Change in future climate due to Antarctic meltwater. Nature 564, 53-58.

Brook, E.J., Buizert, C., 2018. Antarctic and global climate history viewed from ice cores. Nature 558, 200-208.

Brovkin, V., Ganopolski, A., Archer, D., Rahmstorf, S., 2007. Lowering of glacial atmospheric CO_2 in response to changes in oceanic circulation and marine biogeochemistry. Paleoceanography 22, PA4202, doi: 10.1029/2006PA001380.

Buizert, C., Schmittner, A., 2015. Southern Ocean control of glacial AMOC stability and Dansgaard-Oeschger interstadial duration. Paleoceanography 30, 1595-1612.

Buizert, C., Sigl, M., Severi, M., Markle, B.R., Wettstein, J.J., McConnell, J.R., Pedro, J.B., Sodemann, H., Goto-Azuma, K., Kawamura, K., 2018. Abrupt ice-age shifts in southern westerly winds and Antarctic climate forced from the north. Nature 563, 681-685.

Burke, A., Robinson, L.F., 2012. The Southern Ocean's role in carbon exchange during the last deglaciation. Science 335, 557-561.

Capron, E., Govin, A., Stone, E.J., Masson-Delmotte, V., Mulitza, S., Otto-Bliesner, B., Rasmussen, T.L., Sime, L.C., Waelbroeck, C., Wolff, E.W., 2014. Temporal and spatial structure of multi-millennial temperature changes at high latitudes during the Last Interglacial. Quat. Sci. Rev. 103, 116-133.

Chadwick, M., Jones, J., Lawler, K., Prebble, J., Kohfeld, K., Crosta, X., 2019. Understanding glacial-interglacial changes in Southern Ocean sea ice. PAGES Magazine 27, 86.

Chalk, T.B., Hain, M.P., Foster, G.L., Rohling, E.J., Sexton, P.F., Badger, M.P.S., Cherry, S.G., Hasenfratz, A.P., Haug, G.H., Jaccard, S.L., 2017. Causes of ice age intensification across the Mid-Pleistocene Transition. Proceedings of the National Academy of Sciences 114, 13114-13119.

Chappell, J., Shackleton, N.J., 1986. Oxygen isotopes and sea level. Nature 324, 137-140.

Chase, Z., Anderson, R.F., Fleisher, M.Q., Kubik, P.W., 2002. The influence of particle composition and particle flux on scavenging of Th, Pa and Be in the ocean. Earth Planet. Sci. Lett. 204, 215-229.

Chen, T.Y., Robinson, L.F., Burke, A., Southon, J., Spooner, P., Morris, P.J., Ng, H.C., 2015. Synchronous centennial abrupt events in the ocean and atmosphere during the last deglaciation. Science 349, 1537-1541.

Cheng, H., Edwards, R.L., Broecker, W.S., Denton, G.H., Kong, X.G., Wang, Y.J., Zhang, R., Wang, X.F., 2009. Ice Age terminations. Science 326, 248-252.

Cheng, H., Edwards, R.L., Sinha, A., Spötl, C., Yi, L., Chen, S., Kelly, M., Kathayat, G., Wang, X., Li, X., 2016. The Asian monsoon over the past 640,000 years and ice age terminations. Nature 534, 640-646.

Clark, P.U., He, F., Golledge, N.R., Mitrovica, J.X., Dutton, A., Hoffman, J.S., Dendy, S., 2020. Oceanic forcing of penultimate deglacial and last interglacial sea-level rise. Nature 577, 660-664.

Clark, P.U., Pisias, N.G., 2000. Interpreting iceberg deposits in the deep sea. Science 290, 51.

Clark, P.U., Pollard, D., 1998. Origin of the middle Pleistocene transition by ice sheet erosion of regolith. Paleoceanography 13, 1-9.

Cody, R., Levy, R., Crampton, J., Naish, T., Wilson, G., Harwood, D., 2012. Selection and stability of quantitative stratigraphic age models: Plio-Pleistocene glaciomarine sediments in the ANDRILL 1B drillcore, McMurdo Ice Shelf. Glob. Planet. Change 96-97, 143-156.

Colleoni, F., De Santis, L., Montoli, E., Olivo, E., Sorlien, C.C., Bart, P.J., Gasson, E.G.W., Bergamasco, A., Sauli, C., Wardell, N., 2018. Past continental shelf evolution increased Antarctic ice sheet sensitivity to climatic conditions. Sci Rep 8, 11323, doi: 10.1038/s41598-018-29718-7.

Collins, G.E., Hogg, I.D., Convey, P., Sancho, L.G., Cowan, D.A., Lyons, W.B., Adams, B.J., Wall, D.H., Green, T.G.A., 2020. Genetic diversity of soil invertebrates corroborates timing estimates for past collapses of the West Antarctic Ice Sheet. Proceedings of the National Academy of Sciences 117, 22293-22302.

Collins, L.G., Allen, C.S., Pike, J., Hodgson, D.A., Weckström, K., Massé, G., 2013. Evaluating highly branched isoprenoid (HBI) biomarkers as a novel Antarctic sea-ice proxy in deep ocean glacial age sediments. Quat. Sci. Rev. 79, 87-98.

Collins, L.G., Pike, J., Allen, C.S., Hodgson, D.A., 2012. High-resolution reconstruction of southwest Atlantic sea-ice and its role in the carbon cycle during marine isotope stages 3 and 2. Paleoceanography 27, PA3217, doi: 10.1029/2011PA002264.

Colville, E.J., Carlson, A.E., Beard, B.L., Hatfield, R.G., Stoner, J.S., Reyes, A.V., Ullman, D.J., 2011. Sr-Nd-Pb isotope evidence for ice-sheet presence on southern Greenland during the Last Interglacial. Science 333, 620-623.

Conte, M.H., Sicre, M.A., Rühlemann, C., Weber, J.C., Schulte, S., Schulz-Bull, D., Blanz, T., 2006. Global temperature calibration of the alkenone unsaturation index ($U^{K'37}$) in surface waters and comparison with surface sediments. Geochemistry, Geophysics, Geosystems 7, Q02005, doi: 10.1029/2005GC001054.

Cook, C.P., Hill, D.J., van de Flierdt, T., Williams, T., Hemming, S.R., Dolan, A.M., Pierce, E.L., Escutia, C., Harwood, D., Cortese, G., 2014. Sea surface temperature control on the distribution of far-traveled Southern Ocean ice-rafted detritus during the Pliocene. Paleoceanography 29, 533-548.

Cook, C.P., van de Flierdt, T., Williams, T., Hemming, S.R., Iwai, M., Kobayashi, M., Jimenez-Espejo, F.J., Escutia, C., Gonzalez, J.J., Khim, B.K., McKay, R.M., Passchier, S., Bohaty, S.M., Riesselman, C.R., Tauxe, L., Sugisaki, S., Galindo, A.L., Patterson, M.O., Sangiorgi, F., Pierce, E.L., Brinkhuis, H., IODP Expedition 318 Scientists, 2013. Dynamic behaviour of the East Antarctic ice sheet during Pliocene warmth. Nat. Geosci. 6, 765-769.

Cook, M.S., Keigwin, L.D., 2015. Radiocarbon profiles of the NW Pacific from the LGM and deglaciation: evaluating ventilation metrics and the effect of uncertain surface reservoir ages. Paleoceanography 30, 174-195.

Cowan, E.A., Hillenbrand, C.-D., Hassler, L.E., Ake, M.T., 2008. Coarse-grained terrigenous sediment deposition on continental rise drifts: A record of Plio-Pleistocene glaciation on the Antarctic Peninsula. Palaeogeography, Palaeoclimatology, Palaeoecology 265, 275-291.

Croll, J., 1864. XIII. On the physical cause of the change of climate during geological epochs. The London, Edinburgh, and Dublin Philosophical Magazine and Journal of Science 28, 121-137.

Crosta, X., Sturm, A., Armand, L., Pichon, J.-J., 2004. Late Quaternary sea ice history in the Indian sector of the Southern Ocean as recorded by diatom assemblages. Mar. Micropaleontol. 50, 209-223.

Crutzen, P.J., Stoermer, E.F., 2000. The "Anthropocene". Global Change Newsletter 41, 17-18.

Cuffey, K.M., Clow, G.D., Steig, E.J., Buizert, C., Fudge, T., Koutnik, M., Waddington, E.D., Alley, R.B., Severinghaus, J.P., 2016. Deglacial temperature history of West Antarctica. Proceedings of the National Academy of Sciences 113, 14249-14254.

Curry, W.B., Oppo, D.W., 2005. Glacial water mass geometry and the distribution of $\delta^{13}C$ of ΣCO_2 in the western Atlantic Ocean. Paleoceanography 20, PA1017, doi: 10.1029/2004pa001021.

Dahl-Jensen, D., Albert, M.R., Aldahan, A., Azuma, N., Balslev-Clausen, D., Baumgartner, M., Berggren, A.-M., Bigler, M., Binder, T., Blunier, T., 2013. Eemian interglacial reconstructed from a Greenland folded ice core. Nature 493, 489-494.

Dansgaard, W., Johnsen, S.J., Clausen, H.B., Dahljensen, D., Gundestrup, N.S., Hammer, C.U., Hvidberg, C.S., Steffensen, J.P., Sveinbjornsdottir, A.E., Jouzel, J., Bond, G., 1993. Evidence for general instability of past climate from a 250-kyr ice-core record. Nature 364, 218-220.

de Boer, B., Lourens, L.J., van de Wal, R.S.W., 2014. Persistent 400,000-year variability of Antarctic ice volume and the carbon cycle is revealed throughout the Plio-Pleistocene. Nature Communications 5, 2999, doi: 10.1038/ncomms3999.

de la Rocha, C.L., Brzezinski, M.A., DeNiro, M.J., Shemesh, A., 1998. Silicon-isotope composition of diatoms as an indicator of past oceanic change. Nature 395, 680-683.

De Santis, L., Prato, S., Brancolini, G., Lovo, M., Torelli, L., 1999. The Eastern Ross Sea continental shelf during the Cenozoic: implications for the West Antarctic ice sheet development. Glob. Planet. Change 23, 173-196.

DeConto, R.M., Pollard, D., 2016. Contribution of Antarctica to past and future sea-level rise. Nature 531, 591-597.

DeConto, R.M., Pollard, D., Kowalewski, D., 2012. Modeling Antarctic ice sheet and climate variations during Marine Isotope Stage 31. Glob. Planet. Change 96, 181-188.

DeConto, R.M., Pollard, D., Wilson, P.A., Pälike, H., Lear, C.H., Pagani, M., 2008. Thresholds for Cenozoic bipolar glaciation. Nature 455, 652-656.

Denton, G.H., Anderson, R.F., Toggweiler, J.R., Edwards, R.L., Schaefer, J.M., Putnam, A.E., 2010. The last glacial termination. Science 328, 1652-1656.

Di Roberto, A., Colizza, E., Del Carlo, P., Petrelli, M., Finocchiaro, F., Kuhn, G., 2019. First marine cryptotephra in Antarctica found in sediments of the western Ross Sea correlates with englacial tephras and climate records. Sci Rep 9, 10628, doi: 10.1038/s41598-019-47188-3.

Domack, E.W., Jacobson, E.A., Shipp, S., Anderson, J.B., 1999. Late Pleistocene–Holocene retreat of the West Antarctic Ice-Sheet system in the Ross Sea: Part 2-sedimentologic and stratigraphic signature. Geol. Soc. Am. Bull. 111, 1517-1536.

Drysdale, R.N., Hellstrom, J.C., Zanchetta, G., Fallick, A.E., Goni, M.F.S., Couchoud, I., McDonald, J., Maas, R., Lohmann, G., Isola, I., 2009. Evidence for obliquity forcing of Glacial Termination II. Science 325, 1527-1531.

Duplessy, J.C., Roche, D.M., Kageyama, M., 2007. The deep ocean during the last interglacial period. Science 316, 89-91.

Dupont, T.K., Alley, R.B., 2005. Assessment of the importance of ice-shelf buttressing to ice-sheet flow. Geophys. Res. Lett. 32, L04503, doi: 10.1029/2004GL022024.

Dutton, A., Carlson, A.E., Long, A.J., Milne, G.A., Clark, P.U., DeConto, R., Horton, B.P., Rahmstorf, S., Raymo, M.E., 2015. Sea-level rise due to polar ice-sheet mass loss during past warm periods. Science 349, aaa4019, doi: 10.1126/science.aaa4019

Dutton, A., Lambeck, K., 2012. Ice volume and sea level during the last interglacial. Science 337, 216-219.

Dyez, K.A., Hönisch, B., Schmidt, G.A., 2018. Early Pleistocene obliquity-scale pCO_2 variability at ~1.5 million years ago. Paleoceanography and Paleoclimatology 33, 1270-1291.

Edwards, T.L., Brandon, M.A., Durand, G., Edwards, N.R., Golledge, N.R., Holden, P.B., Nias, I.J., Payne, A.J., Ritz, C., Wernecke, A., 2019. Revisiting Antarctic ice loss due to marine ice-cliff instability. Nature 566, 58-64.

Egan, K.E., Rickaby, R.E.M., Leng, M.J., Hendry, K.R., Hermoso, M., Sloane, H.J., Bostock, H., Halliday, A.N., 2012. Diatom silicon isotopes as a proxy for silicic acid utilisation: a Southern Ocean core top calibration. Geochim. Cosmochim. Acta 96, 174-192.

Elderfield, H., Ferretti, P., Greaves, M., Crowhurst, S., McCave, I.N., Hodell, D., Piotrowski, A.M., 2012. Evolution of ocean temperature and ice volume through the Mid-Pleistocene Climate Transition. Science 337, 704-709.

Elderfield, H., Ganssen, G., 2000. Past temperature and $\delta^{18}O$ of surface ocean waters inferred from foraminiferal Mg/Ca ratios. Nature 405, 442-445.

Elderfield, H., Rickaby, R.E.M., 2000. Oceanic Cd/P ratio and nutrient utilization in the glacial Southern Ocean. Nature 405, 305-310.

Emiliani, C., 1955. Pleistocene temperatures. The Journal of Geology 63, 538-578.

EPICA Community Members, 2004. Eight glacial cycles from an Antarctic ice core. Nature 429, 623-628.

EPICA Community Members, 2006. One-to-one coupling of glacial climate variability in Greenland and Antarctica. Nature 444, 195-198.

Escutia, C., Brinkhuis, H., Klaus, A., Expedition 318 Scientists, 2011. Proc. IODP, 318, Wilkes Land glacial history. Integrated Ocean Drilling Program Management International, Tokyo.

Farmer, G.L., Licht, K., Swope, R.J., Andrews, J., 2006. Isotopic constraints on the provenance of fine-grained sediment in LGM tills from the Ross Embayment, Antarctica. Earth Planet. Sci. Lett. 249, 90-107.

Farmer, J.R., Hönisch, B., Haynes, L.L., Kroon, D., Jung, S., Ford, H.L., Raymo, M.E., Jaume-Seguí, M., Bell, D.B., Goldstein, S.L., 2019. Deep Atlantic Ocean carbon storage and the rise of 100,000-year glacial cycles. Nat. Geosci. 12, 355-360.

Farneti, R., Delworth, T.L., Rosati, A.J., Griffies, S.M., Zeng, F., 2010. The role of mesoscale eddies in the rectification of the Southern Ocean response to climate change. Journal of Physical Oceanography 40, 1539-1557.

Ferraccioli, F., Armadillo, E., Jordan, T., Bozzo, E., Corr, H., 2009. Aeromagnetic exploration over the East Antarctic Ice Sheet: A new view of the Wilkes Subglacial Basin. Tectonophysics 478, 62-77.

Ferrari, R., Jansen, M.F., Adkins, J.F., Burke, A., Stewart, A.L., Thompson, A.F., 2014. Antarctic sea ice control on ocean circulation in present and glacial climates. Proc. Natl. Acad. Sci. U. S. A. 111, 8753-8758.

Ferry, A.J., Crosta, X., Quilty, P.G., Fink, D., Howard, W., Armand, L.K., 2015. First records of winter sea ice concentration in the southwest Pacific sector of the Southern Ocean. Paleoceanography 30, 1525-1539.

Fischer, H., Severinghaus, J., Brook, E., Wolff, E., Albert, M., 2013. Where to find 1.5 million yr old ice for the IPICS "Oldest Ice" ice core. Clim. Past. 9, 2489–2505.

Fischer, H., Wahlen, M., Smith, J., Mastroianni, D., Deck, B., 1999. Ice core records of atmospheric CO_2 around the last three glacial terminations. Science 283, 1712-1714.

Fogwill, C.J., Phipps, S.J., Turney, C.S.M., Golledge, N.R., 2015. Sensitivity of the Southern Ocean to enhanced regional Antarctic ice sheet meltwater input. Earth's Future 3, 317-329.

Fogwill, C.J., Turney, C.S.M., Meissner, K.J., Golledge, N.R., Spence, P., Roberts, J.L., England, M.H., Jones, R.T., Carter, L., 2014. Testing the sensitivity of the East Antarctic Ice Sheet to Southern Ocean dynamics: past changes and future implications. J. Quat. Sci. 29, 91-98.

Ford, H.L., Raymo, M.E., 2020. Regional and global signals in seawater $\delta^{18}O$ records across the mid-Pleistocene transition. Geology 48, 113-117.

Foster, G.L., Rae, J.W.B., 2016. Reconstructing ocean pH with boron isotopes in foraminifera. Annual Review of Earth and Planetary Sciences 44, 207-237.

Francois, R., Altabet, M.A., Yu, E.-F., Sigman, D.M., Bacon, M.P., Frank, M., Bohrmann, G., Bareille, G., Labeyrie, L.D., 1997. Contribution of Southern Ocean surface-water stratification to low atmospheric CO_2 concentrations during the last glacial period. Nature 389, 929-935.

Francois, R., Honjo, S., Manganini, S.J., Ravizza, G.E., 1995. Biogenic barium fluxes to the deep sea: Implications for paleoproductivity reconstruction. Glob. Biogeochem. Cycle 9, 289-303.

Fretwell, P., Pritchard, H.D., Vaughan, D.G., Bamber, J.L., Barrand, N.E., Bell, R., Bianchi, C., Bingham, R.G., Blankenship, D.D., Casassa, G., Catania, G., Callens, D., Conway, H., Cook, A.J., Corr, H.F.J., Damaske, D., Damm, V., Ferraccioli, F., Forsberg, R., Fujita, S., Gim, Y., Gogineni, P., Griggs, J.A., Hindmarsh, R.C.A., Holmlund, P., Holt, J.W., Jacobel, R.W., Jenkins, A., Jokat, W., Jordan, T., King,

E.C., Kohler, J., Krabill, W., Riger-Kusk, M., Langley, K.A., Leitchenkov, G., Leuschen, C., Luyendyk, B.P., Matsuoka, K., Mouginot, J., Nitsche, F.O., Nogi, Y., Nost, O.A., Popov, S.V., Rignot, E., Rippin, D.M., Rivera, A., Roberts, J., Ross, N., Siegert, M.J., Smith, A.M., Steinhage, D., Studinger, M., Sun, B., Tinto, B.K., Welch, B.C., Wilson, D., Young, D.A., Xiangbin, C., Zirizzotti, A., 2013. Bedmap2: improved ice bed, surface and thickness datasets for Antarctica. Cryosphere 7, 375-393.

Fürst, J.J., Durand, G., Gillet-Chaulet, F., Tavard, L., Rankl, M., Braun, M., Gagliardini, O., 2016. The safety band of Antarctic ice shelves. Nat. Clim. Chang. 6, 479-482.

Galaasen, E.V., Ninnemann, U.S., Kessler, A., Irvalı, N., Rosenthal, Y., Tjiputra, J., Bouttes, N., Roche, D.M., Kleiven, H.K.F., Hodell, D.A., 2020. Interglacial instability of North Atlantic Deep Water ventilation. Science 367, 1485-1489.

Ganopolski, A., Rahmstorf, S., 2001. Rapid changes of glacial climate simulated in a coupled climate model. Nature 409, 153-158.

Gebbie, G., 2014. How much did Glacial North Atlantic Water shoal? Paleoceanography 29, 190-209.

Gebbie, G., Huybers, P., 2011. How is the ocean filled? Geophys. Res. Lett. 38, L06604, doi: 10.1029/2011GL046769.

Gersonde, R., Barcena, M.A., 1998. Revision of the upper Pliocene - Pleistocene diatom biostratigraphy for the northern belt of the Southern Ocean. Micropaleontology 44, 84-98.

Gersonde, R., Crosta, X., Abelmann, A., Armand, L., 2005. Sea-surface temperature and sea ice distribution of the Southern Ocean at the EPILOG Last Glacial Maximum—a circum-Antarctic view based on siliceous microfossil records. Quat. Sci. Rev. 24, 869-896.

Gersonde, R., Zielinski, U., 2000. The reconstruction of late Quaternary Antarctic sea-ice distribution—the use of diatoms as a proxy for sea-ice. Palaeogeography, Palaeoclimatology, Palaeoecology 162, 263-286.

Ghosh, P., Adkins, J., Affek, H., Balta, B., Guo, W., Schauble, E.A., Schrag, D., Eiler, J.M., 2006. $^{13}C–^{18}O$ bonds in carbonate minerals: a new kind of paleothermometer. Geochim. Cosmochim. Acta 70, 1439-1456.

Gilford, D.M., Ashe, E.L., DeConto, R.M., Kopp, R.E., Pollard, D., Rovere, A., 2020. Could the Last Interglacial constrain projections of future Antarctic ice mass loss and sea-level rise? Journal of Geophysical Research: Earth Surface 125, e2019JF005418, doi: 10.1029/2019JF005418.

Gohl, K., Wellner, J.S., Klaus, A., Expedition 379 Scientists, 2019. Expedition 379 Preliminary Report: Amundsen Sea West Antarctic Ice Sheet History. International Ocean Discovery Program. https://doi.org/10.14379/iodp.pr.379.2019.

Goldstein, S.L., Hemming, S.R., 2003. Long-lived isotopic tracers in oceanography, paleoceanography and ice sheet dynamics, in: Elderfield, H. (Ed.), The Oceans and Marine Geochemistry. Elsevier-Pergamon, Oxford, pp. 453-489.

Golledge, N.R., Levy, R.H., McKay, R.M., Naish, T.R., 2017. East Antarctic ice sheet most vulnerable to Weddell Sea warming. Geophys. Res. Lett. 44, 2343-2351.

Golledge, N.R., Menviel, L., Carter, L., Fogwill, C.J., England, M.H., Cortese, G., Levy, R.H., 2014. Antarctic contribution to meltwater pulse 1A from reduced Southern Ocean overturning. Nature Communications 5, 5107, doi: 10.1038/ncomms6107.

Gomez, N., Weber, M.E., Clark, P.U., Mitrovica, J.X., Han, H.K., 2020. Antarctic ice dynamics amplified by Northern Hemisphere sea-level forcing. Nature 587, 600-604.

Gottschalk, J., Hodell, D.A., Skinner, L.C., Crowhurst, S.J., Jaccard, S.L., Charles, C., 2018. Past carbonate preservation events in the deep Southeast Atlantic Ocean (Cape Basin) and their implications for Atlantic overturning dynamics and marine carbon cycling. Paleoceanography and Paleoclimatology 33, 643-663.

Gottschalk, J., Skinner, L.C., Lippold, J., Vogel, H., Frank, N., Jaccard, S.L., Waelbroeck, C., 2016. Biological and physical controls in the Southern Ocean on past millennial-scale atmospheric CO_2 changes. Nature Communications 7, 11539, doi: 10.1038/ncomms11539.

Gow, A.J., Ueda, H.T., Garfield, D.E., 1968. Antarctic ice sheet: preliminary results of first core hole to bedrock. Science 161, 1011-1013.

Grant, K.M., Rohling, E.J., Ramsey, C.B., Cheng, H., Edwards, R.L., Florindo, F., Heslop, D., Marra, F., Roberts, A.P., Tamisiea, M.E., Williams, F., 2014. Sea-level variability over five glacial cycles. Nature Communications 5, 5076, doi: 10.1038/ncomms6076.

Green, R.A., Menviel, L., Meissner, K.J., Crosta, X., 2020. Evaluating seasonal sea-ice cover over the Southern Ocean from the Last Glacial Maximum. Climate of the Past Discussions, 1-23, doi: 10.5194/cp-2020-155.

Grootes, P.M., Stuiver, M., White, J.W.C., Johnsen, S., Jouzel, J., 1993. Comparison of oxygen isotope records from the GISP2 and GRIP Greenland ice cores. Nature 366, 552-554.

Grousset, F.E., Biscaye, P.E., 2005. Tracing dust sources and transport patterns using Sr, Nd and Pb isotopes. Chemical Geology 222, 149-167.

Gulick, S.P.S., Shevenell, A.E., Montelli, A., Fernandez, R., Smith, C., Warny, S., Bohaty, S.M., Sjunneskog, C., Leventer, A., Frederick, B., 2017. Initiation and long-term instability of the East Antarctic Ice Sheet. Nature 552, 225-229.

Hain, M.P., Sigman, D.M., Haug, G.H., 2010. Carbon dioxide effects of Antarctic stratification, North Atlantic Intermediate Water formation, and subantarctic nutrient drawdown during the last ice age: Diagnosis and synthesis in a geochemical box model. Glob. Biogeochem. Cycle 24, GB4023, doi: 10.1029/2010GB003790.

Hall, I.R., McCave, I.N., Shackleton, N.J., Weedon, G.P., Harris, S.E., 2001. Intensified deep Pacific inflow and ventilation in Pleistocene glacial times. Nature 412, 809-812.

Hambrey, M.J., McKelvey, B., 2000. Neogene fjordal sedimentation on the western margin of the Lambert Graben, East Antarctica. Sedimentology 47, 577-607.

Hasenfratz, A.P., Jaccard, S.L., Martínez-García, A., Sigman, D.M., Hodell, D.A., Vance, D., Bernasconi, S.M., Kleiven, H.K.F., Haumann, F.A., Haug, G.H., 2019. The residence time of Southern Ocean surface waters and the 100,000-year ice age cycle. Science 363, 1080-1084.

Hay, C., Mitrovica, J.X., Gomez, N., Creveling, J.R., Austermann, J., Kopp, R.E., 2014. The sea-level fingerprints of ice-sheet collapse during interglacial periods. Quat. Sci. Rev. 87, 60-69.

Hayes, C.T., Martínez-García, A., Hasenfratz, A.P., Jaccard, S.L., Hodell, D.A., Sigman, D.M., Haug, G.H., Anderson, R.F., 2014. A stagnation event in the deep South Atlantic during the last interglacial period. Science 346, 1514-1517.

Hays, J.D., Imbrie, J., Shackleton, N.J., 1976. Variations in the Earth's orbit: pacemaker of the ice ages. Science 194, 1121-1132.

He, F., Shakun, J.D., Clark, P.U., Carlson, A.E., Liu, Z., Otto-Bliesner, B.L., Kutzbach, J.E., 2013. Northern Hemisphere forcing of Southern Hemisphere climate during the last deglaciation. Nature 494, 81-85.

Hemming, S.R., 2004. Heinrich events: Massive late Pleistocene detritus layers of the North Atlantic and their global climate imprint. Rev. Geophys. 42, RG1005, doi: 10.1029/2003rg000128.

Hemming, S.R., Broecker, W.S., Sharp, W.D., Bond, G.C., Gwiazda, R.H., McManus, J.F., Klas, M., Hajdas, I., 1998. Provenance of Heinrich layers in core V28-82, northeastern Atlantic: $^{40}Ar/^{39}Ar$ ages of ice-rafted hornblende, Pb isotopes in feldspar grains, and Nd–Sr–Pb isotopes in the fine sediment fraction. Earth Planet. Sci. Lett. 164, 317-333.

Henderson, G.M., 2002. New oceanic proxies for paleoclimate. Earth Planet. Sci. Lett. 203, 1-13.

Henry, L.G., McManus, J.F., Curry, W.B., Roberts, N.L., Piotrowski, A.M., Keigwin, L.D., 2016. North Atlantic ocean circulation and abrupt climate change during the last glaciation. Science 353, 470-474.

Higgins, J.A., Kurbatov, A.V., Spaulding, N.E., Brook, E., Introne, D.S., Chimiak, L.M., Yan, Y., Mayewski, P.A., Bender, M.L., 2015. Atmospheric composition 1 million years ago from blue ice in the Allan Hills, Antarctica. Proceedings of the National Academy of Sciences 112, 6887-6891.

Hillenbrand, C.-D., Ehrmann, W., 2005. Late Neogene to Quaternary environmental changes in the Antarctic Peninsula region: evidence from drift sediments. Glob. Planet. Change 45, 165-191.

Hillenbrand, C.-D., Fütterer, D.K., Grobe, H., Frederichs, T., 2002. No evidence for a Pleistocene collapse of the West Antarctic Ice Sheet from continental margin sediments recovered in the Amundsen Sea. Geo-Marine Letters 22, 51-59.

Hillenbrand, C.-D., Kuhn, G., Frederichs, T., 2009. Record of a Mid-Pleistocene depositional anomaly in West Antarctic continental margin sediments: an indicator for ice-sheet collapse? Quat. Sci. Rev. 28, 1147-1159.

Hillenbrand, C.-D., Moreton, S.G., Caburlotto, A., Pudsey, C.J., Lucchi, R.G., Smellie, J.L., Benetti, S., Grobe, H., Hunt, J.B., Larter, R.D., 2008. Volcanic time-markers for Marine Isotopic Stages 6 and 5 in Southern Ocean sediments and Antarctic ice cores: implications for tephra correlations between palaeoclimatic records. Quat. Sci. Rev. 27, 518-540.

Hillenbrand, C.-D., Smith, J.A., Hodell, D.A., Greaves, M., Poole, C.R., Kender, S., Williams, M., Andersen, T.J., Jernas, P.E., Elderfield, H., 2017. West Antarctic Ice Sheet retreat driven by Holocene warm water incursions. Nature 547, 43-48.

Hines, S.K.V., Southon, J.R., Adkins, J.F., 2015. A high-resolution record of Southern Ocean intermediate water radiocarbon over the past 30,000 years. Earth Planet. Sci. Lett. 432, 46-58.

Ho, S.L., Mollenhauer, G., Fietz, S., Martínez-Garcia, A., Lamy, F., Rueda, G., Schipper, K., Méheust, M., Rosell-Melé, A., Stein, R., 2014. Appraisal of TEX_{86} and TEX_{86}^{L} thermometries in subpolar and polar regions. Geochim. Cosmochim. Acta 131, 213-226.

Ho, S.L., Mollenhauer, G., Lamy, F., Martínez-Garcia, A., Mohtadi, M., Gersonde, R., Hebbeln, D., Nunez-Ricardo, S., Rosell-Melé, A., Tiedemann, R., 2012. Sea surface temperature variability in the Pacific sector of the Southern Ocean over the past 700 kyr. Paleoceanography 27, PA4202, doi: 10.1029/2012PA002317.

Hodell, D.A., Channell, J.E.T., Curtis, J.H., Romero, O.E., Röhl, U., 2008. Onset of "Hudson Strait" Heinrich events in the eastern North Atlantic at the end of the middle Pleistocene transition (~640 ka)? Paleoceanography 23, PA4218, doi: 10.1029/2008PA001591.

Hodell, D.A., Venz, K.A., Charles, C.D., Ninnemann, U.S., 2003. Pleistocene vertical carbon isotope and carbonate gradients in the South Atlantic sector of the Southern Ocean. Geochem. Geophys. Geosyst. 4, 1004, doi: 10.1029/2002gc000367.

Hoffman, J.S., Clark, P.U., Parnell, A.C., He, F., 2017. Regional and global sea-surface temperatures during the last interglaciation. Science 355, 276-279.

Hogg, A., Southon, J., Turney, C., Palmer, J., Ramsey, C.B., Fenwick, P., Boswijk, G., Friedrich, M., Helle, G., Hughen, K., 2016. Punctuated shutdown of Atlantic meridional overturning circulation during Greenland Stadial 1. Sci Rep 6, 25902, doi: 10.1038/srep25902.

Holden, P.B., Edwards, N.R., Wolff, E.W., Lang, N.J., Singarayer, J.S., Valdes, P.J., Stocker, T.F., 2010. Interhemispheric coupling, the West Antarctic Ice Sheet and warm Antarctic interglacials. Clim. Past. 6, 431-443.

Holder, L., Duffy, M., Opdyke, B., Leventer, A., Post, A., O'Brien, P., Armand, L., 2020. Controls since the Mid-Pleistocene Transition on sedimentation and primary productivity downslope of Totten Glacier, East Antarctica. Paleoceanography and Paleoclimatology 35, e2020PA003981, doi: 10.1029/2020PA003981.

Holloway, M.D., Sime, L.C., Allen, C.S., Hillenbrand, C.D., Bunch, P., Wolff, E., Valdes, P.J., 2017. The spatial structure of the 128 ka Antarctic sea ice minimum. Geophys. Res. Lett. 44, 11129-11139.

Holloway, M.D., Sime, L.C., Singarayer, J.S., Tindall, J.C., Bunch, P., Valdes, P.J., 2016. Antarctic last interglacial isotope peak in response to sea ice retreat not ice-sheet collapse. Nature Communications 7, 12293, doi: 10.1038/ncomms12293.

Hönisch, B., Hemming, N.G., Archer, D., Siddall, M., McManus, J.F., 2009. Atmospheric carbon dioxide concentration across the mid-Pleistocene transition. Science 324, 1551-1554.

Hönisch, B., Hemming, N.G., Grottoli, A.G., Amat, A., Hanson, G.N., Bijma, J., 2004. Assessing scleractinian corals as recorders for paleo-pH: Empirical calibration and vital effects. Geochim. Cosmochim. Acta 68, 3675-3685.

Hoogakker, B.A.A., Elderfield, H., Schmiedl, G., McCave, I.N., Rickaby, R.E.M., 2015. Glacial–interglacial changes in bottom-water oxygen content on the Portuguese margin. Nat. Geosci. 8, 40-43.

Howe, J.N.W., Piotrowski, A.M., 2017. Atlantic deep water provenance decoupled from atmospheric CO_2 concentration during the lukewarm interglacials. Nature Communications 8, 2003, doi: 10.1038/s41467-017-01939-w.

Huybers, P., 2006. Early Pleistocene glacial cycles and the integrated summer insolation forcing. Science 313, 508-511.

Huybers, P., 2011. Combined obliquity and precession pacing of late Pleistocene deglaciations. Nature 480, 229-232.

Huybers, P., Denton, G., 2008. Antarctic temperature at orbital timescales controlled by local summer duration. Nat. Geosci. 1, 787-792.

Huybers, P., Wunsch, C., 2005. Obliquity pacing of the late Pleistocene glacial terminations. Nature 434, 491-494.

Imbrie, J., Berger, A., Boyle, E.A., Clemens, S.C., Duffy, A., Howard, W.R., Kukla, G., Kutzbach, J., Martinson, D.G., McIntyre, A., Mix, A.C., Molfino, B., Morley, J.J., Peterson, L.C., Pisias, N.G., Prell, W.L., Raymo, M.E., Shackleton, N.J., Toggweiler, J.R., 1993. On the structure and origin of major glaciation cycles 2. The 100,000-year cycle. Paleoceanography 8, 699-735.

Imbrie, J., Boyle, E.A., Clemens, S.C., Duffy, A., Howard, W.R., Kukla, G., Kutzbach, J., Martinson, D.G., McIntyre, A., Mix, A.C., Molfino, B., Morley, J.J., Peterson, L.C., Pisias, N.G., Prell, W.L., Raymo, M.E., Shackleton, N.J., Toggweiler, J.R., 1992. On the structure and origin of major glaciation cycles 1. Linear responses to Milankovitch forcing. Paleoceanography 7, 701-738.

IPCC, 2019. Special Report on the Ocean and Cryosphere in a Changing Climate [H.-O. Pörtner, D.C. Roberts, V. Masson-Delmotte, P. Zhai, M. Tignor, E. Poloczanska, K. Mintenbeck, A. Alegría, M. Nicolai, A. Okem, J. Petzold, B. Rama, N.M. Weyer (eds.)]. IPCC Geneva.

Irvalı, N., Galaasen, E.V., Ninnemann, U.S., Rosenthal, Y., Born, A., Kleiven, H.K.F., 2020. A low climate threshold for south Greenland Ice Sheet demise during the Late Pleistocene. Proceedings of the National Academy of Sciences 117, 190-195.

Jaccard, S.L., Galbraith, E.D., Martínez-García, A., Anderson, R.F., 2016. Covariation of deep Southern Ocean oxygenation and atmospheric CO_2 through the last ice age. Nature 530, 207-210.

Jaccard, S.L., Galbraith, E.D., Sigman, D.M., Haug, G.H., Francois, R., Pedersen, T.F., Dulski, P., Thierstein, H.R., 2009. Subarctic Pacific evidence for a glacial deepening of the oceanic respired carbon pool. Earth Planet. Sci. Lett. 277, 156-165.

Jaccard, S.L., Hayes, C.T., Martínez-García, A., Hodell, D.A., Anderson, R.F., Sigman, D.M., Haug, G.H., 2013. Two modes of change in Southern Ocean productivity over the past million years. Science 339, 1419-1423.

Jakob, K.A., Wilson, P.A., Pross, J., Ezard, T.H.G., Fiebig, J., Repschläger, J., Friedrich, O., 2020. A new sea-level record for the Neogene/Quaternary boundary reveals transition to a more stable East Antarctic Ice Sheet. Proceedings of the National Academy of Sciences 117, 30980-30987.

Jamieson, S.S.R., Sugden, D.E., Hulton, N.R.J., 2010. The evolution of the subglacial landscape of Antarctica. Earth Planet. Sci. Lett. 293, 1-27.

Jansen, J.H.F., Kuijpers, A., Troelstra, S.R., 1986. A mid-Brunhes climatic event: Long-term changes in global atmosphere and ocean circulation. Science 232, 619-622.

Jimenez-Espejo, F.J., Presti, M., Kuhn, G., Mckay, R., Crosta, X., Escutia, C., Lucchi, R.G., Tolotti, R., Yoshimura, T., Huertas, M.O., 2020. Late Pleistocene oceanographic and depositional variations along the Wilkes Land margin (East Antarctica) reconstructed with geochemical proxies in deep-sea sediments. Glob. Planet. Change 184, 103045, doi: 10.1016/j.gloplacha.2019.103045.

Johnsen, S.J., Clausen, H.B., Dansgaard, W., Fuhrer, K., Gundestrup, N., Hammer, C.U., Iversen, P.l., Jouzel, J., Stauffer, B., 1992. Irregular glacial interstadials recorded in a new Greenland ice core. Nature 359, 311-313.

Jones, R.S., Norton, K.P., Mackintosh, A.N., Anderson, J.T.H., Kubik, P., Vockenhuber, C., Wittmann, H., Fink, D., Wilson, G.S., Golledge, N.R., 2017. Cosmogenic nuclides constrain surface fluctuations of an East Antarctic outlet glacier since the Pliocene. Earth Planet. Sci. Lett. 480, 75-86.

Joughin, I., Smith, B.E., Medley, B., 2014. Marine ice sheet collapse potentially under way for the Thwaites Glacier Basin, West Antarctica. Science 344, 735-738.

Jouzel, J., 2013. A brief history of ice core science over the last 50 yr. Clim. Past. 9, 2525–2547.

Jouzel, J., Masson-Delmotte, V., 2010. Deep ice cores: the need for going back in time. Quat. Sci. Rev. 29, 3683-3689.

Jouzel, J., Masson-Delmotte, V., Cattani, O., Dreyfus, G., Falourd, S., Hoffmann, G., Minster, B., Nouet, J., Barnola, J.M., Chappellaz, J., Fischer, H., Gallet, J.C., Johnsen, S., Leuenberger, M., Loulergue, L., Luethi, D., Oerter, H., Parrenin, F., Raisbeck, G., Raynaud, D., Schilt, A., Schwander, J., Selmo, E., Souchez, R., Spahni, R., Stauffer, B., Steffensen, J.P., Stenni, B., Stocker, T.F., Tison, J.L., Werner, M., Wolff, E.W., 2007. Orbital and millennial Antarctic climate variability over the past 800,000 years. Science 317, 793-796.

Jouzel, J., Vimeux, F., Caillon, N., Delaygue, G., Hoffmann, G., Masson-Delmotte, V., Parrenin, F., 2003. Magnitude of isotope/temperature scaling for interpretation of central Antarctic ice cores. Journal of Geophysical Research: Atmospheres 108, 4361, doi: 10.1029/2002JD002677.

Kanfoush, S.L., Hodell, D.A., Charles, C.D., Guilderson, T.P., Mortyn, P.G., Ninnemann, U.S., 2000. Millennial-scale instability of the Antarctic ice sheet during the last glaciation. Science 288, 1815-1818.

Katz, M.E., Cramer, B.S., Franzese, A., Honisch, B., Miller, K.G., Rosenthal, Y., Wright, J.D., 2010. Traditional and emerging geochemical proxies in foraminifera. J. Foraminifer. Res. 40, 165-192.

Kawamura, K., Parrenin, F., Lisiecki, L., Uemura, R., Vimeux, F., Severinghaus, J.P., Hutterli, M.A., Nakazawa, T., Aoki, S., Jouzel, J., Raymo, M.E., Matsumoto, K., Nakata, H., Motoyama, H., Fujita, S., Goto-Azuma, K., Fujii, Y., Watanabe, O., 2007. Northern Hemisphere forcing of climatic cycles in Antarctica over the past 360,000 years. Nature 448, 912-916.

Keeling, R.F., Stephens, B.B., 2001. Antarctic sea ice and the control of Pleistocene climate instability. Paleoceanography 16, 112-131.

Knorr, G., Lohmann, G., 2003. Southern Ocean origin for the resumption of Atlantic thermohaline circulation during deglaciation. Nature 424, 532-536.

Kohfeld, K.E., Chase, Z., 2017. Temporal evolution of mechanisms controlling ocean carbon uptake during the last glacial cycle. Earth Planet. Sci. Lett. 472, 206-215.

Konfirst, M.A., Scherer, R.P., Hillenbrand, C.-D., Kuhn, G., 2012. A marine diatom record from the Amundsen Sea - Insights into oceanographic and climatic response to the Mid-Pleistocene Transition in the West Antarctic sector of the Southern Ocean. Mar. Micropaleontol. 92, 40-51.

Kopp, R.E., Simons, F.J., Mitrovica, J.X., Maloof, A.C., Oppenheimer, M., 2009. Probabilistic assessment of sea level during the last interglacial stage. Nature 462, 863-867.

Kopp, R.E., Simons, F.J., Mitrovica, J.X., Maloof, A.C., Oppenheimer, M., 2013. A probabilistic assessment of sea level variations within the last interglacial stage. Geophysical Journal International 193, 711-716.

Korotkikh, E.V., Mayewski, P.A., Handley, M.J., Sneed, S.B., Introne, D.S., Kurbatov, A.V., Dunbar, N.W., McIntosh, W.C., 2011. The last interglacial as represented in the glaciochemical record from Mount Moulton Blue Ice Area, West Antarctica. Quat. Sci. Rev. 30, 1940-1947.

Kumar, N., Anderson, R.F., Mortlock, R.A., Froelich, P.N., Kubik, P., Dittrich-Hannen, B., Suter, M., 1995. Increased biological productivity and export production in the glacial Southern Ocean. Nature 378, 675-680.

Laepple, T., Werner, M., Lohmann, G., 2011. Synchronicity of Antarctic temperatures and local solar insolation on orbital timescales. Nature 471, 91-94.

Laj, C., Kissel, C., Beer, J., 2004. High resolution global paleointensity stack since 75 kyr (GLOPIS-75) calibrated to absolute values. American Geophysical Union Geophysical Monograph Series, Washington DC 145, 255-265.

Lambert, F., Delmonte, B., Petit, J.R., Bigler, M., Kaufmann, P.R., Hutterli, M.A., Stocker, T.F., Ruth, U., Steffensen, J.P., Maggi, V., 2008. Dust-climate couplings over the past 800,000 years from the EPICA Dome C ice core. Nature 452, 616-619.

Lamy, F., Arz, H.W., Kilianc, R., Lange, C.B., Lembke-Jene, L., Wengler, M., Kaiser, J., Baeza-Urrea, O., Hall, I.R., Harada, N., Tiedemann, R., 2015. Glacial reduction and millennial-scale variations in Drake Passage throughflow. Proc. Natl. Acad. Sci. U. S. A. 112, 13496-13501.

Lamy, F., Gersonde, R., Winckler, G., Esper, O., Jaeschke, A., Kuhn, G., Ullermann, J., Martínez-Garcia, A., Lambert, F., Kilian, R., 2014. Increased dust deposition in the Pacific Southern Ocean during glacial periods. Science 343, 403-407.

Lamy, F., Kaiser, J., Arz, H.W., Hebbeln, D., Ninnemann, U., Timm, O., Timmermann, A., Toggweiler, J.R., 2007. Modulation of the bipolar seesaw in the Southeast Pacific during Termination 1. Earth Planet. Sci. Lett. 259, 400-413.

Lamy, F., Winckler, G., Alvarez Zarikian, C.A., Expedition 383 Scientists, 2019. Expedition 383 Preliminary Report: Dynamics of the Pacific Antarctic Circumpolar Current. International Ocean Discovery Program. https://doi.org/10.14379/iodp.pr.383.2019.

Lang, D.C., Bailey, I., Wilson, P.A., Chalk, T.B., Foster, G.L., Gutjahr, M., 2016. Incursions of southern-sourced water into the deep North Atlantic during late Pliocene glacial intensification. Nat. Geosci. 9, 375-379.

Lang, N., Wolff, E.W., 2011. Interglacial and glacial variability from the last 800 ka in marine, ice and terrestrial archives. Clim. Past. 7, 361-380.

Lawrence, K.T., Liu, Z., Herbert, T.D., 2006. Evolution of the eastern tropical Pacific through Plio-Pleistocene glaciation. Science 312, 79-83.

Lear, C.H., Elderfield, H., Wilson, P.A., 2000. Cenozoic deep-sea temperatures and global ice volumes from Mg/Ca in benthic foraminiferal calcite. Science 287, 269-272.

Levine, J.G., Yang, X., Jones, A.E., Wolff, E.W., 2014. Sea salt as an ice core proxy for past sea ice extent: A process-based model study. Journal of Geophysical Research: Atmospheres 119, 5737-5756.

Levy, R., Cody, R., Crampton, J., Fielding, C., Golledge, N., Harwood, D., Henrys, S., Mckay, R., Naish, T., Ohneiser, C., 2012. Late Neogene climate and glacial history of the Southern Victoria Land coast from integrated drill core, seismic and outcrop data. Glob. Planet. Change 96-97, 157-180.

Licht, K.J., Hemming, S.R., 2017. Analysis of Antarctic glacigenic sediment provenance through geochemical and petrologic applications. Quat. Sci. Rev. 164, 1-24.

Lilly, K., Fink, D., Fabel, D., Lambeck, K., 2010. Pleistocene dynamics of the interior East Antarctic ice sheet. Geology 38, 703-706.

Lisiecki, L.E., Raymo, M.E., 2005. A Pliocene-Pleistocene stack of 57 globally distributed benthic $\delta^{18}O$ records. Paleoceanography 20, PA1003, doi: 10.1029/2004PA001071.

Lopes dos Santos, R.A., Spooner, M.I., Barrows, T.T., De Deckker, P., Sinninghe Damsté, J.S., Schouten, S., 2013. Comparison of organic ($U^{K'}_{37}$, TEX^{H}_{86}, LDI) and faunal proxies (foraminiferal assemblages) for reconstruction of late Quaternary sea surface temperature variability from offshore southeastern Australia. Paleoceanography 28, 377-387.

Lund, D.C., Adkins, J.F., Ferrari, R., 2011. Abyssal Atlantic circulation during the Last Glacial Maximum: Constraining the ratio between transport and vertical mixing. Paleoceanography 26, PA1213, doi: 10.1029/2010PA001938.

Luthi, D., Le Floch, M., Bereiter, B., Blunier, T., Barnola, J.M., Siegenthaler, U., Raynaud, D., Jouzel, J., Fischer, H., Kawamura, K., Stocker, T.F., 2008. High-resolution carbon dioxide concentration record 650,000-800,000 years before present. Nature 453, 379-382.

Lynch-Stieglitz, J., Fairbanks, R.G., 1994. A conservative tracer for glacial ocean circulation from carbon isotope and palaeo-nutrient measurements in benthic foraminifera. Nature 369, 308-310.

Mackensen, A., Schmiedl, G., 2019. Stable carbon isotopes in paleoceanography: Atmosphere, oceans, and sediments. Earth-Sci. Rev. 197, 102893, doi: 10.1016/j.earscirev.2019.102893.

Mackintosh, A., Golledge, N., Domack, E., Dunbar, R., Leventer, A., White, D., Pollard, D., DeConto, R., Fink, D., Zwartz, D., Gore, D., Lavoie, C., 2011. Retreat of the East Antarctic ice sheet during the last glacial termination. Nat. Geosci. 4, 195-202.

Marchitto, T.M., Broecker, W.S., 2006. Deep water mass geometry in the glacial Atlantic Ocean: A review of constraints from the paleonutrient proxy Cd/Ca. Geochem. Geophys. Geosyst. 7, Q12003, doi: 10.1029/2006GC001323.

Marchitto, T.M., Curry, W.B., Lynch-Stieglitz, J., Bryan, S.P., Cobb, K.M., Lund, D.C., 2014. Improved oxygen isotope temperature calibrations for cosmopolitan benthic foraminifera. Geochim. Cosmochim. Acta 130, 1-11.

Marcott, S.A., Bauska, T.K., Buizert, C., Steig, E.J., Rosen, J.L., Cuffey, K.M., Fudge, T.J., Severinghaus, J.P., Ahn, J., Kalk, M.L., 2014. Centennial-scale changes in the global carbon cycle during the last deglaciation. Nature 514, 616-619.

Marino, G., Rohling, E.J., Rodríguez-Sanz, L., Grant, K.M., Heslop, D., Roberts, A.P., Stanford, J.D., Yu, J., 2015. Bipolar seesaw control on last interglacial sea level. Nature 522, 197-201.

Marino, G., Zahn, R., Ziegler, M., Purcell, C., Knorr, G., Hall, I.R., Ziveri, P., Elderfield, H., 2013. Agulhas salt-leakage oscillations during abrupt climate changes of the Late Pleistocene. Paleoceanography 28, 599-606.

Mariotti, V., Paillard, D., Bopp, L., Roche, D.M., Bouttes, N., 2016. A coupled model for carbon and radiocarbon evolution during the last deglaciation. Geophys. Res. Lett. 43, 1306-1313.

Martin, D.F., Cornford, S.L., Payne, A.J., 2019. Millennial-Scale Vulnerability of the Antarctic Ice Sheet to Regional Ice Shelf Collapse. Geophys. Res. Lett. 46, 1467-1475.

Martin, J.H., 1990. Glacial-interglacial CO_2 change: The iron hypothesis. Paleoceanography 5, 1-13.

Martínez-Botí, M.A., Foster, G.L., Chalk, T.B., Rohling, E.J., Sexton, P.F., Lunt, D.J., Pancost, R.D., Badger, M.P.S., Schmidt, D.N., 2015a. Plio-Pleistocene climate sensitivity evaluated using high-resolution CO_2 records. Nature 518, 49-54.

Martínez-Botí, M.A., Marino, G., Foster, G.L., Ziveri, P., Henehan, M.J., Rae, J.W.B., Mortyn, P.G., Vance, D., 2015b. Boron isotope evidence for oceanic carbon dioxide leakage during the last deglaciation. Nature 518, 219-222.

Martinez-Garcia, A., Rosell-Mele, A., Geibert, W., Gersonde, R., Masque, P., Gaspari, V., Barbante, C., 2009. Links between iron supply, marine productivity, sea surface temperature, and CO_2 over the last 1.1 Ma. Paleoceanography 24, PA1207, doi: 10.1029/2008PA001657.

Martinez-Garcia, A., Rosell-Mele, A., Jaccard, S.L., Geibert, W., Sigman, D.M., Haug, G.H., 2011. Southern Ocean dust-climate coupling over the past four million years. Nature 476, 312-315.

Martinez-Garcia, A., Rosell-Melé, A., McClymont, E.L., Gersonde, R., Haug, G.H., 2010. Subpolar link to the emergence of the modern equatorial Pacific cold tongue. Science 328, 1550-1553.

Martinez-Garcia, A., Sigman, D.M., Ren, H., Anderson, R.F., Straub, M., Hodell, D.A., Jaccard, S.L., Eglinton, T.I., Haug, G.H., 2014. Iron fertilization of the Subantarctic Ocean during the last ice age. Science 343, 1347-1350.

Martinson, D.G., Pisias, N.G., Hays, J.D., Imbrie, J., Moore, T.C., Shackleton, N.J., 1987. Age dating and the orbital theory of the Ice Ages: development of a high-resolution 0 to 300,000-year chronostratigraphy. Quat. Res. 27, 1-29.

Martrat, B., Grimalt, J.O., Shackleton, N.J., de Abreu, L., Hutterli, M.A., Stocker, T.F., 2007. Four climate cycles of recurring deep and surface water destabilizations on the Iberian margin. Science 317, 502-507.

Marzocchi, A., Jansen, M.F., 2019. Global cooling linked to increased glacial carbon storage via changes in Antarctic sea ice. Nat. Geosci. 12, doi: 10.1038/s41561-019-0466-8.

Mas e Braga, M., Bernales, J., Prange, M., Stroeven, A.P., Rogozhina, I., 2021. Sensitivity of the Antarctic ice sheets to the warming of marine isotope substage 11c. The Cryosphere 15, 459-478.

Maslin, M.A., Brierley, C.M., 2015. The role of orbital forcing in the Early Middle Pleistocene Transition. Quat. Int. 389, 47-55.

Masson-Delmotte, V., Schulz, M., Abe-Ouchi, A., Beer, J., Ganopolski, A., González Rouco, J., Jansen, E., Lambeck, K., Luterbacher, J., Naish, T., 2013. Information from paleoclimate archives, Climate Change 2013: The Physical Science Basis. Contribution of Working Group I to the Fifth Assessment Report of the Intergovernmental Panel on Climate Change [Stocker, T.F., D. Qin, G.-K. Plattner, M. Tignor, S.K. Allen, J. Boschung, A. Nauels, Y. Xia, V. Bex and P.M. Midgley (eds.)]. Cambridge University Press, Cambridge, United Kingdom and New York, NY, USA.

McCave, I.N., Crowhurst, S.J., Kuhn, G., Hillenbrand, C.D., Meredith, M.P., 2013. Minimal change in Antarctic Circumpolar Current flow speed between the last glacial and Holocene. Nat. Geosci. 7, 113-116.

McCave, I.N., Hall, I.R., 2006. Size sorting in marine muds: Processes, pitfalls, and prospects for paleoflow-speed proxies. Geochem. Geophys. Geosyst. 7, Q10N05, doi: 10.1029/2006GC001284.

McCave, I.N., Manighetti, B., Robinson, S.G., 1995. Sortable silt and fine sediment size composition slicing - parameters for paleocurrent speed and paleoceanography. Paleoceanography 10, 593-610.

McCave, I.N., Thornalley, D.J.R., Hall, I.R., 2017. Relation of sortable silt grain-size to deep-sea current speeds: Calibration of the 'Mud Current Meter'. Deep Sea Research Part I: Oceanographic Research Papers 127, 1-12.

McClymont, E.L., Elmore, A.C., Kender, S., Leng, M.J., Greaves, M., Elderfield, H., 2016. Pliocene-Pleistocene evolution of sea surface and intermediate water temperatures from the southwest Pacific. Paleoceanography 31, 895-913.

McCorkle, D.C., Emerson, S.R., 1988. The relationship between pore water carbon isotopic composition and bottom water oxygen concentration. Geochim. Cosmochim. Acta 52, 1169-1178.

McGee, D., Winckler, G., Borunda, A., Serno, S., Anderson, R.F., Recasens, C., Bory, A., Gaiero, D., Jaccard, S.L., Kaplan, M., 2016. Tracking eolian dust with helium and thorium: Impacts of grain size and provenance. Geochim. Cosmochim. Acta 175, 47-67.

McKay, N.P., Overpeck, J.T., Otto-Bliesner, B.L., 2011. The role of ocean thermal expansion in Last Interglacial sea level rise. Geophys. Res. Lett. 38, L14605, doi: 10.1029/2011GL048280.

McKay, R., Browne, G., Carter, L., Cowan, E., Dunbar, G., Krissek, L., Naish, T., Powell, R., Reed, J., Talarico, F., 2009. The stratigraphic signature of the late Cenozoic Antarctic Ice Sheets in the Ross Embayment. Geol. Soc. Am. Bull. 121, 1537-1561.

McKay, R., Golledge, N.R., Maas, S., Naish, T., Levy, R., Dunbar, G., Kuhn, G., 2016. Antarctic marine ice-sheet retreat in the Ross Sea during the early Holocene. Geology 44, 7-10.

McKay, R., Naish, T., Carter, L., Riesselman, C., Dunbar, R., Sjunneskog, C., Winter, D., Sangiorgi, F., Warren, C., Pagani, M., 2012a. Antarctic and Southern Ocean influences on Late Pliocene global cooling. Proceedings of the National Academy of Sciences 109, 6423-6428.

McKay, R., Naish, T., Powell, R., Barrett, P., Scherer, R., Talarico, F., Kyle, P., Monien, D., Kuhn, G., Jackolski, C., Williams, T., 2012b. Pleistocene variability of Antarctic Ice Sheet extent in the Ross Embayment. Quat. Sci. Rev. 34, 93-112.

McKay, R.M., De Santis, L., Kulhanek, D.K., Expedition 374 Scientists, 2019. Ross Sea West Antarctic Ice Sheet History. Proceedings of the International Ocean Discovery Program, 374. College Station, TX (International Ocean Discovery Program), doi: 10.14379/iodp.proc.374.2019.

McManus, J.F., Oppo, D.W., Cullen, J.L., 1999. A 0.5-million-year record of millennial-scale climate variability in the North Atlantic. Science 283, 971-975.

Melles, M., Brigham-Grette, J., Minyuk, P.S., Nowaczyk, N.R., Wennrich, V., DeConto, R.M., Anderson, P.M., Andreev, A.A., Coletti, A., Cook, T.L., 2012. 2.8 million years of Arctic climate change from Lake El'gygytgyn, NE Russia. Science 337, 315-320.

Mengel, M., Levermann, A., 2014. Ice plug prevents irreversible discharge from East Antarctica. Nat. Clim. Chang. 4, 451-455.

Menviel, L., Spence, P., Yu, J., Chamberlain, M.A., Matear, R.J., Meissner, K.J., England, M.H., 2018a. Southern Hemisphere westerlies as a driver of the early deglacial atmospheric CO_2 rise. Nature Communications 9, 2503, doi: 10.1038/s41467-018-04876-4.

Mercer, J.H., 1978. West Antarctic ice sheet and CO_2 greenhouse effect: a threat of disaster. Nature 271, 321-325.

Milankovitch, M.M., 1941. Canon of insolation and the ice age problem. Royal Serbian Academy Special Publication 132.

Monnin, E., Indermuhle, A., Dallenbach, A., Fluckiger, J., Stauffer, B., Stocker, T.F., Raynaud, D., Barnola, J.M., 2001. Atmospheric CO_2 concentrations over the last glacial termination. Science 291, 112-114.

Morlighem, M., Rignot, E., Binder, T., Blankenship, D., Drews, R., Eagles, G., Eisen, O., Ferraccioli, F., Forsberg, R., Fretwell, P., 2020. Deep glacial troughs and stabilizing ridges unveiled beneath the margins of the Antarctic ice sheet. Nat. Geosci. 13, 132-137.

Mortlock, R.A., Charles, C.D., Froelich, P.N., Zibello, M.A., Saltzman, J., Hays, J.D., Burckle, L.H., 1991. Evidence for lower productivity in the Antarctic Ocean during the last glaciation. Nature 351, 220-223.

Mortyn, P.G., Charles, C.D., Ninnemann, U.S., Ludwig, K., Hodell, D.A., 2003. Deep sea sedimentary analogs for the Vostok ice core. Geochem. Geophys. Geosyst. 4, 8405, doi: 10.1029/2002GC000475.

Mulitza, S., Chiessi, C.M., Schefuß, E., Lippold, J., Wichmann, D., Antz, B., Mackensen, A., Paul, A., Prange, M., Rehfeld, K., 2017. Synchronous and proportional deglacial changes in Atlantic meridional overturning and northeast Brazilian precipitation. Paleoceanography 32, 622-633.

Muschitiello, F., D'Andrea, W.J., Schmittner, A., Heaton, T.J., Balascio, N.L., DeRoberts, N., Caffee, M.W., Woodruff, T.E., Welten, K.C., Skinner, L.C., 2019. Deep-water circulation changes lead North

Atlantic climate during deglaciation. Nature Communications 10, 1272, doi: 10.1038/s41467-019-09237-3.

Nadeau, L.-P., Ferrari, R., Jansen, M.F., 2019. Antarctic sea ice control on the depth of North Atlantic Deep Water. J. Clim. 32, 2537-2551.

Naish, T., Powell, R., Levy, R., Wilson, G., Scherer, R., Talarico, F., Krissek, L., Niessen, F., Pompilio, M., Wilson, T., Carter, L., DeConto, R., Huybers, P., McKay, R., Pollard, D., Ross, J., Winter, D., Barrett, P., Browne, G., Cody, R., Cowan, E., Crampton, J., Dunbar, G., Dunbar, N., Florindo, F., Gebhardt, C., Graham, I., Hannah, M., Hansaraj, D., Harwood, D., Helling, D., Henrys, S., Hinnov, L., Kuhn, G., Kyle, P., Laufer, A., Maffioli, P., Magens, D., Mandernack, K., McIntosh, W., Millan, C., Morin, R., Ohneiser, C., Paulsen, T., Persico, D., Raine, I., Reed, J., Riesselman, C., Sagnotti, L., Schmitt, D., Sjunneskog, C., Strong, P., Taviani, M., Vogel, S., Wilch, T., Williams, T., 2009. Obliquity-paced Pliocene West Antarctic ice sheet oscillations. Nature 458, 322-328.

Nakayama, Y., Manucharyan, G., Zhang, H., Dutrieux, P., Torres, H.S., Klein, P., Seroussi, H., Schodlok, M., Rignot, E., Menemenlis, D., 2019. Pathways of ocean heat towards Pine Island and Thwaites grounding lines. Sci Rep 9, 16649, doi: 10.1038/s41598-019-53190-6.

Narcisi, B., Petit, J.-R., Delmonte, B., Basile-Doelsch, I., Maggi, V., 2005. Characteristics and sources of tephra layers in the EPICA-Dome C ice record (East Antarctica): implications for past atmospheric circulation and ice core stratigraphic correlations. Earth Planet. Sci. Lett. 239, 253-265.

NGRIP Members, 2004. High-resolution record of Northern Hemisphere climate extending into the last interglacial period. Nature 431, 147-151.

Nichols, K.A., Goehring, B.M., Balco, G., Johnson, J.S., Hein, A.S., Todd, C., 2019. New Last Glacial Maximum ice thickness constraints for the Weddell Sea Embayment, Antarctica. The Cryosphere 13, 2935-2951.

Nürnberg, D., Bijma, J., Hemleben, C., 1996. Assessing the reliability of magnesium in foraminiferal calcite as a proxy for water mass temperatures. Geochim. Cosmochim. Acta 60, 803-814.

Ohkouchi, N., Eglinton, T.I., Hayes, J.M., 2003. Radiocarbon dating of individual fatty acids as a tool for refining Antarctic margin sediment chronologies. Radiocarbon 45, 17-24.

Oliver, K.I.C., Hoogakker, B.A.A., Crowhurst, S., Henderson, G.M., Rickaby, R.E.M., Edwards, N.R., Elderfield, H., 2010. A synthesis of marine sediment core $\delta^{13}C$ data over the last 150 000 years. Clim. Past. 6, 645-673.

Paillard, D., Parrenin, F., 2004. The Antarctic ice sheet and the triggering of deglaciations. Earth Planet. Sci. Lett. 227, 263-271.

Paolo, F.S., Fricker, H.A., Padman, L., 2015. Volume loss from Antarctic ice shelves is accelerating. Science 348, 327-331.

Parrenin, F., Masson-Delmotte, V., Köhler, P., Raynaud, D., Paillard, D., Schwander, J., Barbante, C., Landais, A., Wegner, A., Jouzel, J., 2013. Synchronous change of atmospheric CO_2 and Antarctic temperature during the last deglacial warming. Science 339, 1060-1063.

Passchier, S., O'Brien, P.E., Damuth, J.E., Januszczak, N., Handwerger, D.A., Whitehead, J.M., 2003. Pliocene–Pleistocene glaciomarine sedimentation in eastern Prydz Bay and development of the Prydz trough-mouth fan, ODP Sites 1166 and 1167, East Antarctica. Mar. Geol. 199, 279-305.

Patterson, M.O., McKay, R., Naish, T., Escutia, C., Jimenez-Espejo, F.J., Raymo, M.E., Meyers, S.R., Tauxe, L., Brinkhuis, H., IODP Expedition 318 Scientists, 2014. Orbital forcing of the East Antarctic ice sheet during the Pliocene and Early Pleistocene. Nat. Geosci. 7, 841-847.

Paxman, G.J.G., Gasson, E.G.W., Jamieson, S.S.R., Bentley, M.J., Ferraccioli, F., 2020. Long-term increase in Antarctic Ice Sheet vulnerability driven by bed topography evolution. Geophys. Res. Lett. 47, e2020GL090003, doi: 10.1029/2020GL090003.

Paxman, G.J.G., Jamieson, S.S.R., Hochmuth, K., Gohl, K., Bentley, M.J., Leitchenkov, G., Ferraccioli, F., 2019. Reconstructions of Antarctic topography since the Eocene–Oligocene boundary. Paleogeogr. Paleoclimatol. Paleoecol. 535, 109346, doi: 10.1016/j.palaeo.2019.109346.

Paytan, A., Griffith, E.M., 2007. Marine barite: Recorder of variations in ocean export productivity. Deep Sea Research Part II: Topical Studies in Oceanography 54, 687-705.

Pearson, P.N., 2012. Oxygen isotopes in foraminifera: Overview and historical review. The Paleontological Society Papers 18, 1-38.

Peeters, F.J.C., Acheson, R., Brummer, G.J.A., de Ruijter, W.P.M., Schneider, R.R., Ganssen, G.M., Ufkes, E., Kroon, D., 2004. Vigorous exchange between the Indian and Atlantic oceans at the end of the past five glacial periods. Nature 430, 661-665.

Pena, L.D., Goldstein, S.L., 2014. Thermohaline circulation crisis and impacts during the mid-Pleistocene transition. Science 345, 318-322.

Peterson, L.C., Haug, G.H., Hughen, K.A., Röhl, U., 2000. Rapid changes in the hydrologic cycle of the tropical Atlantic during the last glacial. Science 290, 1947-1951.

Petit, J.R., Jouzel, J., Raynaud, D., Barkov, N.I., Barnola, J.M., Basile, I., Bender, M., Chappellaz, J., Davis, M., Delaygue, G., Delmotte, M., Kotlyakov, V.M., Legrand, M., Lipenkov, V.Y., Lorius, C., Pepin, L., Ritz, C., Saltzman, E., Stievenard, M., 1999. Climate and atmospheric history of the past 420,000 years from the Vostok ice core, Antarctica. Nature 399, 429-436.

Phipps, S.J., Fogwill, C.J., Turney, C.S.M., 2016. Impacts of marine instability across the East Antarctic Ice Sheet on Southern Ocean dynamics. The Cryosphere 10, 2317-2328.

Piotrowski, A.M., Goldstein, S.L., Hemming, S.R., Fairbanks, R.G., 2005. Temporal relationships of carbon cycling and ocean circulation at glacial boundaries. Science 307, 1933-1938.

Pollard, D., DeConto, R.M., 2009. Modelling West Antarctic ice sheet growth and collapse through the past five million years. Nature 458, 329-332.

Pollard, D., DeConto, R.M., Alley, R.B., 2015. Potential Antarctic Ice Sheet retreat driven by hydrofracturing and ice cliff failure. Earth Planet. Sci. Lett. 412, 112-121.

Polyak, V.J., Onac, B.P., Fornós, J.J., Hay, C., Asmerom, Y., Dorale, J.A., Ginés, J., Tuccimei, P., Ginés, A., 2018. A highly resolved record of relative sea level in the western Mediterranean Sea during the last interglacial period. Nat. Geosci. 11, 860-864.

Pritchard, H.D., Ligtenberg, S.R.M., Fricker, H.A., Vaughan, D.G., van den Broeke, M.R., Padman, L., 2012. Antarctic ice-sheet loss driven by basal melting of ice shelves. Nature 484, 502-505.

Prothro, L.O., Majewski, W., Yokoyama, Y., Simkins, L.M., Anderson, J.B., Yamane, M., Miyairi, Y., Ohkouchi, N., 2020. Timing and pathways of East Antarctic Ice Sheet retreat. Quat. Sci. Rev. 230, 106166, doi: 10.1016/j.quascirev.2020.106166.

Pugh, R.S., McCave, I.N., Hillenbrand, C.-D., Kuhn, G., 2009. Circum-Antarctic age modelling of Quaternary marine cores under the Antarctic Circumpolar Current: ice-core dust–magnetic correlation. Earth Planet. Sci. Lett. 284, 113-123.

Quilty, P.G., Lirio, J.M., Jillett, D., 2000. Stratigraphy of the Pliocene Sørsdal Formation, Marine Plain, Vestfold Hills, East Antarctica. Antarct. Sci. 12, 205-216.

Rae, J.W.B., Burke, A., Robinson, L.F., Adkins, J.F., Chen, T., Cole, C., Greenop, R., Li, T., Littley, E.F.M., Nita, D.C., Stewart, J.A., Taylor, B.J., 2018. CO_2 storage and release in the deep Southern Ocean on millennial to centennial timescales. Nature 562, 569-573.

Rae, J.W.B., Foster, G.L., Schmidt, D.N., Elliott, T., 2011. Boron isotopes and B/Ca in benthic foraminifera: Proxies for the deep ocean carbonate system. Earth Planet. Sci. Lett. 302, 403-413.

Ragueneau, O., Tréguer, P., Leynaert, A., Anderson, R.F., Brzezinski, M.A., DeMaster, D.J., Dugdale, R.C., Dymond, J., Fischer, G., Francois, R., 2000. A review of the Si cycle in the modern ocean: recent progress and missing gaps in the application of biogenic opal as a paleoproductivity proxy. Glob. Planet. Change 26, 317-365.

RAISED Consortium, 2014. A community-based geological reconstruction of Antarctic Ice Sheet deglaciation since the Last Glacial Maximum. Quat. Sci. Rev. 100, 1-9.

Rampen, S.W., Willmott, V., Kim, J.-H., Uliana, E., Mollenhauer, G., Schefuß, E., Damsté, J.S.S., Schouten, S., 2012. Long chain 1, 13-and 1, 15-diols as a potential proxy for palaeotemperature reconstruction. Geochim. Cosmochim. Acta 84, 204-216.

Raymo, M.E., 1994. The initiation of Northern Hemisphere glaciation. Annual Review of Earth and Planetary Sciences 22, 353-383.

Raymo, M.E., Lisiecki, L.E., Nisancioglu, K.H., 2006. Plio-Pleistocene ice volume, Antarctic climate, and the global δ18O record. Science 313, 492-495.

Raymo, M.E., Mitrovica, J.X., 2012. Collapse of polar ice sheets during the stage 11 interglacial. Nature 483, 453-456.

Reimer, P.J., Bard, E., Bayliss, A., Beck, J.W., Blackwell, P.G., Ramsey, C.B., Buck, C.E., Cheng, H., Edwards, R.L., Friedrich, M., Grootes, P.M., Guilderson, T.P., Haflidason, H., Hajdas, I., Hatte, C., Heaton, T.J., Hoffmann, D.L., Hogg, A.G., Hughen, K.A., Kaiser, K.F., Kromer, B., Manning, S.W., Niu, M., Reimer, R.W., Richards, D.A., Scott, E.M., Southon, J.R., Staff, R.A., Turney, C.S.M., van der Plicht, J., 2013. IntCal13 and Marine13 radiocarbon age calibration curves 0-50,000 years cal BP. Radiocarbon 55, 1869-1887.

Reinardy, B.T.I., Escutia, C., Iwai, M., Jimenez-Espejo, F.J., Cook, C., de Flierdt, T.V., Brinkhuis, H., 2015. Repeated advance and retreat of the East Antarctic Ice Sheet on the continental shelf during the early Pliocene warm period. Paleogeogr. Paleoclimatol. Paleoecol. 422, 65-84.

Reyes, A.V., Carlson, A.E., Beard, B.L., Hatfield, R.G., Stoner, J.S., Winsor, K., Welke, B., Ullman, D.J., 2014. South Greenland ice-sheet collapse during marine isotope stage 11. Nature 510, 525-528.

Rial, J.A., Oh, J., Reischmann, E., 2013. Synchronization of the climate system to eccentricity forcing and the 100,000-year problem. Nat. Geosci. 6, 289-293.

Rickaby, R.E.M., Elderfield, H., Roberts, N., Hillenbrand, C.D., Mackensen, A., 2010. Evidence for elevated alkalinity in the glacial Southern Ocean. Paleoceanography 25, PA1209, doi: 10.1029/2009PA001762.

Rignot, E., Casassa, G., Gogineni, P., Krabill, W., Rivera, A.U., Thomas, R., 2004. Accelerated ice discharge from the Antarctic Peninsula following the collapse of Larsen B ice shelf. Geophys. Res. Lett. 31, L18401, doi: 10.1029/2004GL020697.

Rignot, E., Mouginot, J., Morlighem, M., Seroussi, H., Scheuchl, B., 2014. Widespread, rapid grounding line retreat of Pine Island, Thwaites, Smith, and Kohler glaciers, West Antarctica, from 1992 to 2011. Geophys. Res. Lett. 41, 3502-3509.

Rintoul, S.R., Chown, S.L., DeConto, R.M., England, M.H., Fricker, H.A., Masson-Delmotte, V., Naish, T.R., Siegert, M.J., Xavier, J.C., 2018. Choosing the future of Antarctica. Nature 558, 233-241.

Ritz, C., Edwards, T.L., Durand, G., Payne, A.J., Peyaud, V., Hindmarsh, R.C.A., 2015. Potential sea-level rise from Antarctic ice-sheet instability constrained by observations. Nature 528, 115-118.

Roberts, N.L., Piotrowski, A.M., McManus, J.F., Keigwin, L.D., 2010. Synchronous deglacial overturning and water mass source changes. Science 327, 75-78.

Robinson, L.F., Adkins, J.F., Frank, N., Gagnon, A.C., Prouty, N.G., Roark, E.B., van de Flierdt, T., 2014. The geochemistry of deep-sea coral skeletons: A review of vital effects and applications for palaeoceanography. Deep Sea Research Part II: Topical Studies in Oceanography 99, 184-198.

Robinson, L.F., Siddall, M., 2012. Palaeoceanography: motivations and challenges for the future. Philosophical Transactions of the Royal Society A: Mathematical, Physical and Engineering Sciences 370, 5540-5566.

Robinson, L.F., van de Flierdt, T., 2009. Southern Ocean evidence for reduced export of North Atlantic Deep Water during Heinrich event 1. Geology 37, 195-198.

Roche, D.M., Crosta, X., Renssen, H., 2012. Evaluating Southern Ocean sea-ice for the Last Glacial Maximum and pre-industrial climates: PMIP-2 models and data evidence. Quat. Sci. Rev. 56, 99-106.

Rodríguez-Sanz, L., Mortyn, P.G., Martínez-Garcia, A., Rosell-Mele, A., Hall, I.R., 2012. Glacial Southern Ocean freshening at the onset of the Middle Pleistocene climate transition. Earth Planet. Sci. Lett. 345, 194-202.

Rohling, E.J., 2000. Paleosalinity: confidence limits and future applications. Mar. Geol. 163, 1-11.

Rohling, E.J., Foster, G.L., Grant, K.M., Marino, G., Roberts, A.P., Tamisiea, M.E., Williams, F., 2014. Sea-level and deep-sea-temperature variability over the past 5.3 million years. Nature 508, 477-482.

Rohling, E.J., Hibbert, F.D., Grant, K.M., Galaasen, E.V., Irvalı, N., Kleiven, H.F., Marino, G., Ninnemann, U., Roberts, A.P., Rosenthal, Y., 2019. Asynchronous Antarctic and Greenland ice-volume contributions to the last interglacial sea-level highstand. Nature Communications 10, 5040, doi: 10.1038/s41467-019-12874-3.

Rohling, E.J., Hibbert, F.D., Williams, F.H., Grant, K.M., Marino, G., Foster, G.L., Hennekam, R., de Lange, G.J., Roberts, A.P., Yu, J., Webster, J.M., Yokoyama, Y., 2017. Differences between the last two glacial maxima and implications for ice-sheet, $\delta^{18}O$, and sea-level reconstructions. Quat. Sci. Rev. 176, 1-28.

Rohling, E.J., Marsh, R., Wells, N.C., Siddall, M., Edwards, N.R., 2004. Similar meltwater contributions to glacial sea level changes from Antarctic and northern ice sheets. Nature 430, 1016-1021.

Rosenheim, B.E., Santoro, J.A., Gunter, M., Domack, E.W., 2013. Improving Antarctic sediment ^{14}C dating using ramped pyrolysis: an example from the Hugo Island Trough. Radiocarbon 55, 115-126.

Roy, M., van de Flierdt, T., Hemming, S.R., Goldstein, S.L., 2007. $^{40}Ar/^{39}Ar$ ages of hornblende grains and bulk Sm/Nd isotopes of circum-Antarctic glacio-marine sediments: implications for sediment provenance in the southern ocean. Chemical Geology 244, 507-519.

Ruddiman, W.F., 1977. Late Quaternary deposition of ice-rafted sand in the subpolar North Atlantic (lat 40° to 65° N). Geol. Soc. Am. Bull. 88, 1813-1827.

Ruddiman, W.F., 2006. Orbital changes and climate. Quat. Sci. Rev. 25, 3092-3112.

Ruddiman, W.F., Raymo, M.E., Martinson, D.G., Clement, B.M., Backman, J., 1989. Pleistocene evolution: Northern Hemisphere ice sheets and North Atlantic Ocean. Paleoceanography 4, 353-412.

Sachs, J.P., Anderson, R.F., 2005. Increased productivity in the subantarctic ocean during Heinrich events. Nature 434, 1118-1121.

Sachs, J.P., Lehman, S.J., 1999. Subtropical North Atlantic temperatures 60,000 to 30,000 years ago. Science 286, 756-759.

Sanyal, A., Hemming, N.G., Broecker, W.S., Hanson, G.N., 1997. Changes in pH in the eastern equatorial Pacific across stage 5–6 boundary based on boron isotopes in foraminifera. Glob. Biogeochem. Cycle 11, 125-133.

Scherer, R.P., Aldahan, A., Tulaczyk, S., Possnert, G., Engelhardt, H., Kamb, B., 1998. Pleistocene collapse of the West Antarctic ice sheet. Science 281, 82-85.

Scherer, R.P., Bohaty, S.M., Dunbar, R.B., Esper, O., Flores, J.A., Gersonde, R., Harwood, D.M., Roberts, A.P., Taviani, M., 2008. Antarctic records of precession-paced insolation-driven warming during early Pleistocene Marine Isotope Stage 31. Geophys. Res. Lett. 35, L03505, doi: 10.1029/2007GL032254.

Schloesser, F., Friedrich, T., Timmermann, A., DeConto, R.M., Pollard, D., 2019. Antarctic iceberg impacts on future Southern Hemisphere climate. Nat. Clim. Chang. 9, 672-677.

Schmidt, M.W., Spero, H.J., Lea, D.W., 2004. Links between salinity variation in the Caribbean and North Atlantic thermohaline circulation. Nature 428, 160-163.

Schoof, C., 2007. Ice sheet grounding line dynamics: Steady states, stability, and hysteresis. J. Geophys. Res.-Earth Surf. 112, F03S28, doi: 10.1029/2006JF000664.

Schouten, S., Hopmans, E.C., Schefuß, E., Damste, J.S.S., 2002. Distributional variations in marine crenarchaeotal membrane lipids: a new tool for reconstructing ancient sea water temperatures? Earth Planet. Sci. Lett. 204, 265-274.

Severinghaus, J.P., Beaudette, R., Headly, M.A., Taylor, K., Brook, E.J., 2009. Oxygen-18 of O_2 records the impact of abrupt climate change on the terrestrial biosphere. Science 324, 1431-1434.

Severinghaus, J.P., Brook, E.J., 1999. Abrupt climate change at the end of the last glacial period inferred from trapped air in polar ice. Science 286, 930-934.

Shackleton, N.J., 2000. The 100,000-year ice-age cycle identified and found to lag temperature, carbon dioxide, and orbital eccentricity. Science 289, 1897-1902.

Shackleton, N.J., Duplessy, J.-C., Arnold, M., Maurice, P., Hall, M.A., Cartlidge, J., 1988. Radiocarbon age of last glacial Pacific deep water. Nature 335, 708-711.

Shackleton, N.J., Hall, M.A., Vincent, E., 2000. Phase relationships between millennial-scale events 64,000-24,000 years ago. Paleoceanography 15, 565-569.

Shackleton, S., Baggenstos, D., Menking, J., Dyonisius, M., Bereiter, B., Bauska, T., Rhodes, R., Brook, E., Petrenko, V., McConnell, J., 2020. Global ocean heat content in the Last Interglacial. Nat. Geosci. 13, 77-81.

Shakun, J.D., Clark, P.U., He, F., Marcott, S.A., Mix, A.C., Liu, Z.Y., Otto-Bliesner, B., Schmittner, A., Bard, E., 2012. Global warming preceded by increasing carbon dioxide concentrations during the last deglaciation. Nature 484, 49-54.

Shakun, J.D., Corbett, L.B., Bierman, P.R., Underwood, K., Rizzo, D.M., Zimmerman, S.R., Caffee, M.W., Naish, T., Golledge, N.R., Hay, C.C., 2018. Minimal East Antarctic Ice Sheet retreat onto land during the past eight million years. Nature 558, 284-287.

Shakun, J.D., Lea, D.W., Lisiecki, L.E., Raymo, M.E., 2015. An 800-kyr record of global surface ocean $\delta^{18}O$ and implications for ice volume-temperature coupling. Earth Planet. Sci. Lett. 426, 58-68.

Shemesh, A., Burckle, L.H., Hays, J.D., 1994. Meltwater input to the Southern Ocean during the last glacial maximum. Science 266, 1542-1544.

Shemesh, A., Hodell, D., Crosta, X., Kanfoush, S., Charles, C., Guilderson, T., 2002. Sequence of events during the last deglaciation in Southern Ocean sediments and Antarctic ice cores. Paleoceanography 17, 1056, doi: 10.1029/2000PA000599.

Shepherd, A., Fricker, H.A., Farrell, S.L., 2018. Trends and connections across the Antarctic cryosphere. Nature 558, 223-232.

Sigl, M., Winstrup, M., McConnell, J.R., Welten, K.C., Plunkett, G., Ludlow, F., Büntgen, U., Caffee, M., Chellman, N., Dahl-Jensen, D., 2015. Timing and climate forcing of volcanic eruptions for the past 2,500 years. Nature 523, 543-549.

Sigman, D.M., Boyle, E.A., 2000. Glacial/interglacial variations in atmospheric carbon dioxide. Nature 407, 859-869.

Sigman, D.M., Hain, M.P., Haug, G.H., 2010. The polar ocean and glacial cycles in atmospheric CO_2 concentration. Nature 466, 47-55.

Sikes, E.L., Volkman, J.K., 1993. Calibration of alkenone unsaturation ratios ($U^{k'}_{37}$) for paleotemperature estimation in cold polar waters. Geochim. Cosmochim. Acta 57, 1883-1889.

Silvano, A., Rintoul, S.R., Herraiz-Borreguero, L., 2016. Ocean-ice shelf interaction in East Antarctica. Oceanography 29, 130-143.

Simões Pereira, P., van de Flierdt, T., Hemming, S.R., Hammond, S.J., Kuhn, G., Brachfeld, S., Doherty, C., Hillenbrand, C.-D., 2018. Geochemical fingerprints of glacially eroded bedrock from West Antarctica: Detrital thermochronology, radiogenic isotope systematics and trace element geochemistry in Late Holocene glacial-marine sediments. Earth-Sci. Rev. 182, 204-232.

Skinner, L.C., Fallon, S., Waelbroeck, C., Michel, E., Barker, S., 2010. Ventilation of the deep Southern Ocean and deglacial CO_2 rise. Science 328, 1147-1151.

Skinner, L.C., Muschitiello, F., Scrivner, A.E., 2019. Marine reservoir age variability over the last deglaciation: implications for marine carbon cycling and prospects for regional radiocarbon calibrations. Paleoceanography and Paleoclimatology 34, 1807-1815.

Skinner, L.C., Primeau, F., Freeman, E., de la Fuente, M., Goodwin, P.A., Gottschalk, J., Huang, E., McCave, I.N., Noble, T.L., Scrivner, A.E., 2017. Radiocarbon constraints on the glacial ocean circulation and its impact on atmospheric CO_2. Nature Communications 8, 16010, doi: 10.1038/ncomms16010.

Skinner, L.C., Shackleton, N.J., 2005. An Atlantic lead over Pacific deep-water change across Termination I: implications for the application of the marine isotope stage stratigraphy. Quat. Sci. Rev. 24, 571-580.

Smith, J.A., Graham, A.G.C., Post, A.L., Hillenbrand, C.-D., Bart, P.J., Powell, R.D., 2019. The marine geological imprint of Antarctic ice shelves. Nature Communications 10, 5635, doi: 10.1038/s41467-019-13496-5.

Snow, K., Hogg, A.M., Sloyan, B.M., Downes, S.M., 2016. Sensitivity of Antarctic bottom water to changes in surface buoyancy fluxes. J. Clim. 29, 313-330.

Snyder, C.W., 2016. Evolution of global temperature over the past two million years. Nature 538, 226-228.

Sosdian, S., Rosenthal, Y., 2009. Deep-sea temperature and ice volume changes across the Pliocene-Pleistocene climate transitions. Science 325, 306-310.

Sosdian, S.M., Greenop, R., Hain, M., Foster, G.L., Pearson, P.N., Lear, C.H., 2018. Constraining the evolution of Neogene ocean carbonate chemistry using the boron isotope pH proxy. Earth Planet. Sci. Lett. 498, 362-376.

Spahni, R., Chappellaz, J., Stocker, T.F., Loulergue, L., Hausammann, G., Kawamura, K., Flückiger, J., Schwander, J., Raynaud, D., Masson-Delmotte, V., 2005. Atmospheric methane and nitrous oxide of the late Pleistocene from Antarctic ice cores. Science 310, 1317-1321.

Spooner, P.T., Guo, W., Robinson, L.F., Thiagarajan, N., Hendry, K.R., Rosenheim, B.E., Leng, M.J., 2016. Clumped isotope composition of cold-water corals: A role for vital effects? Geochim. Cosmochim. Acta 179, 123-141.

Spratt, R.M., Lisiecki, L.E., 2016. A Late Pleistocene sea level stack. Clim. Past. 12, 1079-1092.

Steig, E.J., Huybers, K., Singh, H.A., Steiger, N.J., Ding, Q., Frierson, D.M., Popp, T., White, J.W., 2015. Influence of West Antarctic ice sheet collapse on Antarctic surface climate. Geophys. Res. Lett. 42, 4862-4868.

Stein, K., Timmermann, A., Kwon, E.Y., Friedrich, T., 2020. Timing and magnitude of Southern Ocean sea ice/carbon cycle feedbacks. Proceedings of the National Academy of Sciences 117, 4498-4504.

Stenni, B., Buiron, D., Frezzotti, M., Albani, S., Barbante, C., Bard, E., Barnola, J.M., Baroni, M., Baumgartner, M., Bonazza, M., 2011. Expression of the bipolar see-saw in Antarctic climate records during the last deglaciation. Nat. Geosci. 4, 46-49.

Stocker, T.F., Johnsen, S.J., 2003. A minimum thermodynamic model for the bipolar seesaw. Paleoceanography 18, 1087, doi: 10.1029/2003pa000920.

Strugnell, J.M., Pedro, J.B., Wilson, N.G., 2018. Dating Antarctic ice sheet collapse: Proposing a molecular genetic approach. Quat. Sci. Rev. 179, 153-157.

Studer, A.S., Sigman, D.M., Martínez-García, A., Benz, V., Winckler, G., Kuhn, G., Esper, O., Lamy, F., Jaccard, S.L., Wacker, L., 2015. Antarctic Zone nutrient conditions during the last two glacial cycles. Paleoceanography 30, 845-862.

Suganuma, Y., Miura, H., Zondervan, A., Okuno, J.i., 2014. East Antarctic deglaciation and the link to global cooling during the Quaternary: Evidence from glacial geomorphology and 10Be surface exposure dating of the Sør Rondane Mountains, Dronning Maud Land. Quat. Sci. Rev. 97, 102-120.

Sugden, D.E., Marchant, D.R., Denton, G.H., 1993. The case for a stable East Antarctic ice sheet: the background. Geografiska Annaler: Series A, Physical Geography 75, 151-154.

Sutter, J., Eisen, O., Werner, M., Grosfeld, K., Kleiner, T., Fischer, H., 2020. Limited retreat of the Wilkes Basin ice sheet during the Last Interglacial. Geophys. Res. Lett. 47, e2020GL088131, https://doi.org/10.1029/2020GL088131.

Sutter, J., Fischer, H., Grosfeld, K., Karlsson, N.B., Kleiner, T., Van Liefferinge, B., Eisen, O., 2019. Modelling the Antarctic Ice Sheet across the mid-Pleistocene transition–implications for Oldest Ice. The Cryosphere 13, 2023-2041.

Sutter, J., Gierz, P., Grosfeld, K., Thoma, M., Lohmann, G., 2016. Ocean temperature thresholds for Last Interglacial West Antarctic Ice Sheet collapse. Geophys. Res. Lett. 43, 2675-2682.

Svensson, A., Andersen, K.K., Bigler, M., Clausen, H.B., Dahl-Jensen, D., Davies, S.M., Johnsen, S.J., Muscheler, R., Parrenin, F., Rasmussen, S.O., 2008. A 60 000 year Greenland stratigraphic ice core chronology. Clim. Past. 4, 47-57.

Swann, G.E.A., Leng, M.J., 2009. A review of diatom $\delta^{18}O$ in palaeoceanography. Quat. Sci. Rev. 28, 384-398.

Teitler, L., Florindo, F., Warnke, D.A., Filippelli, G.M., Kupp, G., Taylor, B., 2015. Antarctic Ice Sheet response to a long warm interval across Marine Isotope Stage 31: A cross-latitudinal study of iceberg-rafted debris. Earth Planet. Sci. Lett. 409, 109-119.

Teitler, L., Warnke, D.A., Venz, K.A., Hodell, D.A., Becquey, S., Gersonde, R., Teitler, W., 2010. Determination of Antarctic Ice Sheet stability over the last ~500 ka through a study of iceberg-rafted debris. Paleoceanography 25, PA1202, doi: 10.1029/2008PA001691.

Thöle, L.M., Amsler, H.E., Moretti, S., Auderset, A., Gilgannon, J., Lippold, J., Vogel, H., Crosta, X., Mazaud, A., Michel, E., 2019. Glacial-interglacial dust and export production records from the Southern Indian Ocean. Earth Planet. Sci. Lett. 525, 115716, doi: 10.1016/j.epsl.2019.115716.

Thomas, A.L., Henderson, G.M., Deschamps, P., Yokoyama, Y., Mason, A.J., Bard, E., Hamelin, B., Durand, N., Camoin, G., 2009. Penultimate deglacial sea-level timing from uranium/thorium dating of Tahitian corals. Science 324, 1186-1189.

Tigchelaar, M., Timmermann, A., Pollard, D., Friedrich, T., Heinemann, M., 2018. Local insolation changes enhance Antarctic interglacials: Insights from an 800,000-year ice sheet simulation with transient climate forcing. Earth Planet. Sci. Lett. 495, 69-78.

Toggweiler, J.R., 1999. Variation of atmospheric CO_2 by ventilation of the ocean's deepest water. Paleoceanography 14, 571-588.

Toggweiler, J.R., Russell, J.L., Carson, S.R., 2006. Midlatitude westerlies, atmospheric CO_2, and climate change during the ice ages. Paleoceanography 21, PA2005, doi: 10.1029/2005PA001154.

Tolotti, R., Bárcena, M.A., Macrì, P., Caburlotto, A., Bonci, M.C., De Santis, L., Donda, F., Corradi, N., Crosta, X., 2018. Wilkes Land Late Pleistocene diatom age model: From bio-events to quantitative biostratigraphy. Revue de Micropaléontologie 61, 81-96.

Tooze, S., Halpin, J.A., Noble, T.L., Chase, Z., O'Brien, P.E., Armand, L., 2020. Scratching the surface: a marine sediment provenance record from the continental slope of central Wilkes Land, East Antarctica. Geochemistry, Geophysics, Geosystems 21, e2020GC009156, doi: 10.1029/2020GC009156.

Toyos, M.H., Lamy, F., Lange, C.B., Lembke-Jene, L., Saavedra-Pellitero, M., Esper, O., Arz, H.W., 2020. Antarctic Circumpolar Current dynamics at the Pacific entrance to the Drake Passage over the past 1.3 million years. Paleoceanography and Paleoclimatology 35, e2019PA003773, doi: 10.1029/2019PA003773.

Turner, J., Orr, A., Gudmundsson, G.H., Jenkins, A., Bingham, R.G., Hillenbrand, C.D., Bracegirdle, T.J., 2017. Atmosphere-ocean-ice interactions in the Amundsen Sea Embayment, West Antarctica. Rev. Geophys. 55, 235-276.

Turney, C.S.M., Fogwill, C.J., Golledge, N.R., McKay, N.P., van Sebille, E., Jones, R.T., Etheridge, D., Rubino, M., Thornton, D.P., Davies, S.M., 2020. Early Last Interglacial ocean warming drove substantial ice mass loss from Antarctica. Proceedings of the National Academy of Sciences 117, 3996-4006.

Vallelonga, P., Gabrielli, P., Balliana, E., Wegner, A., Delmonte, B., Turetta, C., Burton, G., Vanhaecke, F., Rosman, K.J.R., Hong, S., Boutron, C.F., Cescon, P., Barbante, C., 2010. Lead isotopic compositions in the EPICA Dome C ice core and Southern Hemisphere Potential Source Areas. Quat. Sci. Rev. 29, 247-255.

van de Flierdt, T., Griffiths, A.M., Lambelet, M., Little, S.H., Stichel, T., Wilson, D.J., 2016. Neodymium in the oceans: a global database, a regional comparison and implications for palaeoceanographic research. Philosophical Transactions of the Royal Society A: Mathematical, Physical and Engineering Sciences 374, doi: 10.1098/rsta.2015.0293.

Vázquez Riveiros, N., Govin, A., Waelbroeck, C., Mackensen, A., Michel, E., Moreira, S., Bouinot, T., Caillon, N., Orgun, A., Brandon, M., 2016. Mg/Ca thermometry in planktic foraminifera: Improving

paleotemperature estimations for *G. bulloides* and *N. pachyderma* left. Geochemistry, Geophysics, Geosystems 17, 1249-1264.

Villa, G., Lupi, C., Cobianchi, M., Florindo, F., Pekar, S.F., 2008. A Pleistocene warming event at 1 Ma in Prydz Bay, East Antarctica: evidence from ODP site 1165. Palaeogeography, Palaeoclimatology, Palaeoecology 260, 230-244.

Vorrath, M.-E., Müller, J., Esper, O., Mollenhauer, G., Haas, C., Schefuß, E., Fahl, K., 2019. Highly branched isoprenoids for Southern Ocean sea ice reconstructions: a pilot study from the Western Antarctic Peninsula. Biogeosciences 16, 2961-2981.

Waelbroeck, C., Labeyrie, L., Michel, E., Duplessy, J.C., McManus, J.F., Lambeck, K., Balbon, E., Labracherie, M., 2002. Sea-level and deep water temperature changes derived from benthic foraminifera isotopic records. Quat. Sci. Rev. 21, 295-305.

WAIS Divide Project Members, 2013. Onset of deglacial warming in West Antarctica driven by local orbital forcing. Nature 500, 440-444.

WAIS Divide Project Members, 2015. Precise interpolar phasing of abrupt climate change during the last ice age. Nature 520, 661-665.

Wang, X., Auler, A.S., Edwards, R.L., Cheng, H., Cristalli, P.S., Smart, P.L., Richards, D.A., Shen, C.-C., 2004. Wet periods in northeastern Brazil over the past 210 kyr linked to distant climate anomalies. Nature 432, 740-743.

Wang, X.T., Sigman, D.M., Prokopenko, M.G., Adkins, J.F., Robinson, L.F., Hines, S.K., Chai, J., Studer, A.S., Martínez-García, A., Chen, T., 2017. Deep-sea coral evidence for lower Southern Ocean surface nitrate concentrations during the last ice age. Proceedings of the National Academy of Sciences 114, 3352-3357.

Wang, Y.J., Cheng, H., Edwards, R.L., An, Z.S., Wu, J.Y., Shen, C.C., Dorale, J.A., 2001. A high-resolution absolute-dated Late Pleistocene monsoon record from Hulu Cave, China. Science 294, 2345-2348.

Watson, A.J., Vallis, G.K., Nikurashin, M., 2015. Southern Ocean buoyancy forcing of ocean ventilation and glacial atmospheric CO2. Nat. Geosci. 8, 861-864.

Weaver, A.J., Saenko, O.A., Clark, P.U., Mitrovica, J.X., 2003. Meltwater pulse 1A from Antarctica as a trigger of the Bolling-Allerod warm interval. Science 299, 1709-1713.

Webb, P.-N., Harwood, D.M., 1991. Late Cenozoic glacial history of the Ross embayment, Antarctica. Quat. Sci. Rev. 10, 215-223.

Weber, M.E., Clark, P.U., Kuhn, G., Timmermann, A., Sprenk, D., Gladstone, R., Zhang, X., Lohmann, G., Menviel, L., Chikamoto, M.O., Friedrich, T., Ohlwein, C., 2014. Millennial-scale variability in Antarctic ice-sheet discharge during the last deglaciation. Nature 510, 134-138.

Weber, M.E., Kuhn, G., Sprenk, D., Rolf, C., Ohlwein, C., Ricken, W., 2012. Dust transport from Patagonia to Antarctica–a new stratigraphic approach from the Scotia Sea and its implications for the last glacial cycle. Quat. Sci. Rev. 36, 177-188.

Weber, M.E., Raymo, M.E., Peck, V.L., Williams, T., Expedition 382 Scientists, 2019. Expedition 382 Preliminary Report: Iceberg Alley and Subantarctic Ice and Ocean Dynamics. International Ocean Discovery Program. https://doi.org/10.14379/iodp.pr.382.2019.

Weertman, J., 1974. Stability of the junction of an ice sheet and an ice shelf. Journal of Glaciology 13, 3-11.

Whittaker, T.E., Hendy, C.H., Hellstrom, J.C., 2011. Abrupt millennial-scale changes in intensity of Southern Hemisphere westerly winds during marine isotope stages 2-4. Geology 39, 455-458.

Willeit, M., Ganopolski, A., Calov, R., Brovkin, V., 2019. Mid-Pleistocene transition in glacial cycles explained by declining CO_2 and regolith removal. Science Advances 5, eaav7337, doi: 10.1126/sciadv.aav7337.

Wilson, D.J., Bertram, R.A., Needham, E.F., van de Flierdt, T., Welsh, K.J., McKay, R.M., Mazumder, A., Riesselman, C.R., Jimenez-Espejo, F.J., Escutia, C., 2018. Ice loss from the East Antarctic Ice Sheet during late Pleistocene interglacials. Nature 561, 383-386.

Wilson, D.J., Piotrowski, A.M., Galy, A., Banakar, V.K., 2015. Interhemispheric controls on deep ocean circulation and carbon chemistry during the last two glacial cycles. Paleoceanography 30, 621-641.

Wilson, D.J., Struve, T., van de Flierdt, T., Chen, T., Li, T., Burke, A., Robinson, L.F., 2020. Sea-ice control on deglacial lower cell circulation changes recorded by Drake Passage deep-sea corals. Earth Planet. Sci. Lett. 544, 116405. doi: 10.1016/j.epsl.2020.116405.

Winckler, G., Anderson, R.F., Fleisher, M.Q., McGee, D., Mahowald, N., 2008. Covariant glacial-interglacial dust fluxes in the equatorial Pacific and Antarctica. Science 320, 93-96.

Winter, K., Woodward, J., Dunning, S.A., Turney, C.S., Fogwill, C.J., Hein, A.S., Golledge, N.R., Bingham, R.G., Marrero, S.M., Sugden, D.E., 2016. Assessing the continuity of the blue ice climate record at Patriot Hills, Horseshoe Valley, West Antarctica. Geophys. Res. Lett. 43, 2019-2026.

Wolff, E.W., Fischer, H., Fundel, F., Ruth, U., Twarloh, B., Littot, G.C., Mulvaney, R., Rothlisberger, R., de Angelis, M., Boutron, C.F., Hansson, M., Jonsell, U., Hutterli, M.A., Lambert, F., Kaufmann, P., Stauffer, B., Stocker, T.F., Steffensen, J.P., Bigler, M., Siggaard-Andersen, M.L., Udisti, R., Becagli, S., Castellano, E., Severi, M., Wagenbach, D., Barbante, C., Gabrielli, P., Gaspari, V., 2006. Southern Ocean sea-ice extent, productivity and iron flux over the past eight glacial cycles. Nature 440, 491-496.

Wouters, B., Martin-Español, A., Helm, V., Flament, T., van Wessem, J.M., Ligtenberg, S.R.M., Van den Broeke, M.R., Bamber, J.L., 2015. Dynamic thinning of glaciers on the Southern Antarctic Peninsula. Science 348, 899-903.

Wu, L., Wang, R., Xiao, W., Ge, S., Chen, Z., Krijgsman, W., 2017. Productivity-climate coupling recorded in Pleistocene sediments off Prydz Bay (East Antarctica). Palaeogeography, Palaeoclimatology, Palaeoecology 485, 260-270.

Wu, L., Wilson, D.J., Wang, R., Passchier, S., Krijgsman, W., Yu, X., Wen, T., Xiao, W., Liu, Z., 2021. Late Quaternary dynamics of the Lambert Glacier-Amery Ice Shelf system, East Antarctica. Quat. Sci. Rev. 252, 106738, doi: 10.1016/j.quascirev.2020.106738.

Xiao, W., Esper, O., Gersonde, R., 2016. Last Glacial-Holocene climate variability in the Atlantic sector of the Southern Ocean. Quat. Sci. Rev. 135, 115-137.

Yamane, M., Yokoyama, Y., Abe-Ouchi, A., Obrochta, S., Saito, F., Moriwaki, K., Matsuzaki, H., 2015. Exposure age and ice-sheet model constraints on Pliocene East Antarctic ice sheet dynamics. Nature Communications 6, 7016, doi: 10.1038/ncomms8016.

Yan, Y., Bender, M.L., Brook, E.J., Clifford, H.M., Kemeny, P.C., Kurbatov, A.V., Mackay, S., Mayewski, P.A., Ng, J., Severinghaus, J.P., 2019. Two-million-year-old snapshots of atmospheric gases from Antarctic ice. Nature 574, 663-666.

Yau, A.M., Bender, M.L., Blunier, T., Jouzel, J., 2016a. Setting a chronology for the basal ice at Dye-3 and GRIP: implications for the long-term stability of the Greenland Ice Sheet. Earth Planet. Sci. Lett. 451, 1-9.

Yau, A.M., Bender, M.L., Robinson, A., Brook, E.J., 2016b. Reconstructing the last interglacial at Summit, Greenland: Insights from GISP2. Proceedings of the National Academy of Sciences 113, 9710-9715.

Yeung, N.K.H., Menviel, L., Meissner, K.J., Sikes, E., 2019. Assessing the spatial origin of Meltwater Pulse 1A using oxygen-isotope fingerprinting. Paleoceanography and Paleoclimatology 34, 2031-2046.

Yin, Q., Berger, A., 2015. Interglacial analogues of the Holocene and its natural near future. Quat. Sci. Rev. 120, 28-46.

Yokoyama, Y., Esat, T.M., Thompson, W.G., Thomas, A.L., Webster, J.M., Miyairi, Y., Sawada, C., Aze, T., Matsuzaki, H., Okuno, J.i., 2018. Rapid glaciation and a two-step sea level plunge into the Last Glacial Maximum. Nature 559, 603-607.

Yu, J., Anderson, R.F., Rohling, E.J., 2014. Deep ocean carbonate chemistry and glacial-interglacial atmospheric CO_2 changes. Oceanography 27, 16-25.

Yu, J., Elderfield, H., 2007. Benthic foraminiferal B/Ca ratios reflect deep water carbonate saturation state. Earth Planet. Sci. Lett. 258, 73-86.

Zachos, J., Pagani, M., Sloan, L., Thomas, E., Billups, K., 2001. Trends, rhythms, and aberrations in global climate 65 Ma to present. Science 292, 686-693.

Figures and tables

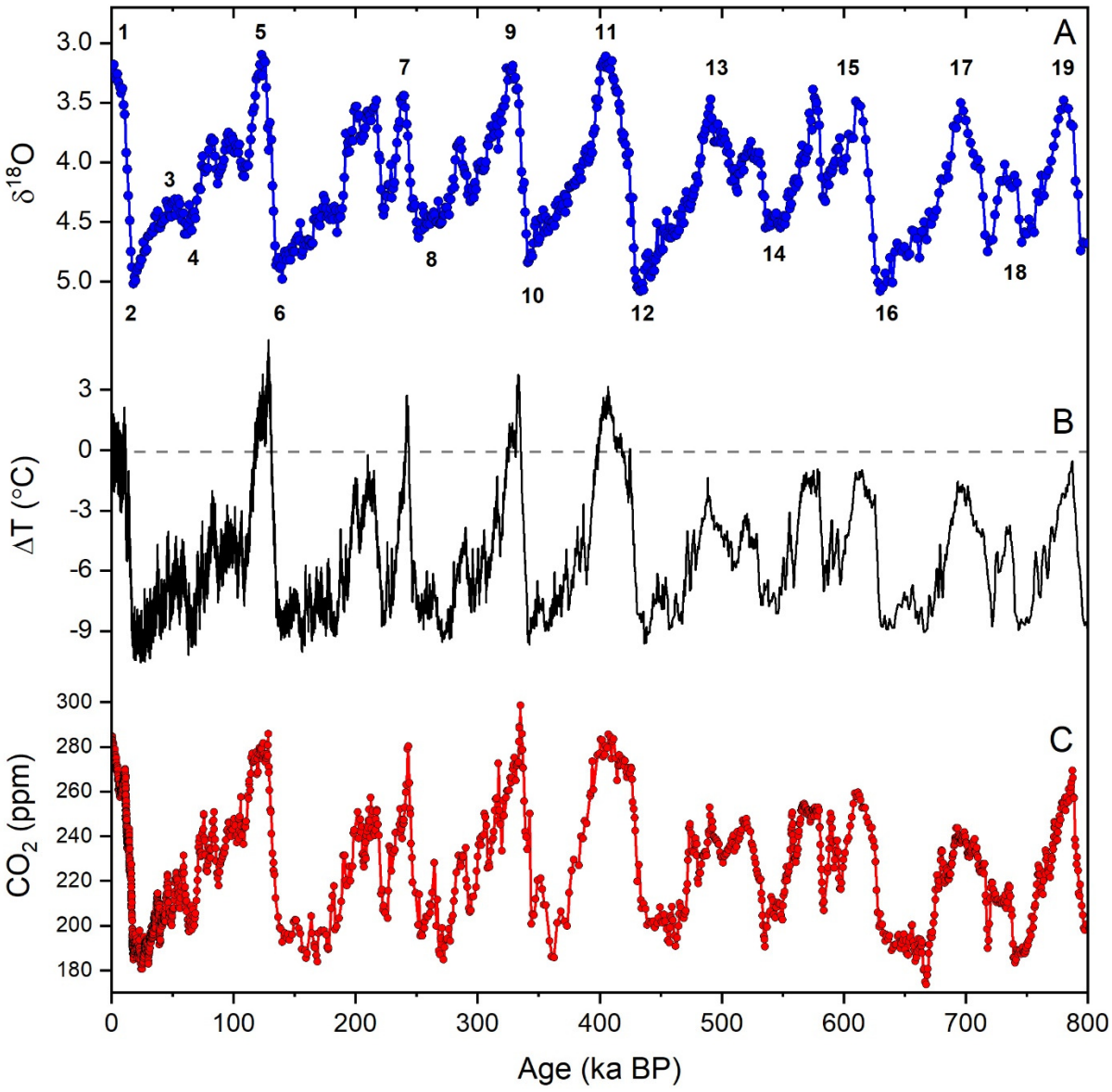

Figure 11.1: Marine and ice core records of late Pleistocene climate variability. (a) "LR04" benthic foraminiferal oxygen isotope ($\delta^{18}O$) stack (Lisiecki and Raymo, 2005). (b) Antarctic ice core temperature reconstruction (ΔT, difference from the mean of the last millennium) based on deuterium isotopes (δD_{ice}) in EDC (Jouzel et al., 2007). (c) Atmospheric carbon dioxide (CO_2) concentrations from Antarctic ice cores (Bereiter et al., 2015). Marine Isotope Stage numbers are shown in (a). Note (i) the strong connection between Antarctic temperatures, benthic foraminiferal $\delta^{18}O$ values, and atmospheric CO_2; (ii) the dominance of quasi-100 kyr cycles for the last 800 kyr; and (iii) the enhanced warmth and elevated atmospheric CO_2 of Antarctic interglacials since MIS 11 (i.e. the Mid-Brunhes Event at ~430 ka).

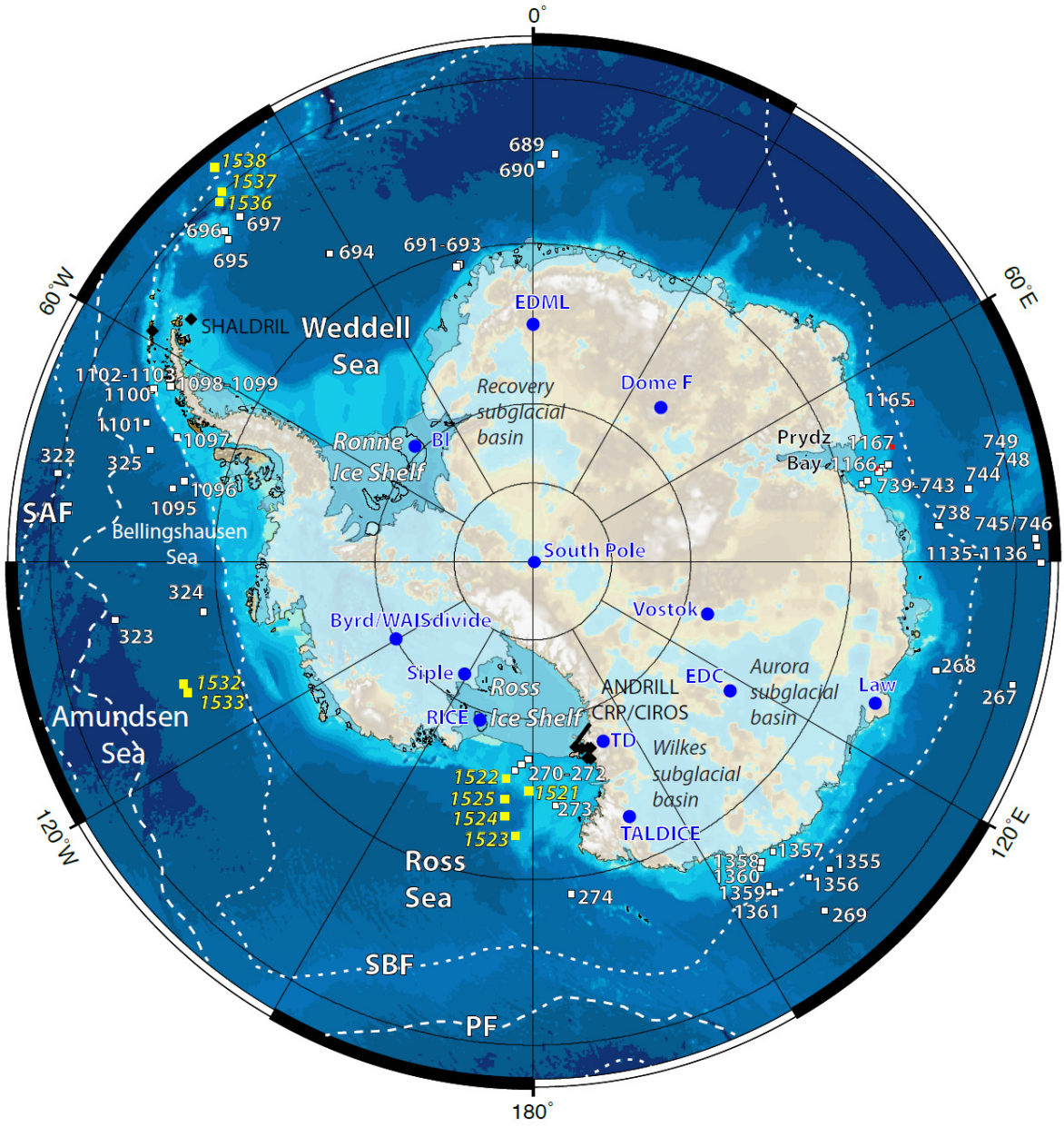

Figure 11.2: Locations of key climate archives from Antarctica, including selected ice cores (blue circles) and marine sediment cores (white squares, yellow squares, black diamonds), and subglacial topography of Antarctica (Bedmap2; Fretwell et al., 2013). Sediment core sites from DSDP/ODP/IODP expeditions (white squares) include: DSDP Leg 28 (Ross Sea), DSDP Leg 35 (Bellingshausen Sea), ODP Leg 113 (Weddell Sea), ODP Legs 119 and 188 (Prydz Bay), ODP Leg 178 (Antarctic Peninsula), and IODP Expedition 318 (Wilkes Land). Sites from recent IODP drilling legs (yellow squares) include: IODP Expedition 374 (Ross Sea), IODP Expedition 379 (Amundsen Sea), and IODP Expedition 382 (Iceberg Alley). Nearshore drilling sites (black diamonds) include: Cape Roberts Project (CRP), Cenozoic Investigations in the Western Ross Sea (CIROS), and Antarctic Drilling Project (ANDRILL) in the Ross Sea, and SHALDRILL on the Antarctic Peninsula. Abbreviations for ice cores: BI, Berkner Island; EDC, EPICA Dome C; EDML, EPICA Dronning Maud Land; RICE, Roosevelt Island Climate Evolution; TALDICE, Talos Dome Ice Core; TD, Taylor Dome; WAIS Divide, West Antarctic Ice Sheet Divide. Abbreviations for ocean fronts (white dashed lines): SBF, Southern Boundary Front; PF, Polar Front; SAF, Subantarctic Front.

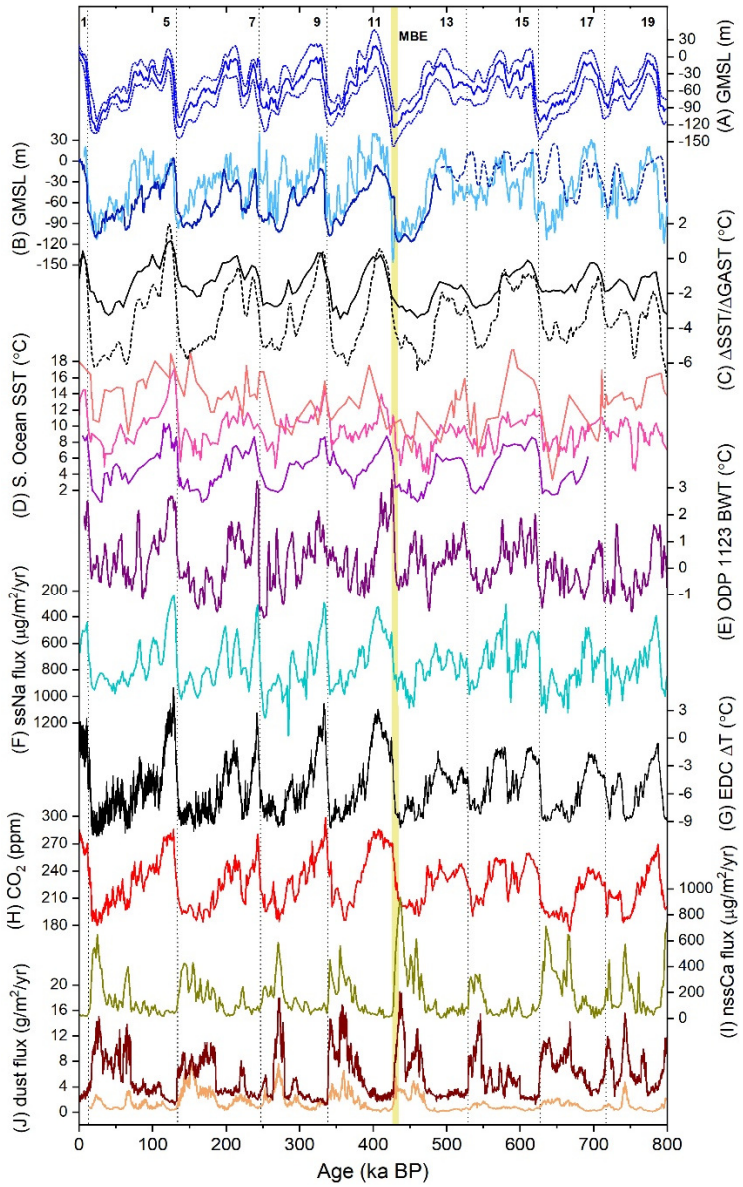

Figure 11.3: Global and Antarctic climate from 0-800 ka based on ice core and marine records. (a) Global mean sea level (GMSL) stack, with dashed lines showing 95 % confidence interval (Spratt and Lisiecki, 2016). (b) Global mean sea level (GMSL) based on combined benthic $\delta^{18}O$ and Mg/Ca in ODP Site 1123 (light blue; Elderfield et al., 2012), and based on modelling of planktonic $\delta^{18}O$ in the Red Sea (solid blue, 0-492 ka; Grant et al., 2014) and the Mediterranean Sea (dashed blue, 492-800 ka; Rohling et al., 2014). (c) Change in global sea surface temperature (ΔSST) from an alkenone-based stack (solid; Martínez-Botí et al., 2015a) and change in global average surface temperature (ΔGAST) from a combined data-modelling approach (dashed; Snyder, 2016). (d) Southern Ocean SSTs based on alkenones from the subantarctic Southeast Pacific (purple, PS75/34-2; Ho et al., 2012), subantarctic South Atlantic (pink, PS2489-2/ODP Site 1090; Martinez-Garcia et al., 2010), and subtropical Tasman Sea (orange, DSDP Site 593; McClymont et al., 2016). (e) Southwest Pacific bottom water temperatures (BWT) from benthic foraminiferal Mg/Ca (ODP Site 1123; Elderfield et al., 2012). (f) Sea-salt sodium (ssNa) flux as a sea ice proxy in EDC ice core (Wolff et al., 2006). (g) Antarctic temperature difference (ΔT) from δD_{ice} in EDC ice core (Jouzel et al., 2007). (h) Atmospheric CO_2 concentration from an ice core compilation (Bereiter et al., 2015). (i) Non sea-salt calcium (nssCa) fluxes as a dust proxy in EDC ice core (Wolff et al., 2006). (j) Dust fluxes to Southern Ocean marine cores in the Atlantic (brown, ODP 1090; Martinez-Garcia et al., 2011) and Pacific (orange, PS75/076-2; Lamy et al., 2014) sectors. Marine Isotope Stage numbers for interglacials are shown at the top. Vertical dotted lines indicate glacial terminations I-VIII. Yellow bar indicates approximate timing of Mid Brunhes Event (MBE). For clarity, uncertainties are not plotted on individual records.

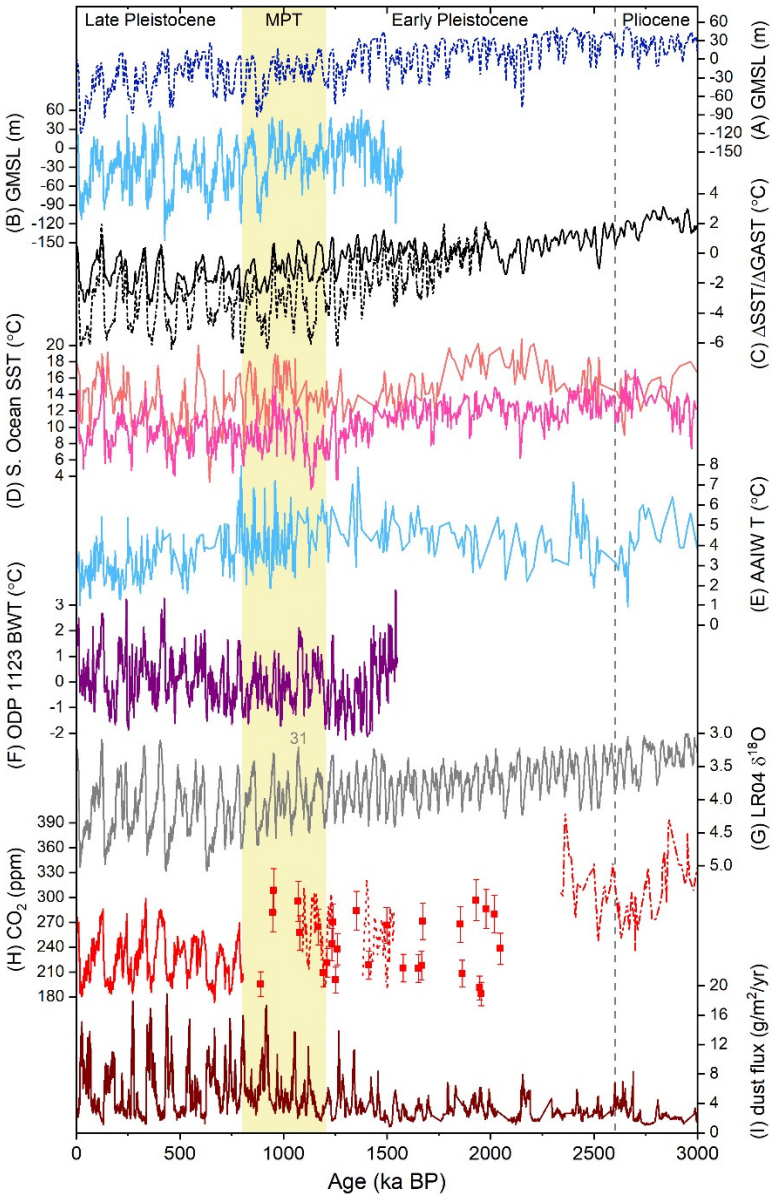

Figure 11.4: Global and Antarctic climate from 0-3 Ma based on marine records. (a) Global mean sea level (GMSL) based on modelling of planktonic $\delta^{18}O$ in the Mediterranean Sea (Rohling et al., 2014). (b) Global mean sea level (GMSL) based on combined benthic $\delta^{18}O$ and Mg/Ca in ODP Site 1123 (Elderfield et al., 2012). (c) Change in global sea surface temperature (ΔSST) from an alkenone-based stack (solid; Martínez-Botí et al., 2015a) and change in global average surface temperature (ΔGAST) from a combined data-modelling approach (dashed; Snyder, 2016). (d) Southern Ocean SSTs based on alkenones from the subantarctic South Atlantic (pink, PS2489-2/ODP Site 1090; Martinez-Garcia et al., 2010) and the subtropical Tasman Sea (orange, DSDP Site 593; McClymont et al., 2016). (e) Antarctic Intermediate Water (AAIW) temperatures from the subtropical Tasman Sea (DSDP Site 593; McClymont et al., 2016). (f) Southwest Pacific bottom water temperatures (BWT) from benthic foraminiferal Mg/Ca (ODP Site 1123; Elderfield et al., 2012). (g) LR04 benthic $\delta^{18}O$ stack (Lisiecki and Raymo, 2005). (h) Atmospheric CO_2 concentration from ice cores (solid line; Bereiter et al., 2015) and from marine boron isotope records: low resolution Pleistocene data (symbols and error bars; Hönisch et al., 2009); early MPT (dashed line; Chalk et al., 2017); early Pleistocene (dotted line; Dyez et al., 2018); late Pliocene-Pleistocene (dash-dot line; Martínez-Botí et al., 2015a; Sosdian et al., 2018). Note that uncertainties on those marine records are typically ~30-40 ppm in the Pleistocene and ~100 ppm in the Pliocene. (i) Dust fluxes to a Southern Ocean marine core in the Atlantic sector (ODP 1090; Martinez-Garcia et al., 2011). Vertical dashed grey line indicates Plio-Pleistocene boundary. Yellow bar indicates approximate timing of Mid Pleistocene Transition (MPT). Super-interglacial MIS 31 is indicated on panel (g). For clarity, uncertainties are not plotted on individual records.

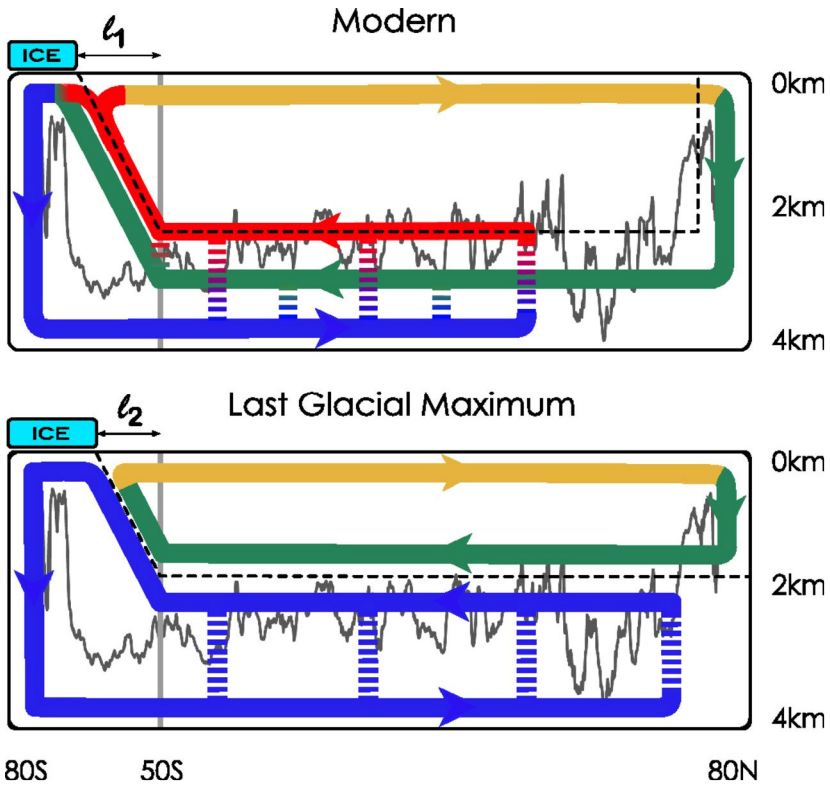

Figure 11.5: Schematic representation of ocean circulation structure during (a) the modern interglacial state, and (b) the Last Glacial Maximum. Ribbons represent water masses: green, NADW; blue, AABW; red, Pacific and Indian deep waters; yellow, AAIW. During glacial periods, extended Southern Ocean sea ice is proposed to shift the boundary between buoyancy loss and buoyancy gain northwards, reducing the width of the channel between the sea ice margin and 50 °S (l_2 versus l_1). Because interior isopycnal slopes in the channel are largely unchanged, the effect is to shoal the interface (dashed line) between the upper northern-sourced cell (NADW) and the lower southern-sourced cell (AABW). Shoaling of that water mass boundary places it above the depth of most rough seafloor bathymetry (black line), leading to reduced vertical mixing (vertical dashed lines) between the northern and southern cells, increased deep stratification, and an enhanced capacity for carbon storage in the lower cell. Figure reproduced from Ferrari et al. (2014). *Credit: Ferrari, R., Jansen, M.F., Adkins, J.F., Burke, A., Stewart, A.L., Thompson, A.F., 2014. Antarctic sea ice control on ocean circulation in present and glacial climates. Proc. Natl. Acad. Sci. U. S. A. 111, 8753-8758. [p. 8755]*

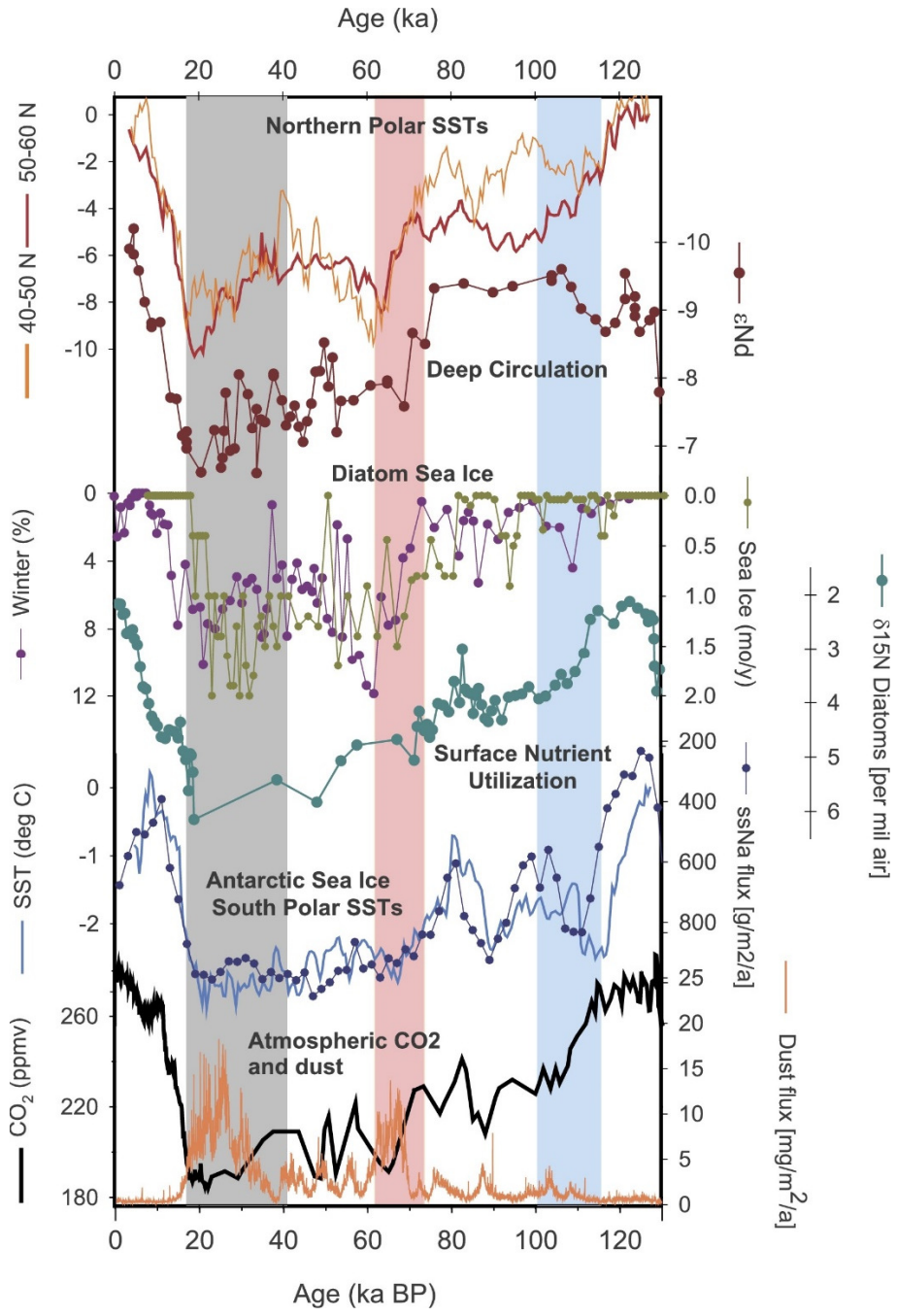

Figure 11.6: Controls on the carbon cycle and climate through the last glacial cycle from 0-130 ka. Coloured bars indicate three intervals of CO_2 drawdown: MIS 5e to 5d transition (blue), MIS 5 to MIS 4 transition (red), LGM (grey). Records are (top to bottom): Northern Hemisphere SST stacks (Kohfeld and Chase, 2017); deep Indian Ocean circulation from neodymium isotopes (Wilson et al., 2015); sea ice proxies in the Southeast Atlantic Ocean (winter sea ice extent from % *F. curta*; Gersonde and Zielinski, 2000) and Southeast Indian Ocean (sea ice duration; Crosta et al., 2004); surface nutrient utilisation from nitrogen isotopes in the Antarctic Zone of the Pacific Ocean (Studer et al., 2015); Antarctic SST stack from 50-60 °S plotted as relative change (Kohfeld and Chase, 2017); sea ice proxy from ice core ssNa flux (Wolff et al., 2006); dust flux based on nssCa in EDC ice core (Lambert et al., 2008); and atmospheric CO_2 from EDC ice core (EPICA Community Members, 2004). Figure reproduced from Kohfeld and Chase (2017). *Credit: Kohfeld, K.E., Chase, Z., 2017. Temporal evolution of mechanisms controlling ocean carbon uptake during the last glacial cycle. Earth Planet. Sci. Lett. 472, 206-215. [p. 210]*

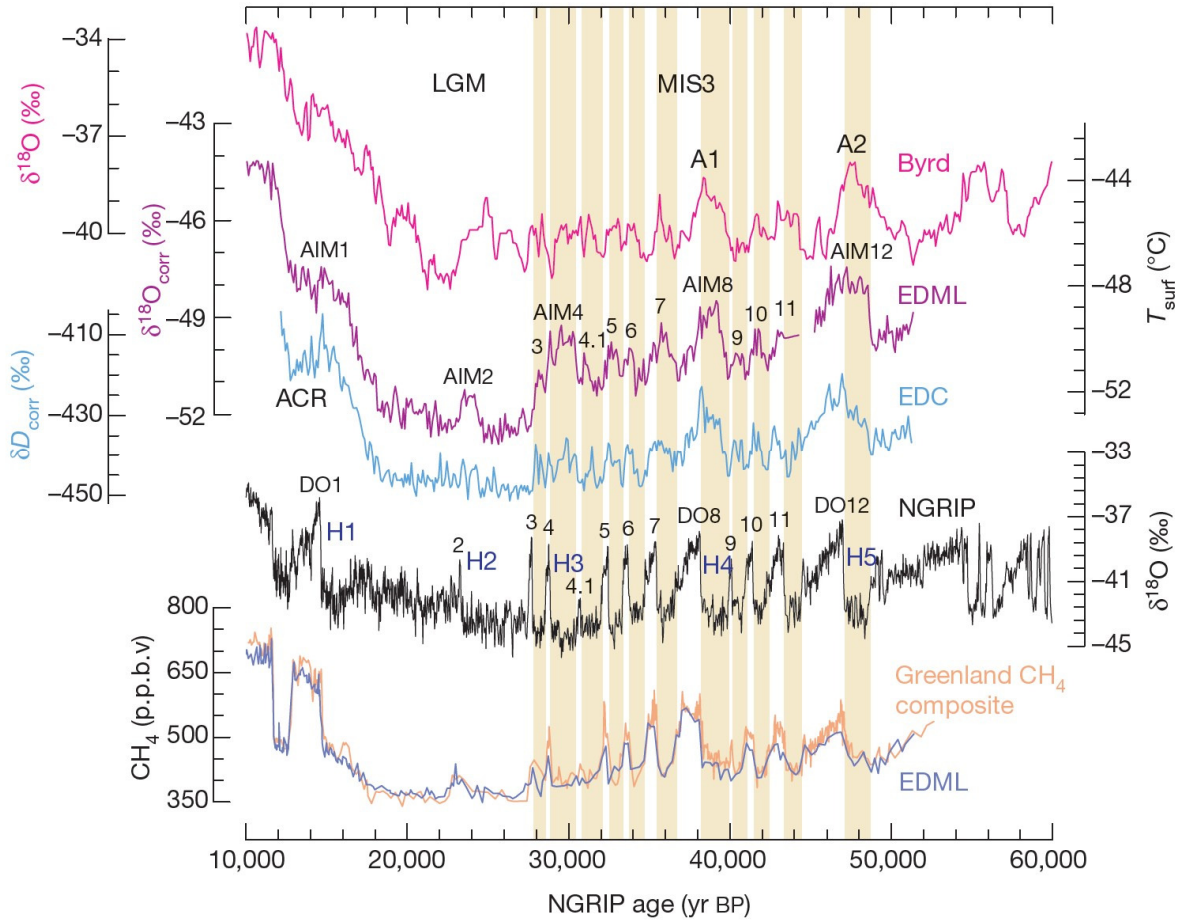

Figure 11.7: Record of the bipolar seesaw in ice core climate records. Upper curves: Antarctic δD_{ice} or $\delta^{18}O_{ice}$ in different ice cores (Byrd, pink; EDML, purple; EDC, blue), with temperature scale on the right corresponding to the EDML record. Middle curve: Greenland $\delta^{18}O_{ice}$ (NGRIP, black). Lower curves: methane records from Antarctica (EDML, blue) and Greenland (composite, orange) used to synchronise the age scales. Yellow bars indicate warming events in Antarctica coinciding with Northern Hemisphere stadials. Ax, Antarctic warm events. AIMx, Antarctic Isotope Maximum events. DOx, Dansgaard-Oeschger events. Hx, Heinrich events. LGM, Last Glacial Maximum. ACR, Antarctic Cold Reversal. Figure reproduced from EPICA Community Members (2006). *Credit: EPICA Community Members, 2006. One-to-one coupling of glacial climate variability in Greenland and Antarctica. Nature 444, 195-198. [p. 196]*

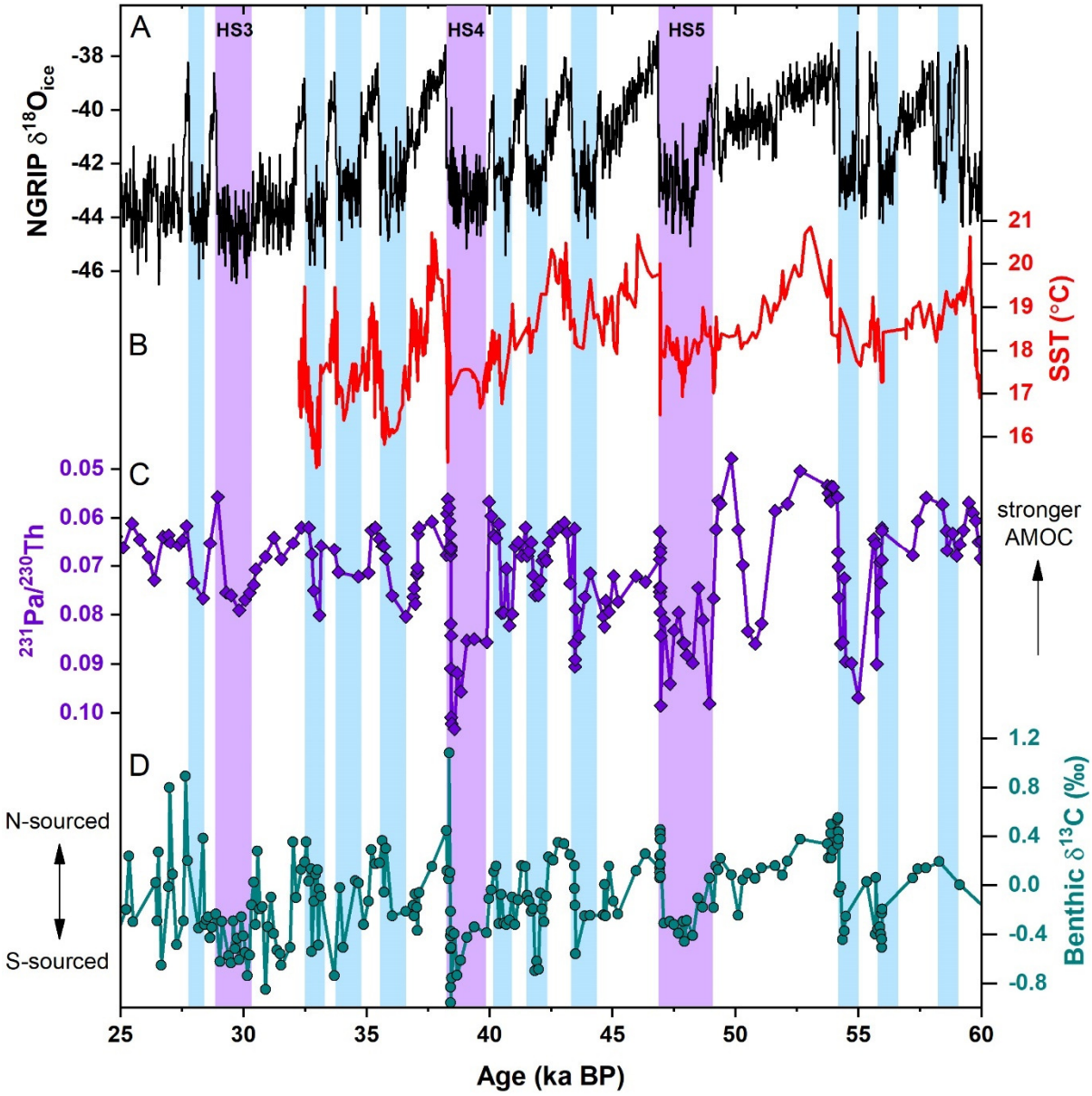

Figure 11.8: Records of surface climate and deep ocean circulation from the North Atlantic region during the last glacial period. (a) Greenland $\delta^{18}O_{ice}$ in NGRIP (NGRIP Members, 2004; Svensson et al., 2008). (b) North Atlantic SST at Bermuda Rise (Sachs and Lehman, 1999). (c) Proxy for AMOC strength based on protactinium/thorium ($^{231}Pa/^{230}Th$) ratios at Bermuda Rise (Henry et al., 2016). (d) Proxy for water mass mixing based on benthic foraminiferal $\delta^{13}C$ at Bermuda Rise (Henry et al., 2016). Vertical blue bars indicate stadials, and purple bars indicate Heinrich Stadials (labelled HSx).

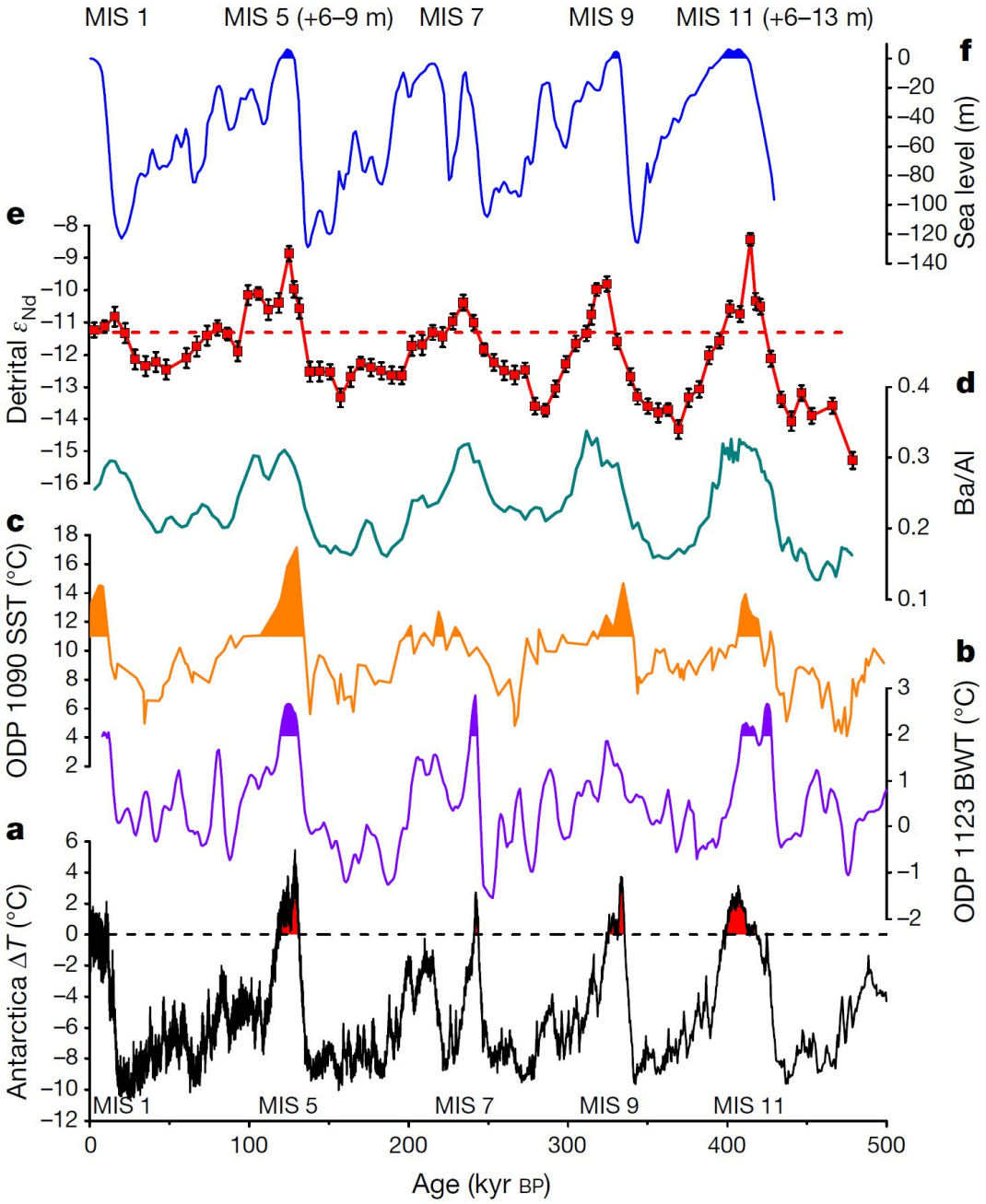

Figure 11.9: Late Pleistocene variability of the EAIS in the Wilkes Subglacial Basin inferred from geochemical proxies at Site U1361 in relation to global sea level and climate reconstructions. (a) Antarctic temperature change (ΔT, difference from mean values of the last millennium) from δD in EDC ice core (Jouzel et al., 2007). (b) Southern Ocean bottom water temperature (BWT) from benthic foraminiferal Mg/Ca at ODP Site 1123 (Elderfield et al., 2012). (c) Southern Ocean SST from alkenones at ODP Site 1090 (Martinez-Garcia et al., 2009). (d) Ba/Al ratios in U1361A (XRF-scanner counts, three-point smoothed; Wilson et al., 2018), with higher values indicating higher marine productivity. (e) Bulk detrital sediment Nd isotopes in U1361A (Wilson et al., 2018), as an indicator of inland (more radiogenic, up) versus coastal (less radiogenic, down) erosion. (f) Global sea level proxy from benthic $\delta^{18}O$ (Waelbroeck et al., 2002), labelled with MIS numbers and sea level estimates from MIS 5e and MIS 11 (Dutton et al., 2015). Shading in (a-c, f) represents intervals with values above modern or late Holocene; red dashed line in (e) indicates the core top value. Figure reproduced from Wilson et al. (2018). *Credit: Wilson, D.J., Bertram, R.A., Needham, E.F., van de Flierdt, T., Welsh, K.J., McKay, R.M., Mazumder, A., Riesselman, C.R., Jimenez-Espejo, F.J., Escutia, C., 2018. Ice loss from the East Antarctic Ice Sheet during late Pleistocene interglacials. Nature 561, 383-386. [p. 385]*

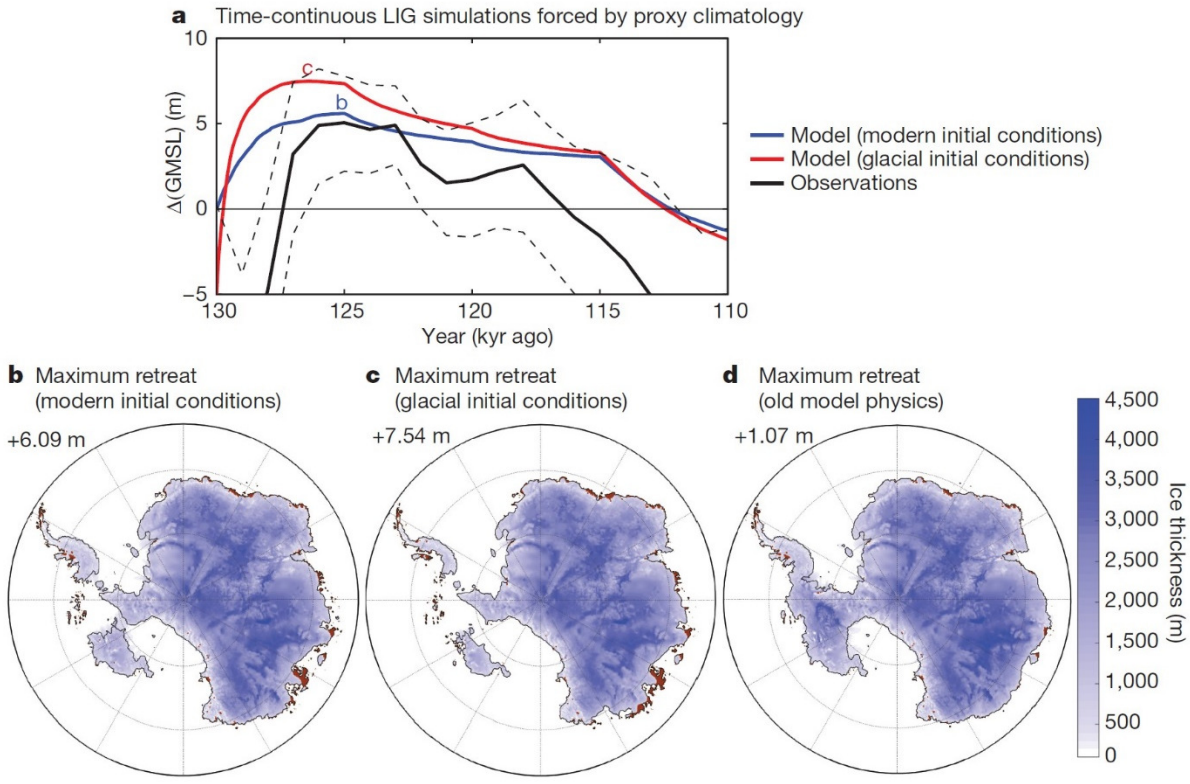

Figure 11.10: Ice sheet modelling results for MIS 5e based on the Penn State University ice sheet model (DeConto and Pollard, 2016). (a) Time series evolution of the Antarctic contribution to global mean sea level during MIS 5e, based on the outputs from two different models starting at 130 ka (panels b and c) and a probabilistic data-based assessment with uncertainties (16th and 84th percentiles) (Kopp et al., 2009). (b-d) Maps showing modelled ice thickness (with numbers indicating Antarctic contributions to global mean sea level) for three different model scenarios. The models are all driven by the same time-evolving proxy-based atmosphere and ocean climatologies and the results are plotted for the maximum MIS 5e retreat state. (b) New model incorporating ice shelf hydrofracture and cliff failure processes, based on modern initial conditions. (c) New model as for (b), but based on glacial initial conditions. (d) Old model physics, based on modern initial conditions. Comparing (b) with (c) indicates the modest effect of initiating the model run from glacial rather than interglacial initial conditions (i.e. deeper bed elevations for glacial initial conditions). Comparing (b) with (d) indicates the major effect of incorporating new processes (i.e. ice shelf hydrofracture and cliff failure) in the models. Brown areas are ice-free land surfaces. Figure reproduced from DeConto and Pollard (2016). *Credit: DeConto, R.M., Pollard, D., 2016. Contribution of Antarctica to past and future sea-level rise. Nature 531, 591-597. [p. 594]*

Table 11.1: Key paleoceanographic parameters and their reconstruction from proxy measurements.

Parameter	Proxy	Notes	References
Ice volume	Benthic foraminiferal oxygen isotopes ($\delta^{18}O$)	need benthic Mg/Ca data or climate modelling to remove temperature effect	(Shackleton, 2000; Bintanja et al., 2005; Elderfield et al., 2012)
Deep ocean temperature	Benthic foraminiferal oxygen isotopes ($\delta^{18}O$)	need to remove ice volume effect; also sensitive to salinity	(Zachos et al., 2001; Marchitto et al., 2014)
	Benthic foraminiferal Mg/Ca ratios	potential additional carbonate ion influence	(Lear et al., 2000; Elderfield et al., 2012)
	Clumped isotopes of oxygen and carbon (Δ_{47}) in carbonates	independent of fluid composition, but need to consider species-dependent vital effects in corals	(Ghosh et al., 2006; Spooner et al., 2016)
Sea surface temperature (SST)	Planktonic foraminiferal oxygen isotopes ($\delta^{18}O$)	need to remove ice volume effect; also sensitive to salinity	(Emiliani, 1955; Pearson, 2012)
	Planktonic foraminiferal Mg/Ca ratios	need species- and/or location-specific calibrations; foraminifera cleaning method is important	(Nürnberg et al., 1996; Elderfield and Ganssen, 2000; Barker et al., 2005; Vázquez Riveiros et al., 2016)
	Unsaturation index in alkenones derived from coccoliths ($U^{k'}_{37}$ and variants)	calibrations for different regions and temperature ranges; coccoliths can be absent near the poles; need to consider seasonality effects	(Sikes and Volkman, 1993; Conte et al., 2006)
	Tetraether index in organic membrane lipids (TEX_{86} and variants)	versions of the index exist for different latitudes; regional calibrations may be useful	(Schouten et al., 2002; Ho et al., 2014)
	Long Chain Diol Index (LDI)	wide distribution including high latitudes; calibration extends to cold temperatures; research needed on source of diols, mechanism, and seasonality effect	(Rampen et al., 2012; Lopes dos Santos et al., 2013)
	Heterocyst diol and triol indices (HDIs and HTIs)	developed in lakes; application in the ocean is in its infancy	(Bauersachs et al., 2015)
Salinity	Foraminiferal oxygen isotopes ($\delta^{18}O$)	need to couple with other proxies to remove temperature and ice volume effects; salinity effects of sea ice are not readily resolved	(Rohling, 2000; Schmidt et al., 2004)
Meltwater input	Diatom oxygen isotopes ($\delta^{18}O$)	promising tracer in polar regions where foraminifera are absent; need to consider species, size fraction, vital effects, and diagenesis	(Shemesh et al., 1994; Swann and Leng, 2009)
Water mass sourcing	Authigenic neodymium isotopes (ε_{Nd})	need to constrain water mass endmembers; additional influences from weathering changes and boundary exchange	(Goldstein and Hemming, 2003; van de Flierdt et al., 2016)
	Benthic foraminiferal carbon isotopes ($\delta^{13}C$)	need to constrain water mass endmembers; also influenced by nutrient regeneration (linked to surface productivity and deep ocean ventilation rate)	(Lynch-Stieglitz and Fairbanks, 1994; Curry and Oppo, 2005; Mackensen and Schmiedl, 2019)
	Benthic foraminiferal Cd/Ca ratios	need to constrain water mass endmembers; also influenced by nutrient regeneration (linked to surface productivity and deep ocean ventilation rate)	(Boyle, 1988a; Marchitto and Broecker, 2006)

Deep ocean ventilation	Radiocarbon in benthic foraminifera or deep-sea corals ($\Delta^{14}C$)	need to compare measured $\Delta^{14}C$ to $\Delta^{14}C$ of contemporaneous surface ocean or atmosphere	(Shackleton et al., 1988; Adkins et al., 1998; Cook and Keigwin, 2015)
Deep water export rates	Protactinium/thorium ($^{231}Pa/^{230}Th$)	significant controls from productivity and particle scavenging	(Chase et al., 2002; Bradtmiller et al., 2014)
Local current strength	Mean grain size of sortable silt fraction (SS)	need to test that the sediment is current-transported; require local calibrations for quantitative reconstructions	(McCave et al., 1995; McCave and Hall, 2006; McCave et al., 2017)
Export productivity	Organic carbon % or mass accumulation rate (can be based on specific organic molecules)	strongly influenced by preservation (linked to factors such as sedimentation rate, temperature, and oxygenation)	(Sachs and Anderson, 2005; Martinez-Garcia et al., 2009)
	Opal content	influenced by preservation (linked to sedimentation rate)	(Mortlock et al., 1991; Ragueneau et al., 2000)
	Barite content, barium concentrations, or Ba/Al ratios	may be less sensitive to preservation than other productivity proxies	(Francois et al., 1995; Paytan and Griffith, 2007)
Nutrient utilisation	Stable nitrogen isotopes in bulk or microfossil-bound organic matter ($\delta^{15}N$)	microfossil-bound data are less susceptible to transport and diagenesis than bulk data; consider diatom species and seasonality	(Francois et al., 1997; Studer et al., 2015)
	Stable silica isotopes in diatoms ($\delta^{30}Si$)	need to ensure separation from clay; isotopic fractionation is size and species-dependent	(de la Rocha et al., 1998; Egan et al., 2012)
Surface pH or atmospheric CO_2	Planktonic foraminiferal or coral boron isotopes ($\delta^{11}B$)	calibrations are species-dependent; conversion to atmospheric CO_2 requires ocean-atmosphere equilibrium	(Sanyal et al., 1997; Hönisch et al., 2004; Foster and Rae, 2016)
Deep ocean pH	Benthic foraminiferal or deep-sea coral boron isotopes ($\delta^{11}B$)	calibrations are species-dependent; need to understand internal pH modification of calcifying fluid (particularly for corals)	(Sanyal et al., 1997; Rae et al., 2011; Foster and Rae, 2016)
Deep ocean carbonate ion	Benthic B/Ca ratios	calibrations are species-dependent	(Yu and Elderfield, 2007; Yu et al., 2014)
	Carbonate percent, mass accumulation rate, Ca/Ti ratios, or preservation indices	also influenced by surface ocean productivity and porewater dissolution; method is most sensitive near lysocline depth	(Broecker and Clark, 2001; Anderson and Archer, 2002; Gottschalk et al., 2018)
Deep ocean nutrient content	Benthic foraminiferal Cd/Ca ratios	also influenced by water mass mixing	(Boyle and Keigwin, 1982; Marchitto and Broecker, 2006)
	Benthic foraminiferal carbon isotopes ($\delta^{13}C$)	also influenced by changes in water mass endmembers and mixing	(Lynch-Stieglitz and Fairbanks, 1994; Gebbie, 2014; Mackensen and Schmiedl, 2019)
Deep ocean oxygen content	$\Delta\delta^{13}C$ gradient between epifaunal and deep infaunal benthic foraminifera	requires suitable foraminifera species to co-exist; calibration appears best at low to moderate oxygen levels	(McCorkle and Emerson, 1988; Hoogakker et al., 2015)
	Alkenone preservation	need independent tracer for surface productivity	(Anderson et al., 2019)
	Authigenic U, Mo, Mn, or other redox-sensitive trace metals	controlled by porewater chemistry so need independent tracer for productivity to infer deep water oxygenation	(Jaccard et al., 2009)

Iceberg rafting (i.e. iceberg rafted debris, IRD)	% or accumulation rate of coarse grain size fraction (e.g. >125 μm)	other potential controls from ocean current transport, iceberg survival (linked to ocean temperature), and debris content of icebergs	(Ruddiman, 1977; Patterson et al., 2014)
Provenance of iceberg rafted debris	U-Pb, K-Ar, Ar-Ar ages on specific minerals in coarse grain size fraction	potential for biases due to nature of source lithology, grain size, and transport processes	(Hemming et al., 1998; Licht and Hemming, 2017)
Provenance of fine-grained detrital sediment	Nd, Pb, Sr isotopes in fine-grained or bulk fraction	need to remove authigenic fraction; need to consider transport, grain size, and weathering effects (particularly for Sr)	(Farmer et al., 2006; Licht and Hemming, 2017)
Dust input fluxes	Fe concentrations or mass accumulation rates (or Fe/Al, Fe/Ti ratios by scanning-XRF)	sediment redistribution can be addressed using method of ^{230}Th normalisation	(Kumar et al., 1995; Martinez-Garcia et al., 2009)
	^{232}Th mass accumulation rate	^{232}Th is a lithogenic tracer but grain size and provenance can be additional influences	(Winckler et al., 2008; McGee et al., 2016)
Sea ice extent	Diatom and radiolarian assemblages	most effective for winter sea ice extent; consider seasonality; location of cores is critical	(Gersonde et al., 2005; Benz et al., 2016)
	Biomarkers (e.g. highly branched isoprenoids, HBIs)	new approach still in development; potential to additionally resolve summer sea ice extent and seasonality	(Collins et al., 2013; Vorrath et al., 2019)